Future Changes in Extreme Rainfall Events and African Easterly Waves over West Africa

TEMITOPE SAMUEL EGBEBIYI

(EGBTEM001)

Dissertation Submitted for the Degree of

Master of Science

Department of Environmental and Geographical Science,

University of Cape Town

Supervisor

Dr. Babatunde J. Abiodun

March, 2016

Climate System Analysis Group

University of Cape Town • iYunivesithi yaseKapa • Universiteit van Kaapstad

SPES BONA

NRF

Declaration

I know the meaning of plagiarism and declare that all the work in the dissertation, save that which is properly acknowledged, is my own.

Signed by candidate

Signature Removed

Temitope S. Egbebiyi

Abstract

This study examines the relationship between African Easterly Waves (AEWs) and extreme rainfall events over West Africa, and investigates how climate change could alter this relationship in the future. Satellite observations, reanalysis data, and regional climate model (RCA4) simulations (forced with eight global climate simulations) were analysed for the study. The study used the 95th percentile of daily rainfall as a threshold to identify extreme rainfall events, and applied spectral analysis to extract 3-5 days and 6-9 days AEWs from 700hPa meridional wind component over West Africa. The capability of RCA4 to reproduce the rainfall climatology, extreme rainfall events, the characteristics of AEWs and the contribution of AEWs to extreme rainfall events over the region during the past climate (1971-2005) was examined and quantified using statistical analysis. The future changes (2031-2065) in these parameters were projected for the RCP4.5 and RCP8.5 climate-change scenarios.

The results of the study show that RCA4 gives a realistic simulation of the West African climate, including the annual rainfall pattern, the structure of AEWs, and the characteristics of the African Easterly Jet that feeds AEWs. The bias in the simulated threshold of extreme rainfall is within the uncertainty of the observed values. The model also captures the link between the structure of AEWs and the rainfall pattern over West Africa, and shows that the percentage contribution of AEWs to extreme rainfall events over the region ranges from 20 to 60%, as depicted by reanalysis data. For the RCP4.5 and RCP8.5 scenarios, the RCA4 ensemble mean projects a future increase in annual rainfall and in the frequency and intensity of extreme rainfall events over the sub-continent, but the increase is generally higher for the RCP8.5 scenario. It also projects a decrease in the frequency of rain days, no changes in the structure of the AEWs, and an increase in the variance of the waves. However, the simulations from the ensemble mean shows no substantial changes in the contribution of AEWs to the extreme rainfall events, suggesting that the increase in the frequency and intensity of the extreme rainfall events may not be attributable to the changes in AEWs. The study's application is in understanding and mitigating the future impact of climate extremes over West Africa.

Keywords: Extreme rainfall events, African Easterly Waves, Climate change, Dynamical downscaling, West Africa

Acknowledgements

First and foremost, I want to appreciate the goodness of God for his protection, provision, guidance, and wisdom for the successful completion of this Degree. Thanks and glory to His name.

I really want to honour my supervisor, Dr Babatunde J. Abiodun, whose mentorship and tutelage helped in the successful completion of this work. Words are insufficient to describe or quantify your immense contribution to my life, family and career. May God always be there for you and your family in times of need, in Jesus' Name (Amen). Many thanks also to his generous wife, Mrs Ruth F. Abiodun, and to his friendly boys (Shalom, Emmanuel, Joel, Samuel and Daniel), for their love towards my family.

To my lovely wife, Oluwabukola, and my daughter, Praise, thanks for your endless understanding, support and encouragement. Your love and prayers have made this degree a great success.

I am also grateful to the South African Government via the National Research Foundation (NRF) for its financial support, without which I would not have been able to complete this degree. Also, my appreciation goes to the University of Cape Town's Postgraduate Funding Office for the International/Refugee Student Scholarship. To you all I say many thanks. I equally want to thank all the institutions that provided the data for this work: the Climate System Analysis Group (CSAG), Swedish Meteorological and Hydrological Institute–Rossby Centre and the various climate modelling groups who provided the GCM/RCM data, TRMM, GPCP and the European Centre for Medium-Range Weather Forecasts for the ERA-Interim data (ERAINT). Many thanks to Drs Chris Lennard and Nikulin Grigory for their assistance in securing the data for the study. Dr Tristan Hauser, thanks for your interest in my work, and for your assistance and guidance on how to compute the easterly wave. I would like to thank Philip Mukwenha for all his technical support with this work.

To my peer-review group members (Kamoru Lawal, Gemma Bluff, Linda Maoyi Molulaqua, Arlindo Meque, Romaric Odulami and Johnson Oloruntade), thanks for the shared knowledge, reviews and critiques. Special thanks to my fellow graduate students in the department, Myra Naik, Stefaan Conradie, Lerato Thekoadi, Shakirudeen Lawal for the many wonderful chats, your intellectual input, the editing and encouragement. To Sabina Abba Omar (my lecturer) and Riddick

Takong, thanks for helping out with the codes.

I cannot forget to thank my family members, friends and benefactors. To my parents, Mr. and Mrs. Gabriel Egbebiyi and Mrs Grace Aderomi, thanks for your prayers and your efforts to give me education. My siblings, Omowumi and Oluwatosin Egbebiyi, and my in-laws, the Aderomis, thanks for the love and encouragement. To my uncle, Dr Yinka Awopetu, thanks for your concern, financial support and encouragement.

To all my benefactors, my father in the Lord, Pastor M. K Adaramola, and his wife, Daddy, thanks for your prayers, encouragement and financial support. I also do not want to forget Mr and Mrs Sayikanmi, Pastor Adelae, Mr and Mrs Oluwole Adekunle and others for their support, which has been crucial in getting me where I am today.

To my friends Mr and Dr (Mrs) Steve Arowolo, many thanks for your love, prayers and encouragement. Thanks for being there; you are indeed covenant friends. To Joshua Adejare Adeleke, thanks for the prayers and the editing; I really appreciate your concern and effort. Greater heights in Jesus' Name.

To everyone whom time and space will not allow me to mention: Thank you.

Dedication

To the Almighty GOD (the Alpha and Omega)

To the Holy Spirit, my teacher and comforter through this journey

To my darling wife and daughter

Table of Contents

List of Figures

List of Tables

List of Abbreviations

ABL – Atmospheric Boundary Layer

AEJ – African Easterly Jet

AEWs – African Easterly Waves

AR – Assessment Report

AV – Added Value

CAPE – Convective Available Potential Energy

CMIP – Coupled Model Intercomparison Project

CORDEX - Coordinated Regional Climate Downscaling Experiment

DD – Dynamical Downscaling

ECMWF – European Centre for Medium-Range Weather Forecasts

ERAINT – ERA-Interim reanalysis

FAO – Food and Agriculture Organisation

GCMs – Global Climate Models

GEV – Generalised Extreme Value

GHGs – Greenhouse Gases

GPCP – Global Precipitation Climatology Project

GP – Generalised Pareto

GRB – Government of Republic of Benin

IPCC – Intergovernmental Panel on Climate Change

ITCZ – Inter-Tropical Convergence Zone

ITD – InterTropical Discontinuity

MCSs – Mesoscale Convective Systems

NED – Number of Extreme Rainfall Days

NRD – Numbers of Rain Days

RCMs – Regional Climate Models

RCP – Representative Concentration Pathways

SD – Statistical Downscaling

SST – Sea Surface Temperature

TEJ – Tropical Easterly Jet

TRMM – Tropical Rainfall Measurement Mission

TMI – TRMM Microwave Imager

VIRS – Visible Infrared Scanner

WAM – West Africa Monsoon

WMO – World Meteorological Organisation

WRF – Weather Research and Forecasting

Chapter 1: Introduction

1.1 The West African Region

West Africa, a geographical area located north of the equator of the African continent, lies between latitudes 4°N and 28°N and longitudes 16°W and 15°E (Figure 1.1). The region is made up of 16 developing countries that form the Economic Community of West African States (ECOWAS). ECOWAS is made up of 16 countries, namely: Benin Republic, Burkina Faso Cape Verde, Gambia, Ghana, Guinea, Guinea-Bissau, Ivory Coast, Liberia, Mali, Mauritania, Niger, Nigeria, Senegal, Sierra Leone and Togo (Figure 1.1). ECOWAS has the mission to promote economic integration within member states across the region. The West African region has a large area of land mass—over 6 million square kilometres, which is about one-fifth of the African continent[1]. The region is bounded by the Gulf of Guinea to the south, and to the north by the northern part of Mali, Mauritania and Niger. While the Adamawa Highlands/Cameroon Mountains form its eastern boundary, the Atlantic Ocean is its boundary to the west. Some of the important topographical features of West Africa are the Adamawa Highlands (up to 2042m above mean sea level), Fouta Djallon (1537m), Guinea Highlands (1656m), Jos Plateau (1690m), the Mandara Mountains (1142m), Nimba Mountains (1752m), Plateau of Djado (1120m) in northern Niger, the Sierra Leone Mountains (1948m) and the Saharan Uplands of Air (1850m) (FAO, 1985). West Africa has 5 major rivers systems, the largest being the Niger River, which traverses most of the countries, over a distance of 4180km.

The West African region has a population of more than 375 million people in 2014[1]. With an average annual growth rate of 3%, the population is projected to increase to about 430 million people by 2020[1]. About 80% of the total population operates in the farming sector; the majority of these people practise subsistence rain-fed farming[2]. The socio-economic activities of most countries in West Africa depend largely on agriculture (Omotosho and Abiodun, 2007). Agriculture accounts for about 60% of the active labour force of the region, and about 35% of the Gross Domestic Product (GDP), which has grown at a rate of about 5.9% annually over the last ten years[3]. However, variability in the West African climate, with regard to extreme rainfalls, droughts, and heat waves, is a serious threat to agricultural production, food security, and many socio-economic activities across the region (Abatan, 2011).

[1] http://global.britannica.com/place/western-Africa
[2] http://www.oecd.org/migration/38481393.pdf
[3] http://www.feedthefuture.gov/country/west-africa-regional

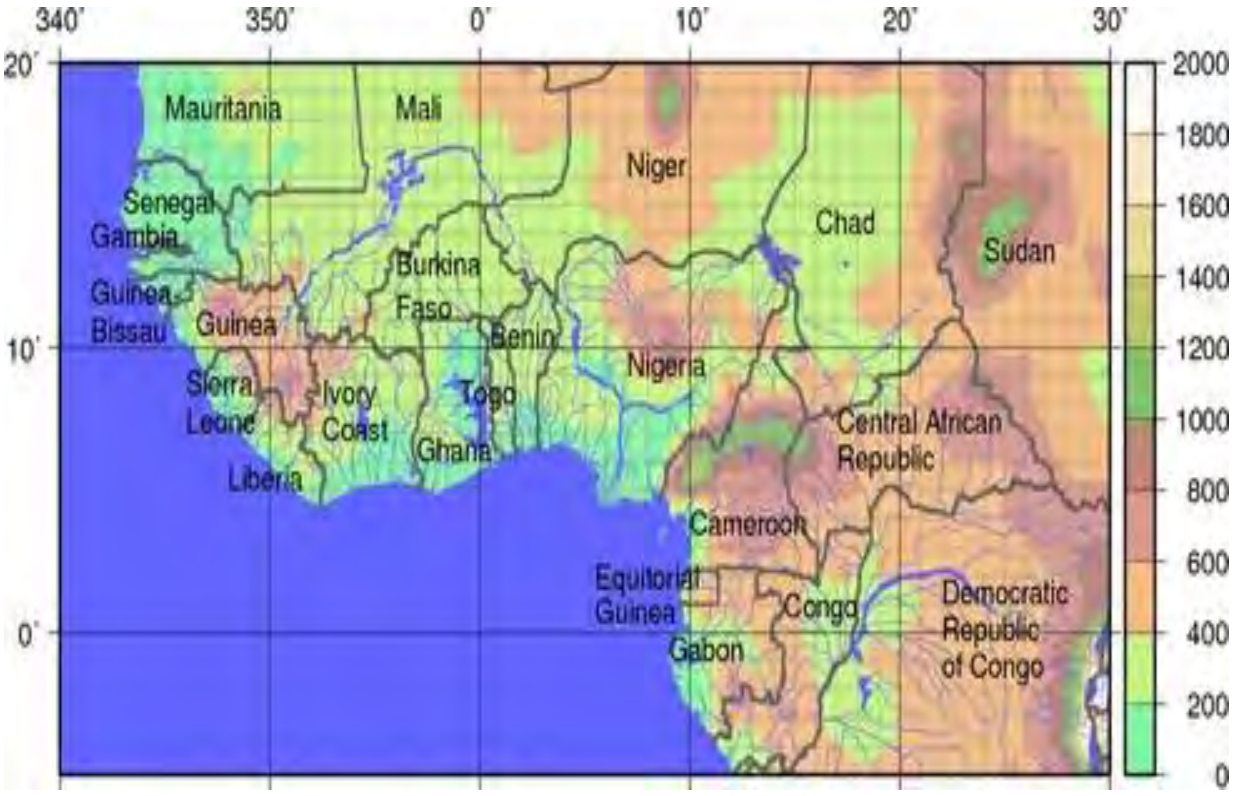

Figure 1.1: The West African topography (shaded, in meters) and rivers (in blue), obtained from http://aaron.boone.free.fr/work.html

1.2 The Climate of West Africa

Two major air masses influence the climate of West Africa. The first air mass is a warm, moist, tropical maritime air mass, which transports moisture inland from the Atlantic Ocean and supplies most of the moisture for the rainfall over the region. This moist air mass reaches its northernmost extent (between 18 and 21^{o}N) in July or August (FAO, 1985). The second air mass is the hot, dusty and dry continental air mass, which originates from the Sahara high-pressure system and blows from the north-east over the region (FAO, 1985, Nicholson 2008, 2009). This air mass is characterised by hot and dry condition over land and reaches its southernmost position over the Guinea zone in January between 5 and 7^{o}N. These air masses contribute significantly to the temperature and rainfall variability over West Africa. The position where the two air masses meet is called the Inter-Tropical Convergence Zone (ITCZ) when it occurs over the ocean, and the Intertropical Discontinuity (ITD) when it occurs over land (Abiodun et al., 2008, Nicholson 2008, 2009). The ITD reaches its southernmost position at about 7^{o}N in January over the Guinea zone and about 22^{o}N in August over the Sahel (Peter and Tetzlaff, 1988).

The Köppen's climate classification (Peel et al., 2007) categorises the climate of West Africa into two major climate zones: the Tropical climate zone and the Dry climate zone (Figure 1.2). The Tropical climate zone consists of three climate zones: the Tropical Forest Climate (wet equatorial) (Af), the Tropical Monsoon Climate (Am), and the Tropical Wet and Dry Climate (Aw). Af covers a small area in West Africa (i.e. it is limited to the south-west coast of Liberia). The climate of Af is dominated by the doldrums low-pressure system all year round and experiences an average monthly temperatures between 24 and 30^{o}C and at least 60mm month^{-1} rainfall every month of the year[4]. Am, which covers a wider area than Af, is found along the west coast of Guinea and Liberia, along the southern borders of Cote d'Ivoire and Ghana, and along the south coast of Nigeria down to its southern border with Cameroon. This climate is mainly controlled by the monsoon circulation, a seasonal reversal in trade-winds direction. (A detailed description of West Africa monsoon system is given in Section 1.4.1.) The areas with the Am climate type are characterised by monthly mean temperatures above 18^{o}C. These areas experience mean annual rainfall of 1500-3000mm year^{-1} and have wet and dry seasons; the driest months have precipitation of less than 60mm month^{-1}. The rainy season, which begins around February or March and ends around November or December, has a bimodal monsoon rainfall with two peaks in May and September following the ITD movement. Aw has a recognised but extended dry season during winter, compared to Am[3]. It affects the large part of the region, from Guinea to the southernmost part of the Savannah zone (about 10^{o}N from the equator). The Aw climate zone is characterised by wet-season precipitations usually below 1000mm, and precipitation totals of less than 60mm, or 1/25th of the total annual rainfall, during dry-season months. The mean annual temperature is about 26^{o}C, with a diurnal range of 1.7-2.8^{o}C.

[4] http://www.britannica.com/science/Koppen-climate-classification

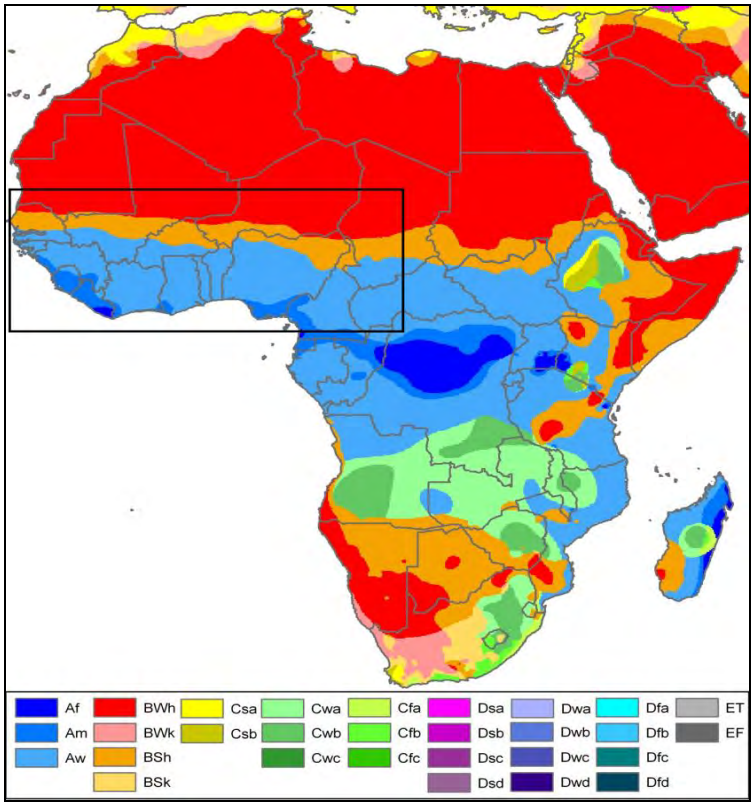

Figure 1.2: The Köppen climate classification over Africa. The West Africa region (study area) is indicated with a rectangle on the Map of Africa (Peel et al., 2007).

The Dry climate has two climate types over West Africa: the Hot Desert (BWh) and the Hot Semi-Arid (BSh) climates. The Hot Desert (BWh) can be found over the southern part of the Sahara (north of Savannah and Sahel zone, north of 10^{o}N). The major feature of BWh is that rainfall over this part of West Africa is less than 50% of the potential evapotranspiration. Rainfall over these areas is very unreliable and irregular due to the area's aridity and low relative humidity. The annual temperature is above 18^{o}C and daily minimum temperatures can go below 0^{o}C during winter. Bwh has the highest percentage of sunshine compared to the other climate types, and the maximum daily temperature is very high. The diurnal temperature range can reach about 5.6-8.3^{o}C, with a mean monthly temperature of 30^{o}C and an annual temperature range of 9^{o}C (FAO, 1985). Furthermore, windy conditions persist during the day. The major factor controlling the BWh is the dominance of the subtropical high-pressure system throughout the year. Thus, the Savannah and Sahel are characterised by cloudless skies during the day and low temperatures at night (FAO, 1985). On the

other hand, the Hot Semi-Arid Climate (BSh) covers the central Sahara and north of the Sahel zone of West Africa. Under this climate type, the difference between the potential evapotranspiration and mean precipitation is less than that of BWh. The annual rainfall, which exceeds that of BWh, is between 250mm and 500mm. The rainfalls are sporadic and are caused by the brief incursions of the Inter-Tropical Convergence Zone. The average temperature is above 18^{o}C. The highest temperatures are observed in this zone and the temperature can be as high as 58^{o}C at daytime and as low as 4^{o}C at night (FAO, 1985). The weather over this region transitions between desert and humid climates. The dominant controlling weather factor is the subtropical high-pressure system that occurs throughout the year.

1.3 Factors Influencing Rainfall-producing System in West Africa

There are many factors responsible for West African rainfall, which includes the West African monsoon systems, sea surface temperature, land use changes and aerosols. In addition, the land ocean/sea thermal gradients or contrasts derived from the monsoon system also influence the rainfall pattern in the region (Adedokun, 1978; Odekunle et al., 205). The complex interaction of these rain-producing systems account for the variation in rainfall amount across the different zones of West Africa (Abiodun et al., 2008). Therefore, a good understanding of these systems is very important for reliable prediction of the variability in rainfall pattern and even extremes over the region.

1.3.1 The West African Monsoon

The pattern of rainfall in West Africa is mainly controlled by a system called West Africa Monsoon (WAM) (Nicholson, 2013). WAM is produced from the reversal of the land and ocean differential heating and dictates the seasonal pattern of rainfall over West Africa. In summer, it is very crucial to and a dynamic feature of the West African climate (Janicot et al., 2011), and it is mostly referred to as the south-westerly portion of the wind that conveys moist air from the Atlantic Ocean into the continent[5] (see Fig. 1.3). In West Africa, WAM is the main source of moisture and also has a strong impact on the onset and variability of rainfall, and high proportion of annual rainfall in the region (Omotosho and Abiodun, 2007). WAM consists of different atmospheric processes, which include: the African Easterly Jet (AEJ), African Easterly Waves (AEWs) and the Tropical Easterly Jet (TEJ), the monsoon flow and Mesoscale Convective Systems (MCSs) (Abiodun et al., 2008). All these processes interact together in a complex manner enhanced by the supply of moisture by the monsoon flow thus leading to summer monsoon rainfall over the region (Abiodun et al., 2008, Janicot et al., 2011). Moreover, the AEJ and TEJ at 700hPa and 200hPa respectively, are also

important processes for this interaction (Ilesanmi, 1971; Omotosho, 1992). This is because a weaker AEJ and stronger TEJ are responsible for wet years, while over the Sahel zone it is the strength and not the latitudinal position of the AEJ that is more important for rainfall (Grist and Nicholson, 2001). Also, important in transporting moisture into Sahel is a low-level jet between 8-11^{o}N, the West African Westerly Jet (WAWJ) whose strength can vary independently of the south-westerly monsoon flow (Pu and Cook, 2010). In addition, another dominant weather feature of WAM in the summer monsoon season is the AEWs, a synoptic scale system (Nicholson, 2013; Bain et al., 2014).

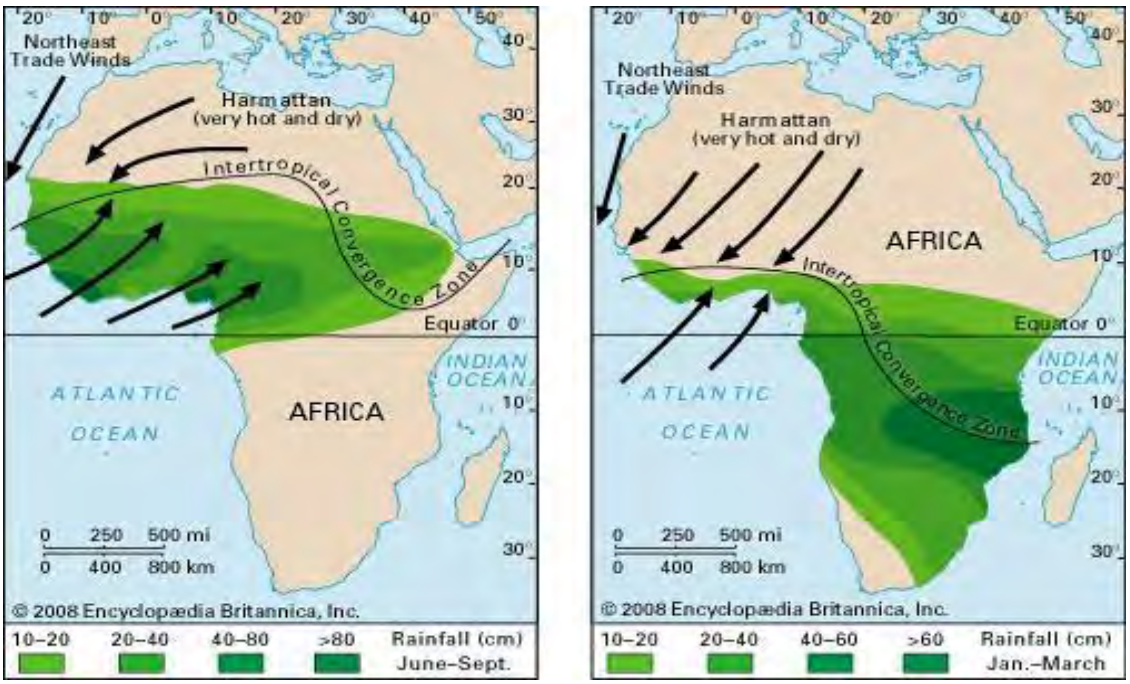

Figure 1.3: Wind and rainfall patterns of the West African monsoon in (a) Jun–Sept. and (b) Jan-Mar[5]

1.3.2 Sea Surface Temperature

Sea Surface Temperature (SST) also influences rainfall variability over West Africa. Studies have shown how Rainfall variability over the region is strongly linked with the variation of SST over the global oceans (Janicot et al., 1996; Fontaine et al., 1998; Giannini et al., 2003; Biasutti et al., 2008). For instance, since West African monsoon, which transports moisture to West Africa, driven by temperature gradient between the Atlantic Ocean and the sub-continent, a warm SST over the Atlantic Ocean may weaken the temperature gradient, thereby weakening the monsoon flow and its moisture transport. This may lead to delay the onset of rainfall less rainfall over West Africa. Also, the convection and rainfall in the Gulf of Guinea are associated with SST variation along the eastern

[5]Encyclopaedia Britannica accessed online 10th July, 2015 at **http://www.britannica.com/science/West-African-monsoon**

Atlantic (Gu and Adler, 2004). Thus, SST variability may be responsible for the observed increase in rainfall over the Guinea coast and equatorial West Africa and the decrease in the Sahel (Deser et al., 2010; Tokinaga and Xie, 2011).

1.3.3 Land Use

Changes in land use influence the West African climate. It has been shown that land-use changes (i.e. desertification and deforestation) in West Africa alter (i.e. decrease) rainfall due to their impact on surface albedo, soil moisture and evapotranspiration (Charney et al., 1975; Abiodun et al., 2008). The implementations of interactive land surface schemes in RCMs has helped improved the simulation of hydrological processes and circulation features, and has fostered a better prediction of land surface processes (Druyan et al., 2004; Konare et al., 2008; Wang et al., 2012). This has enhanced our understanding of the link between land surface processes/feedback and convection (Nicholson et al., 2013).

Surface fluxes of moisture and heat impact convective rainfall (Clarke et al., 2004). Also, convection can be generated from surface changes relationship with temperature and moisture that influence the boundary layer and cloud development (Adler et al., 2011a, b). In addition, land-use changes affect the variability of rainfall in West Africa owing to its effect on the dynamics of monsoon circulation (Paeth et al., 2009; Abiodun et al., 2012a; Zaroug et al., 2013). Hence, understanding land-use change patterns (such as deforestation, urbanisation, vegetation cover and reforestation) is crucial because land-use patterns influence convection and affect the hydrological cycle in West Africa and vice versa (Nicholson et al., 2013).

1.3.4 Aerosols

Aerosols play a crucial role on radiation and convection processes, thereby influencing West African climate. They help in cloud formation as ice and cloud condensation nuclei are majorly from dust (Hui et al., 2008; Wiacek et al., 2010). The influence of dust on the atmospheric radiation budget can induce rainfall variability (DeMott et al., 2003). A decrease in rainfall over West Africa has been linked to an increase in dust (Kluser et al., 2010; Solmon et al., 2012). Aerosols can also induce West African rainfall variability though their indirectly influence on the dynamics of West African monsoon systems. For instance, studies have shown that aerosol can weaken the TEJ and strengthen AEJ the play important roles on rainfall over West Africa (Konare et al., 2008). However, AEWs are important for initialising and transporting dust (Skinner and Diffenbaugh, 2014).

1.4 The African Easterly Waves

AEWs are synoptic-scale disturbances that move from east to west over West Africa and over the Atlantic oceans. These westward propagating waves are observed between June and September during the summer monsoon season in West Africa (Viltard et al., 1998). AEWs evolve, grow and develop through variability in baroclinic and barotropic processes due to the African Easterly Jet (AEJ) strong vertical and horizontal wind shear, in the mid-troposphere (at 600mb) (Burpee, 1972, 1974; Hall et al., 2006; Skinner and Diffenbaugh, 2014). They are associated with TEJ. AEWs are important in initiating convective systems (Carlson, 1969; Mekonnen et al., 2006) and they interact with convection (Cornforth et al., 2009; Berry and Thorncroft, 2012; Crétat et al., 2014). However, they set off from the eastern and central Africa (Berry and Thorncroft, 2005; Hsieh and Cook; 2008, Crétat et al., 2014) through convective heating along, and to the south of the AEJ (Reed et al., 1988; Wang and Gillies, 2011). The structure and wavelength of the AEWs are controlled by the AEJ (Norquist et al., 1977; Hsieh and Cook, 2008). AEWs have two periods (3-5 and 6-9 days) that are prevalent during the summer monsoon season, but they differ in their wavelength and phase speed (Diedhiou et al., 1998, 1999; Vitard et al., 1997; Wu et al. 2012, 2013; Crétat et al. 2014). The average wavelength and phase speed of the 3-5 days AEWs are 3000 km and 8 m/s and 5000 km and 12 m/s to the north and south of the AEJ respectively, while 6-9 days AEWs has a longer wavelength of 5000-6000km but slower phase speed, 7 m/s (De Felice et al., 1990, Diedhiou et al., 1999; Pytharoulis and Thorncroft, 1999). Nevertheless, the two AEWs periods influence and modulate rain-producing systems over West Africa (Fortune 1980; Gaye et al., 2005) and may even lead to extreme rainfall in the region (Laurent et al., 1998; Fink et al., 2006).

1.5 What are Extreme Rainfall Events?

Extreme events are weather hazards or natural disasters that threaten humans' lives, properties and the environment. Different ways have been used in defining extreme events (e.g. extreme rainfall events). The Third Assessment Report (AR3) of the Intergovernmental Panel on Climate Change (IPCC, 2001) defines an extreme weather event as:

"*an event that is rare within its statistical reference distribution at a particular place. Definitions of rare vary, but an extreme weather event would normally be as rare as or rarer than the 10th or 90th percentile. By definition, the characteristics of what is called extreme weather may vary from place to place.*"

However, in the literature (e.g. Groisman et al., 2001; Frich et al. 2002), an extreme rainfall event (ERE) is often defined in three ways. Firstly, when an event exceeds a predefined threshold value, it is called an extreme event. Secondly, the return interval (period of re-occurrence) of an event of specific magnitude is used to describe an extreme event. Lastly, an extreme event is defined as an event that is above a set percentile threshold of a given variable distribution. In the present study, an event is defined as an extreme rainfall event if the rainfall amount is equal to or exceeds the 95th percentile threshold of the daily rainfall distributions.

1.6 Impacts of Extreme Rainfall Events in West Africa

Extreme rainfall events are among the most destructive natural disasters that continue to threaten socio-economic activities in West Africa (Hountondji et al., 2011). Occurrence of extreme rainfall events often cause flooding and erosion, resulting in loss of lives, destruction of property, and displacement of communities (Pathe et al., 2011). Table 1.1 highlights some of the destructive impacts of extreme rainfall events in West Africa for the period 1953-2015. For instance, between 1970 and 2015, extreme rainfall events killed 980 people and injured about 54 individuals across the region. In 2007 alone, more than 869 human deaths, with over 2 million people displaced from their homes in West Africa due to floods induced by extreme rainfall (Tschakert et al., 2010). Furthermore, for the period 1970-2015, about 5 million people were displaced and rendered homeless across the region; 47 communities and 680,000 persons were affected as a result of this destructive weather hazard (Tschakert et al., 2010). In the region, the three countries were mostly affected, namely: Ghana (56 killed and over 330,000 affected), Burkina Faso (46 killed, 28,000 displaced and 93,000 affected,), and Togo (23 killed, 13,700 displaced and over 125,000 affected) respectively (Tschakert et al., 2010).

Furthermore, extreme rainfall events are often responsible for soil erosion and crop damage thus affecting agricultural production (e.g. see Fig. 1.5);; they cause infrastructural damage (e.g. see Fig. 1.4) and increase the risk of infection and outbreak of water-borne diseases (Pathe et al., 2011; Hountondji et al., 2011). It was reported that extreme rainfall events damaged infrastructure worth about US$270 million in West Africa in the period 1970-2013, and also destroyed US$ 2 million or 7,000 hectares worth of rice fields in Guinea (WMO Report, 2015), thus emphasising the disastrous nature of such events in West Africa. Therefore, a major source of concern to West African residents is the damaging impacts of floods from extreme rainfall. Hence, there is a need for a skilful prediction or projection of the future characteristics of extreme rainfall events. This will help the community to adapt to (or mitigate) the impact of extreme rainfall events in West Africa. The present study is oriented in that direction.

Table 1.1: The impacts of extreme rainfall events on human lives, agriculture, and infrastructure in West Africa.

Year (and Location) of extreme rainfall events	Damages	References
1954-2000 (West Africa) 79 events	• Destroyed 5,850 houses • Destroyed bridges, roads and industrial complexes in 1974, 1984 and 1998 respectively. • About $1million hard cash were washed away during the events • Led to nine months famine that affected about five million people in 1954	Grolle (1997) Tarhule (2005)
2007 (West Africa)	• Killed over 869 people • Displaced over 2 million people	Tschakert et al., (2010)
2009 (Burkina Faso)	• Killed 8 people • Displaced 150,000 people • Destroyed major infrastructures, 25,000 homes and the main hospital in the capital city. • Damaged 300 hectares of crops	Panthou et al. (2012); Sighomnou et al., 2013
2010 (Benin)	• Killed 42 people • Rendered 150,000 homeless • Destroyed completely or partially 55,000 houses, 450 schools and 92 health centres. • Destroyed 680,000 tonnes of agricultural products and about 201,600 crop hectares • 81,000 livestock lost • Estimated total loss of US$ 260 million damages after the event	GRB (2010)
2013 (Niger and Guinea)	• Killed 32 people • Rendered 135,000 people homeless • Destroyed rice field of 7,000 hectares worth US$ 2 million in Guinea	WMO Report (2015)
2015 (Burkina Faso)	• Killed 8 people • Injured 54 individuals • Displaced 19,779 people	The Watcher (2015)[6]

[6] The Watcher, accessed online on 27th August, 2015 at http://thewatchers.adorraeli.com/2015/08/08/heavy-flooding-across-west-africa-8-people-dead-and-19-779-affected-in-burkina-faso

Figure 1.4: A collapsed building[7] and flooded settlement[8] after a heavy rainfall in Burkina Faso and Nigeria respectively.

Figure 1.5: A flooded maize farm and road in Benin after heavy rains in 1998 (Yabi and Afouda, 2012)

1.7 Aim and Objectives

1.7.1 Aim

The aim of this thesis is to study the impact of future climate changes under the carbon emission Representative Concentration Pathways 4.5 and 8.5 (RCP4.5 & RCP8.5) on the characteristics of extreme rainfall events and AEWs, and on the contribution of AEWs to the occurrence of extreme rainfall events. The characteristics of the extreme rainfall events considered include the spatial

[7]The Watcher, accessed online on 27th August, 2015 at http://thewatchers.adorraeli.com/2015/08/08/heavy-flooding-across-west-africa-8-people-dead-and-19-779-affected-in-burkina-faso

[8]Okpara et al. (2013)

variation, intensity and frequency of the events. And the characteristics of the AEWs examined include the spatial structure, phase speed and variance of 3-5 and 6-9 days AEWs.

1.7.2 Objectives

The objectives of the present thesis are to:

- understand the characteristics of extreme rainfall events and AEWs over West Africa in the past climate;
- evaluate how well a regional climate model (RCA4), driven by multi-GCM simulations, reproduces the characteristics of extreme rainfall events and AEWs in the present climate;
- investigate how climate change may influence the future characteristics (intensity and frequency) of extreme rainfall in West Africa under two emission scenarios (RCP4.5 and RCP8.5);
- examine how future climate change might influence the contribution of AEWs to the occurrence of extreme rainfall events.

1.8 Structure of Dissertation

The dissertation is structured as follows: Chapter Two reviews past studies on methods of identifying extreme rainfall events, climate downscaling approaches, and the impact of climate change on extreme rainfall. Chapter Three describes the data and methods used for the study. The results and discussion of the study are presented in the next two chapters (Chapters Four and Five). Chapter Four discusses the observed characteristics of extreme rainfall events and AEWs in the past climate, and how well these characteristics are reproduced in the models, while Chapter Five discusses the projected impact of climate change on both extreme rainfall events and AEWs under the two future emission scenarios (RCP4.5 and RCP8.5). Chapter Six provides concluding remarks on the studies and provides recommendations for future studies.

Chapter 2: Literature Review

In this chapter, past studies on extreme rainfall events over West Africa are reviewed. First, it provides an overview of the three main methods used for identifying and defining extreme rainfall, discusses the trend and atmospheric conditions that influences extreme rainfall in West Africa. Also, a summary of previous findings on the capability of climate models to simulate extreme rainfall and the impact of climate change on extreme rainfall over West Africa was presented. Finally, the uncertainties in future characteristics of extreme rainfall as projected by climate models over the region were presented in the chapter.

2.1 Identification of Extreme Rainfall Events

As there is no one universal definition for extreme rainfall events, previous studies (e.g. Tarhule, 2005; Barnston and Mason, 2011) have adopted different methods to identify extreme rainfall events. These methods vary from using the characteristics of extreme rainfall events to identify the event to using the impacts of extreme rainfall events to detect the events. For example, while Groisman et al. (2001) and Klein Tank and Zwiers (2009) defined and identified extreme rainfall events based on the characteristics of the events (i.e. frequency, persistence, intensity, and amplitude), Tarhule (2005) and Barnston and Mason (2011) defined and identified the extreme rainfall events based on the devastating and destructive impacts of the event on the society. However, the review in this section focuses on the three prominent methods (as identified by Groisman et al., 2001) that are relevant for the present study. These methods are return periods, threshold values, and percentiles.

2.1.1 The Return-Period Method

Several studies have given different attributes for return-period methods (e.g. Sanderson, 2010; Chu et al., 2009). For instance, Sanderson (2010) indicated that return period is the frequency of an event, while the magnitude of the associated rainfall event is called return value. Chu et al. (2009) and Vezzoli et al. (2012) referred to the return period, also known as recurrence interval, as the average interval (in years) between rainfall events of a given magnitude or greater. This method, which is common among building engineers and hydrologists, has been used to describe the characteristics of extreme events in different parts of the world. With this method, Sanderson (2010) used a 46-year period to calculate the return value of daily rainfall events over 40 towns and cities in the United Kingdom. Melice and Reason (2007) applied the method over a 65-year data series to

estimate the frequency of the occurrence of a destructive rainfall in George (South Africa). Over West Africa, Panthou et al. (2012) estimated the frequency of extreme rainfall events with a 100-year return value in the Central Sahel Zone using the return period. The main shortcoming of this method is that it requires a long rainfall time series. Sanderson (2010) shows that applying the return period method on a short time rainfall series may lead to high uncertainties in return values.

2.1.2 Identifying Extreme Rainfall Events Using Threshold Values

The use of threshold values for identifying extreme rainfall is common, and the method is well established in the literature (e.g. Groisman et al., 2001; Dyson et al., 2009; Zhang et al., 2011). With this method, an extreme event over an area is identified by using a rainfall threshold value that is suitable for the area. Any rainfall amount equal to or greater than the threshold value is considered an extreme event. Because of its simplicity (when compared to the return period), this method is widely used and preferred to the return-period approach. Panthou et al. (2014) used threshold values of 30.0 and 60.0 mm day^{-1} to identify and study the characteristics of extreme rainfall events in the north and south of the Central Sahel, respectively. Hountondji et al. (2011) applied a threshold value of 79.6 mm day^{-1} to obtain extreme rainfall events over 21 stations in Benin for the period 1960-2000. Groisman et al. (2001) studied the spatial distribution of very heavy rain events over the United States using 100 mm day^{-1} at a 1° x 1° grid resolution. However, some studies (i.e. Dyson et al., 2009; Zhang et al., 2011; Abba Omar, 2014) have that pointed out that this method has a major weakness. The weakness is that, as various regions of the world receive different amount of rainfall and require different threshold value, it is difficult to compare extreme rainfall events over the regions. Moreover, Klein Tank and Zwiers (2009) and Zhang et al. (2011) showed that the threshold value method is inappropriate for the spatial comparison of extreme rainfall distribution over an area or a region.

2.1.3 Percentile Values

To overcome the shortcomings of the threshold-values method, some studies have used percentile values method in identifying an extreme rainfall event (i.e. Grimm and Tedeschi, 2009; Abiodun et al., 2013; Ly et al., 2013). For example, Ly et al. (2013) defined an event as extreme rainfall if it is equal to or above the 99th percentile of daily rainfall in the Sahel zone of West Africa. Abiodun et al. (2013) described the spatial distribution of extreme rainfall events using the 99.5th percentile of daily rainfall over Nigeria. Moreover, other studies employ a different approach in the application of this method. Grimm and Tedeschi (2009) defined an extreme rainfall using the mean of three consecutive rainfall days above the 90th percentile distribution. Moreover, Yabi and Afouda (2012)

identified any year with 20% increase in total annual rainfall above the mean total annual rainfall as an extreme rainfall year over Benin. However, the percentile value method seems to be a more useful approach compared to the return period or threshold values. This reason is that there is an even distribution of the days equal to or greater than the set percentile. Unlike the return period method, this method does not need a long-term dataset and it is applicable to all regions (Klein Tank & Zwiers, 2009; Zhang et al., 2011; Abba Omar, 2014). Moreover, this method is suitable for evaluating the changes in event characteristics, intensity and frequency as well as allows the spatial comparison of complex topography over a region as West Africa (Zhang et al., 2011). Therefore, of these three methods described above, the percentile-threshold method seems to be the most appropriate method for the present study. Following Crétat et al. (2014), the present study used the 95th percentile of daily rainfall to define an extreme rainfall event over West Africa. The implementation of the method for this study is detailed in Chapter Three.

2.2 Trends in Extreme Rainfall Events in West Africa

Using different methods (as described above), many studies have reported an increasing trend in the frequency and intensity of extreme rainfall over different parts of West Africa. For instance, Panthou et al. (2014) found an increasing trend in the frequency of extreme rainfall in the central Sahel. Over a 40 year period (1960-2000), Hountondji et al. (2011) showed an increasing trend in the frequency of extreme rainfall over 21 stations in Benin Republic. Other studies have reported more vulnerability from increased extreme rainfall over Nigeria (New et al. 2006) and Western Niger (A. Ozer and P. Ozer, 2005). Gachon et al. (2007) also found a positive trend in the 90th percentile of daily total rain and frequency of days with rainfall above the 90th percentile in the period 1961-1990 over West Africa. Moreover, Ly et al. (2013) showed a positive statistical significance trend in the 99th percentile of daily rainfall in most locations of West African Sahel, and confirm that the frequency of extreme rainfall events has increased in the last decades (1991-2010) in the West African Sahel compared to the 1961-1990 period. From the above studies, different independent findings have clearly shown there is an increasing trend in extreme rainfall event intensity and frequency over West Africa. The increasing positive trend in the occurrence of extreme rainfall has motivated studies that identify the favourable conditions for these events and try to understand the future characteristics of the events. The present study will improve knowledge in these areas.

2.3 Favourable Atmospheric Conditions for Extreme Rainfall Event in West Africa

Past studies have identified different processes that favour extreme rainfall over West Africa (Reed et al., 1977; Fortune, 1980; Lavaysse et al., 2006, Pathe et al., 2009). While some studies (i.e. Pathe et al., 2009) attribute heavy rainfall over West Africa to warm SST conditions over the Tropical Atlantic Ocean and El Nino conditions over the Pacific Ocean, other studies (i.e. Reed et al. 1977; Fortune, 1980; Lavaysse et al. 2006) attribute the phenomenon to the complex interaction and variability in rainfall-producing features in the WAM systems (i.e. MCSs, AEJ, TEJ and AEWs). For example, Nicholson (2008 and 2009) found that an increase in the strength of TEJ usually lead to an increase in extreme rainfall in the West African Sahel. Laurent et al. (1998) and Fink et al. (2006) found that more MCSs lead to more extreme rainfall in the Sahel. However, Ruti and Dell' Aquila (2010), Abatan, (2011), and Crétat et al. (2014) have reported a strong link between extreme rainfall and AEWs over West Africa. Their findings reveled that extreme rainfall strongly depends on the wave pattern of the AEWs. Crétat et al. (2014), in particular, found that there is a link between extreme rainfall and the two AEWs types (3-5 days and 6-9 days wave periods) over West Africa. Furthermore, the study showed that the 3-5 days AEWs mostly account for extreme rainfall over West Africa (especially south of latitude 15^{o}N). Also, some studies argued that most of heavy rainfall in West Africa comes from MCSs, and that these MCSs are usually embedded in the AEWs (Fink and Reiner, 2003; Fink et al. 2006; Crétat et al. 2014). Hence, a good understanding of the relationship between AEWs and extreme rainfall is crucial to understanding the characteristics of extreme rainfall over West Africa. Therefore, the emphasis of the present study will be on understanding the link between AEWs and extreme rainfall in West Africa in the past and future climates.

2.4 Simulating Extreme Rainfall Events

Global Climate Models (GCMs) are accredited tools for climate simulation. The capability of GCMs in simulating the characteristics of extreme rainfall at the global and continental scales have been documented by many studies (e.g. Kamiguchi et al., 2006; IPCC, 2007; Vigaud et al., 2009; Crétat et al., 2013; Niang et al. 2014). For example, Crétat et al. (2013) found that three out of the four GCMs used in their study simulated a realistic magnitude of intense rainfall over Africa. Kamiguchi et al. (2006) demonstrated the ability of the GCMs in extreme rainfall projection over the continent. However, while GCMs may be skilful in rainfall at the global or continental scale, they cannot resolve the regional circulation patterns that lead to hydrological extreme events like extreme rainfall events at regional scale due to their coarse horizontal resolution (Christensen and

Christensen, 2003). Giorgi et al. (2001), Wang et al. (2004) and Rummukainen (2010) pointed out that GCMs' low and coarse horizontal resolution results in their inability to simulate the finer scale regional and local forcings (e.g. complex terrain and topography, land-ocean contrasts) that controls the regional climate. Giorgi et al. (2009) argued that the low resolution of the GCMs hinders them from simulating extreme events that are important to climate information users. Sylla et al. (2012) and Crétat et al. (2013) also found that GCMs failed to correctly reproduce key features of the local atmospheric circulation due to the low resolution of the models. These shortcomings have been shown to be a major source of uncertainty in projecting future changes in rainfall (Douville et al. 2006; Joly et al. 2007; Vigaud et al., 2009; Caminade and Terray, 2010) and in simulating extreme rainfall characteristics, frequency and intensity, over West Africa (Cook and Vizy, 2006; Sylla et al. 2012; Crétat et al. 2013). For instance, Crétat et al. (2013) stated that GCMs simulations often overestimate the frequency (and underestimate the intensity) of extreme rainfall over West Africa. In light of these shortcomings, downscaling, a method to improve outputs from GCM outputs was initiated to meet the increasing demand for climate variability and projection at a regional scale (Endris et al., 2015). Downscaling, a means of acquiring small-grid scale information from fields with lower resolution provides decision makers with the needed information for impact assessment at local scale in connection with information from the GCMs (Benestad, 2008). Two approaches to downscaling are reported in the literature: Statistical and Dynamical downscaling.

2.4.1 Statistical Downscaling

Statistical Downscaling (SD) has been used to obtain regional climate information from GCMs in previous studies (e.g. Hewitson and Crane, 1996; Di Vittorio and Miller, 2013). SD (i.e. statistical modelling) is used to establish a statistical correlation between global scale climate variables (surface pressure) and local climate variables such as rainfall of an area (Endris et al., 2015). The resultant relationship is used in acquiring regional climate information by mapping them to a GCM data (Hewitson and Crane, 1996). According to Di Vittorio and Miller (2013), SD method adopts the statistical relationships between low-resolution GCM or RCM data and the point measurement at an observation station. Statistical relationships are estimated for a calibration period, validated for separate time period, and applied for another time period assuming temporal stationarity (Di Vittorio and Miller, 2013). Furthermore, regional information can be obtained by the use of equation to downscale GCM outputs. This involves the use of equation to investigate the differences between global and local or regional climate. Abiodun et al. (2013) statistically downscaled different GCMs simulations and found an increase in frequency of extreme rainfall days across the ecological zones of Nigeria due to global warming.

Goswani et al. (2006), however, revealed that large spatial contradictions and the inability to account for topographic effect on extreme rainfall events are some of the defects of the SD technique. Hence, discarding the geomorphology of the study area makes SD inappropriate in forecasting extreme rainfall events (Goswani et al., 2006). In addition, Endris et al. (2015) showed that a major flaw in the SD approach is that the approach is built on a temporal stationarity, thus it assumes the obtained statistical relationship will not be altered by climate change impact. Nevertheless, SD is not appropriate for the present study because it is not suitable for downscaling the dynamic fields (i.e. wind) needed for the study. In addition, since the method downscale variables differently, it may compromise the relationship between the AEWs and rainfall that is crucial for the study.

2.4.2 Dynamical Downscaling

The use of dynamical downscaling (DD) techniques for providing regional information or generating future climate projections from GCMs has been documented by several studies (i.e. Wang et al., 2004; Seth et al., 2007; and Endris et al., 2015). Unlike SD, the DD method applies conservation laws to provide regional climate information over the chosen domain about climate variability and change projections via numerical models (Endris et al., 2015). In this technique, a GCM provides an initial condition and a continuous lateral boundary condition to a RCM's integration, while the RCM provides the finer-scale regional information (Fig 2.1). Many studies have used the DD technique to provide regional climate information for different purposes, including climate predictability studies (Lawal et al., 2015), seasonal climate prediction (Wang et al., 2004), climate change projection (Giorgi and Mearns, 1991 and Giorgi, 2006), and the impact of land-cover change on projected future climate (Abiodun et al 2012; Naik and Abiodun, 2016). The technique has also been successfully used over West Africa for climate-change studies (Vigaud et al., 2009; Diallo et al., 2012). For example, Diallo et al. (2012) employed the DD approach to project future changes in precipitation and temperature over West Africa for the early twenty-first century, using four RCMs (RegCM3, RCA, REMO and HadRM3P) to downscale two GCM (ECHAM5 and HadCM3) outputs. Some of the advantages of the DD method are that it captures atmospheric processes like rainfall induced by topography and uses coarse resolution GCMs output to provide higher-resolution information up to 10-50 km (Giorgi et al., 2009), as well as the fact that it responds to different external forcings and does not assume temporal stationarity in the SD method (Endris et al., 2015). For this study, the dynamical downscaling approach of using a RCM to downscale a GCM output was used.

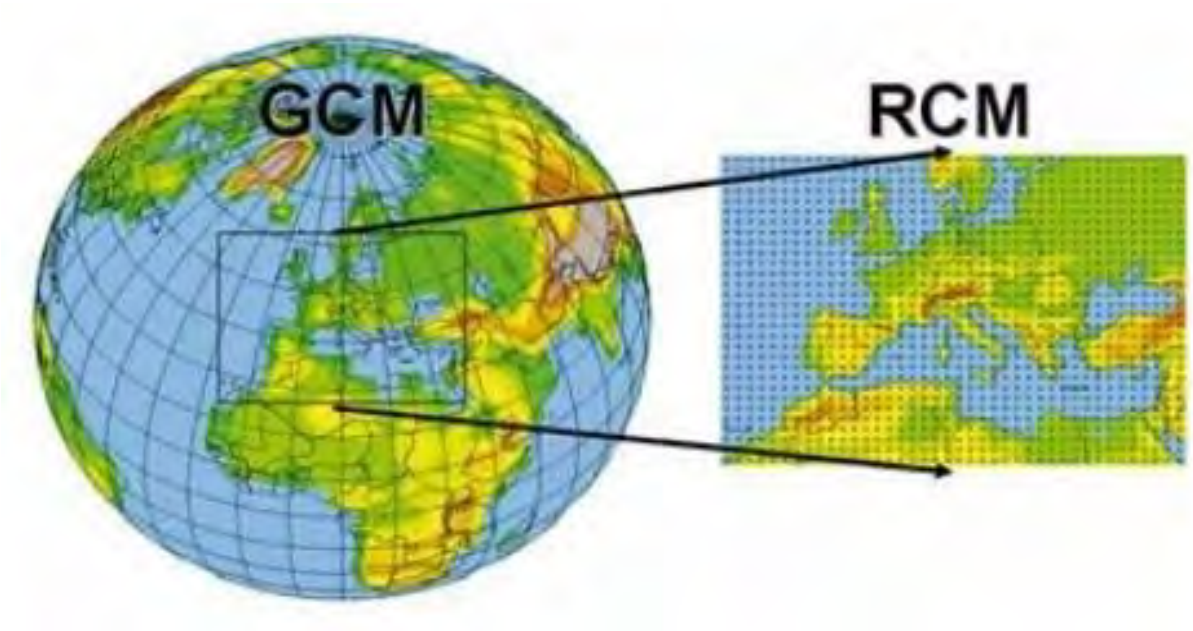

Figure 2.1: A dynamical downscaling technique, showing how regional scale information is obtained from a large scale global dataset[9].

2.5 Application of RCMs over West Africa

The ability of RCMs in reproducing the West African climatology and its variability have been established in many studies (e.g. Vizy and Cook, 2002; Afiesimama et al., 2006; Abiodun et al., 2008; Vigaud et al., 2009; Sylla et al. 2010). Abiodun et al. (2008) showed that RegCM3 simulates the inter-annual variability of WAM. Vigaud et al. (2009) showed the Weather Research and Forecasting (WRF) model simulates well the spatio-temporal variability of rainfall season. The study further revealed that variability in spatial and temporal characteristics of the atmospheric circulations (Saharan heat low and AEJ) and the relationship between AEJ dynamics and observed rainfall over West Africa. Moreover, our knowledge about the different interactions amongst the atmospheric features that induce precipitation over the region has improved by the use of RCMs (Jenkins et al., 2005; Moufouma-Okia and Rowell, 2010; Sylla et al., 2011; Browne and Sylla, 2012). De Elia and Laprise (2003) reported that RCMs simulate well the seasonal cycle of rainfall events. Furthermore, the nesting of RCM (WRF 3.5) reproduces spatial and temporal characteristics of extreme rainfall events as observation over Africa (Crétat et al., 2013). Also, Sylla et al. (2012) and Haensler et al. (2013) successfully applied RCM to reveal how topography can induce extreme rainfall in West Africa, showing RCMs' ability to capture and resolve complex topography. Hence,

[9] http://www.slideshare.net/ipsantika/statistical-downscaling-sdsm

the present study will build on the successful application of RCM over West Africa in studying the relationship between AEWs and extreme rainfall events in a warming climate.

2.6 Impact of Climate Change on Extreme Rainfall Events in West Africa

Several studies have projected that, due to the increase in GHG concentrations, the severity and frequency of extreme rainfall events may increase in West Africa. For example, Christiansen et al. (2007) showed that an increase in GHG concentration will result in about 20% increase in flooding due to an increase in intensity and frequency of extreme rainfall events in the next decade across the region. Also, Sylla et al. (2012) and Haensler et al. (2013) projects the intensity and frequency of extreme rainfall will increase due to increasing GHG concentrations , by the end of the 21st century, notably over the Guinea Highlands and Cameroun Mountains. Similarly, Vizy and Cook (2012) project an increase in the frequency of extreme rainfall days over West Africa between May and July. Moreover, Skinner and Diffenbaugh (2014) further revealed that north of the AEJ along the Sahel-Sahara border the strength of AEWs will increase due to global warming over West Africa. This is a crucial issue because the AEJ and AEW are part of the modulating factor that influences rainfall, which in turn might affect extreme rainfall characteristics in the region. Hence, there is a need to use RCMs to further examine how the increasing global warming and its impact on AEWs may alter the future characteristics of extreme rainfall over West Africa (Sylla et al. 2012; Skinner and Diffenbaugh, 2014). This study is in that direction.

2.7 Uncertainty in Extreme Rainfall Predictions over West Africa

There are uncertainties in projected future changes in extreme rainfall events over West Africa. For instance, while Kamiguchi et al. (2006), Vizy and Cook (2012) and Haensler et al. (2013) have shown projected increase in heavy precipitation from GCMs and RCMs future projections over West Africa, Seneviratne et al. (2012) and Sylla et al. (2012) showed conflicting results that heavy precipitation are projected to decrease over the region. Vizy and Cook (2012) also projected an increase in the number of extreme rainfall days over West Africa and the Sahel during May and July. Sylla et al. (2012) and Haensler et al. (2013) projected an increase in the intensity and frequency of extreme rainfall over the topography and high complex terrain areas (the Guinea Highlands and Cameroon Mountains). All the above studies agree that the intensity and frequency of extreme rainfall will increase over West Africa. On the other hand, Seneviratne et al. (2012) and IPCC, AR5 (2013) showed that there is uncertainty in the projected changes of heavy precipitation, low to medium confidence, at the end of the 21st century based on Coupled Model Intercomparison

Project 3 (CMIP-3) GCMs simulations over West Africa. Moreover, Sylla et al. (2012) turned up contrasting results in their investigation of the impact of increasing GHG concentrations on extreme rainfall events over West Africa using ECHAM5 and RegCM3. While ECHAM5 projected wetter conditions over West Africa (especially, the Sahel and Gulf of Guinea), RegCM3 projected a drying in the area under the same conditions. Hence, there is a need to use another set of GCMs and RCMs in investing these uncertainties. The present study will use ensemble simulation from a regional climate model forced with nine GCMs to address the uncertainty in the future projections of extreme rainfall events over West Africa.

In summary, findings from previous work have shown that there are three prominent methods for defining and identifying extreme rainfall events but in comparison with return period and threshold value methods, the percentile is a better method. Furthermore, the review found that the trend in extreme rainfall characteristics is increasing over West Africa and underlined the atmospheric conditions that influence the occurrence as shown in past studies. In addition, the study of extreme rainfall events over the region from climate models such as GCMs simulations and the different downscaling techniques (statistical and dynamical), as well as the use of RCMs were discussed. Moreover, past studies revealed that the impact of climate change may lead to an increase in extreme rainfall events over West Africa, however further studies over the region showed there are uncertainties on the future characteristics of extreme rainfall events from GCM and RCM projections. Hence, there is a need for further research. Therefore, it is expedient using ensembles of global and regional climate models to evaluate these characteristics in order to provide regional and local climate-change information on the future characteristics of extreme rainfall events over West Africa, before making a firm conclusion. The Coupled Model Intercomparison Project, Phase 5 (CMIP5) GCMs (Taylor et al., 2012) and the Coordinated Regional Climate Downscaling Experiment (CORDEX) models (Giorgi et al. 2009) provide the opportunity for such an evaluation, which is the approach used in the present study.

Chapter 3: Data and Methodology

This chapter describes the study domain, datasets and methods used in this study. The first part gives a brief description of the study area. The second part provides information about the data used. Finally, the last part describes the methods and approach used in analysing the data for this study.

3.1 Study Area

The study area for this research is West Africa, located at latitude 4-20^{o}N and longitude 16^{o}W and 20^{o}E. The West African domain can be divided into three climatic zones namely, the Guinea Coast (4-8°N), Savannah (8-12°N) and Sahel (12–20°N) (Omotosho and Abiodun, 2007, Abiodun et al., 2012a). Hence, the same climatic zone is used in the present study, as shown in Figure 3.1 below.

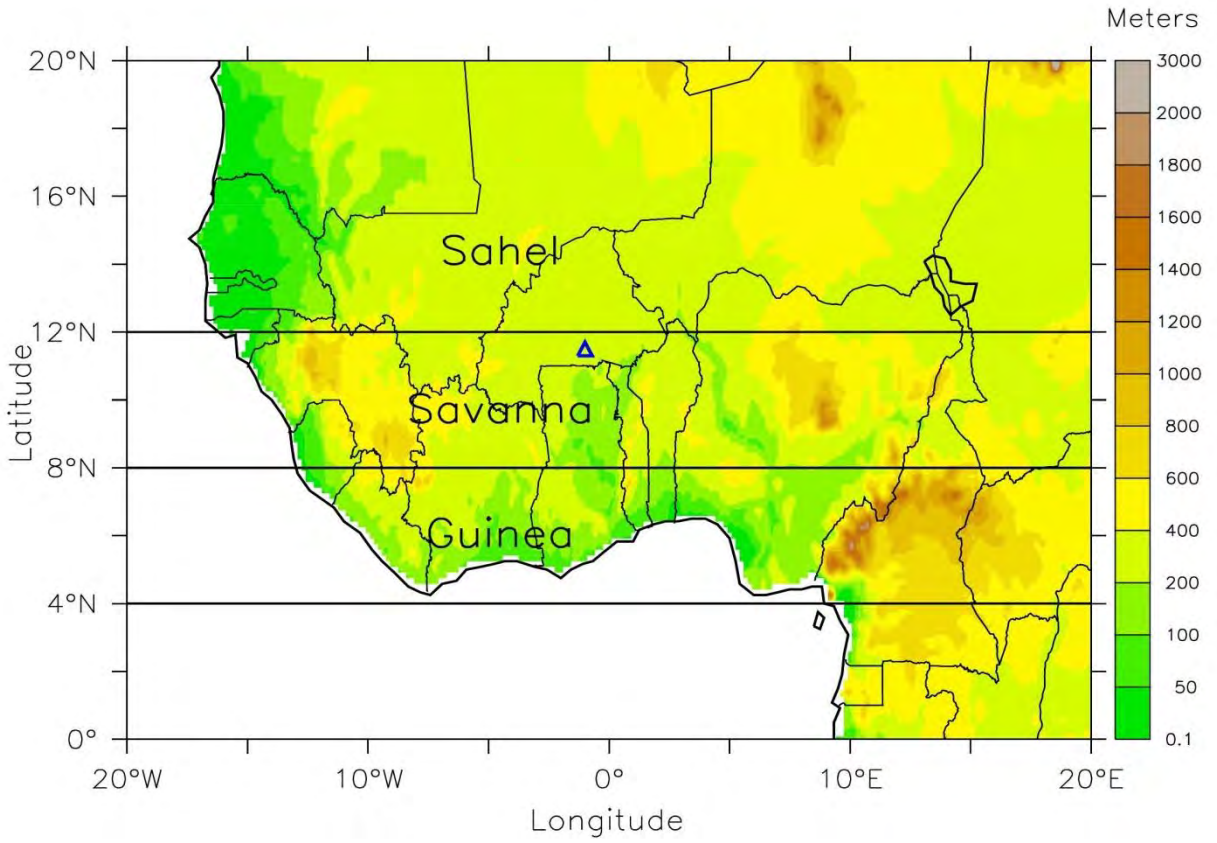

Figure 3.1: The study domain, showing the West African topography and ecological zones, designated as Guinea, Savannah and Sahel, respectively.

3.2 Data

Three different types of datasets (satellite, re-analysis, and model simulation) were analysed for the study. While the satellite dataset was used as observation data to validate the model simulations, the re-analysis data were used to provide boundary forcing for the regional climate-model simulations,

and to examine the capability of the model in simulating the characteristics of AEWs.

3.2.1 Satellite Data

Satellite-derived rainfall datasets were used as observation data because of the lack of high-quality station data over West Africa and the inaccessibility of the existing data available. Also, station data are often characterised by coarse resolution spatially and temporally, and are not evenly distributed in some regions. This constitutes a major challenge when evaluating RCMs simulation over West Africa (Nikulin et al*.,* 2012). However, the use of satellite measurements has been employed in solving the scarcity and inadequacy of data in the region. These types of datasets provide an alternative to station data (Williams et al., 2010, Abiodun et al., 2015).

Two satellite-derived rainfall datasets were used for the study. The first one is the Tropical Rainfall Measurement Mission (TRMM 3B-42, version 6, hereafter TRMM). TRMM is a merged microwave-infrared product that provides rainfall estimates based on the merged microwave infrared estimates, such as the TRMM microwave imager (TMI), the visible infrared scanner (VIRS) and the TRMM precipitation radar. It is computed at 3-hourly temporal and 0.25° x 0.25° spatial resolutions. A full description of the TRMM datasets is given by Huffman et al. (2007). For this study, we used TRMM daily rainfall values averaged at 3-hourly values and re-gridded from 0.25° x 0.25° to 0.44° x 0.44° for the period of 1998-2013. The second satellite dataset, the Global Precipitation Climatology Project (GPCP, version 1.1), is a gridded observation dataset. GPCP estimates rainfall at daily intervals and at a 1° x 1° spatial resolution using a combination of geosynchronous satellite infrared readings and low earth polar orbit satellite (Huffman et al., 2001). Like TRMM, we re-gridded GPCP rainfall data to a 0.44° x 0.44° grid resolution for the period 1998-2013.

The use of two observation datasets helps us address the differences and uncertainties in the observation data. However, some studies (i.e. Sylla et al., 2013) have shown that, in comparison with the TRMM dataset, the GPCP dataset gives closer values to rain gauge observation over West Africa. Hence, in the present study, GPCP is used as the reference observation dataset for calculating the rainfall biases in TRMM, reanalysis, and model simulations.

3.2.2 Re-analysis Dataset

For the re-analysis dataset, we used the European Centre for Medium-Range Weather Forecasts (ECMWF) ERA-Interim reanalysis (hereafter, ERAINT). The gridded products from reanalysis include three-hourly surface products and 6-hourly interval upper air field data covering the

troposphere and stratosphere at 1.5^{o} x 1.5^{o} spatial resolutions (Berrisford et al., 2009; Dee et al., 2011). ERAINT is produced via a data-assimilation scheme that provides prior information from the short-range forecast model, which updates available observation data every 12 hours (Dee et al.,2011). We used ERAINT daily rainfall and wind data at700hPa for the period of 1981-2005. ERAINT data were regridded from a 1.5° x 1.5° to a 0.44° x 0.44° grid resolution.

3.2.3 Simulated Data

Two sets of climate-simulation datasets were used for the study. The first set consists of global climate simulations from eight global climate models (GCMs), which are part of the Coupled Model Inter-comparison Project Phase 5 (CMIP5, Taylor et al., 2012). The descriptions of these GCMs are presented in Table (3.1). All the GCM datasets were re-gridded from their different native resolutions to a 0.44^{o} x 0.44^{o} grid resolution. The second set of climate simulations analysed for the study is from regional climate-model simulations that were forced with ERAINT and with the eight GCMs data. The regional climate simulation was obtained from the Swedish Meteorological and Hydrological Institute–Rossby Centre's regional atmospheric model (SMHI-RCA4, hereafter RCA4 [Samuelson et al., 2011]).

3.2.3.1 RCA4

The RCA model is the climate version of the operational model HIRLAM (Dieterich et al., 2013). The model was developed at the Rossby Centre of the Swedish Meteorological and Hydrological Institute, Sweden. Since its inception in 1997, the Rossby Centre has released four different versions of RCA, the latest being the RCA4 (Samuelson et al., 2011). The RCA4 is based on the numerical weather-prediction model HILRAM (Unden et al., 2002). It is a primitive-equation, hydrostatic model that uses a terrain following hybrid vertical coordinates with 40 grid points. The model has a spatial horizontal resolution of 0.44^{o} (50km) and two dynamical cores, a two time-level, semi-lagrangian and semi-implicit scheme with a six-order horizontal diffusion applied to the prognostic variables (Jones et al., 2004). The convective scheme used follows that of Kain and Fritsch (1990, 1993). The time used is 1200s. The radiation scheme is based on a HILRAM radiation scheme (Savi arvi, 1990; Sass et al., 1994). The turbulence vertical diffusion follows Cuxart et al. (2000). The cloud microphysics scheme derives from the work of Rasch and Kristjanson (1998). The land surface scheme follows that described by Samuelson et al. (2006).

All the RCA4 simulations used in the study were performed by the Coordinated Regional Climate Downscaling Experiment (CORDEX). CORDEX was formed by the World Climate Research

Program (WCRP), with two objectives and phases. The objectives are to evaluate the model's performance and design experiments to improve the methods of downscaling global climate projections to produce multi-model downscaled regional climate information for impact and adaption studies (Giorgi et al., 2009). The first phase of CORDEX involves forcing the RCMs with the latest ECMWF, ERA-Interim reanalysis, using a reference period of 1980-2010. The second phase is to downscale the RCMs forced with GCMs from the fifth Coupled Model Inter-Comparison Projects (CMIP5) for past climate (1951-2005) and future climate (2006-2100) under a carbon emission Representative Concentration Pathways 4.5 and 8.5 (RCP 4.5 & RCP 8.5) (Giorgi et al., 2009; Kalognomou et al., 2013). CORDEX RCM simulations used 50km (0.44° x 0.44°) horizontal grid resolutions for the dynamical downscaling. The simulation domain (about 25^{o}W-60^{o}E and 44^{o}S-42^{o}N [Nikulin et al., 2012]) is much wider than our study domain (West Africa; 20^{o}W-20^{o}E, 0^{o}-20^{o}N). This domain consists of the interior boundaries and does not include the lateral relaxation zones. It is large enough to fully capture the primary features controlling the annual cycle of the West African Monsoon (WAM) and to minimise lateral boundary conditions problem. The RCA simulations analysed for our study consist of past climate simulations (1971-2005) and future climate simulations (2031-2065) under the RCP4.5 and RCP8.5 scenarios. As part of CORDEX, the RCA4 past climate simulations were forced with ERAINT and GCMs data (1971-2005), while the RCA4 future climate simulations were forced with GCMs data (2031-2065).

Table 3.1: List of forcing GCMs used in forcing Regional Climate Model, RCA4

Modelling Centre	Institute ID	Model Name	Resolution
Canadian centre for climate modelling and analysis	CCCMA	CanESM2	2.8^o x 2.8^o
Centre National de Recherches Meteorolo-Giques /Centre Europeen de Recherche et Formation Avanceesencalcul scientifiqu	CNRM-CERFACS	CNRM-CM5	1.4^o x 1.4^o
European centre for medium-range weather forecast	ECMWF	EC-EARTH	1.5^o x 1.5^o
NOAA geophysical fluid dynamic laboratory	NOAA-GDFL	GFDL_ESM2M	2.5^o x 2.0^o
EC-EARTH consortium	EC-EARTH	ICHEC	1.25^o x 1.25^o
Atmosphere and Ocean Research Institute (University of Tokyo), National Institute for Environmental studies and Japan agency for Marine-Earth Science and Technology	MIROC	MIROC5	1.4^o x 1.4^o
UK Met Office Hadley centre	MOHC	HadGEM2-ES	1.9^o x 1.3^o
Max Planck institute for meteorology	MPI	MPI-ESM-LR	1.9^o x 1.9^o
Norwegian climate centre	NCC	NorESM1-M	2.5^o x 1.9^o

3.3 Methods

3.3.1 Identification of Extreme Rainfall Events

In this study, the threshold for an extreme rainfall event over a grid point is defined as the 95^{th} percentile (threshold) of the daily rainfall over the point. We use this definition because it allows for both spatial and inter-dataset comparisons, since the same part of the probability distribution of the datasets is sampled (Klein Tank et al., and Zwiers, 2009). For each dataset (GPCP, TRMM, ERAINT, RCA, and GCMs), the extreme rainfall threshold was calculated at each grip point over West Africa, using the daily rainfall (> 0.5 mm) in 12 months of the year. The extreme rainfall threshold was obtained for the past and future climates. Any day that the rainfall amount exceeds the threshold is considered an extreme rainfall day (or event). For easy comparison, the extreme rainfall threshold for past climate was used in identifying the extreme rainfall event for both past and future climates. A comparison of the simulated and observed spatial patterns of extreme rainfall

threshold in the past climate over West Africa was used to assess how well the models simulate the intensity of extreme events over the region, while the difference between the simulated threshold in the future and past climates (future-past) was used to quantify the projected future changes in the intensity of extreme events for the two scenarios. The projected changes in the number of rainfall days and the number of extreme rainfall events were also obtained.

3.3.2 Extraction of African Eastern Waves

To study the characteristics of AEWs, we applied a spectral band pass filter on the time series of the 700hPa meridional wind (V700) in the observed and simulated datasets. Several studies (De Felice et al. 1990; Diedhiou et al. 1998, 1999; Crétat et al. 2014) have demonstrated the suitability of this technique in identifying and studying wave structures. To extract the 3-5 days AEWs, we used the following 4-step procedure (obtained from Crétat et al, 2014):

- A 3-5 days spectral band pass filter was applied to the daily V700 time series from January 1st to December 31st of the years used in the study at 1^{o}W and 11.5^{o}N, but zero padding was used for all values out of the July-September (JAS) seasons. We used this point because the 11.5^{o}N latitude is located between the two observed tracks of 3–5 days AEWs, and the 1^{o}W corresponds to the centre of the Sahel.
- Then, the JAS season of each year was extracted from the 3-5 days filtered V700 time series, and concatenated as a single vector for each dataset.
- All days for which the values of the 3-5 days V700 time series are above the last 90^{th} percentile were selected. The corresponding values of the non-filtered 700 hPa wind and rainfall were averaged to capture when the southerly phase of the mean 3-5 days AEWs is centred at 1^{o}W and 11.5^{o}N at a reference time t_o. The same procedure was repeated for all days for which the values of the 3-5 days V700 time series are below the 10^{th} percentile to capture the atmospheric state during the northerly phase of the mean 3-5 days AEWs
- Next, composite anomalies are obtained by computing the difference between the averaged northerly and southerly phases of the 3-5 days AEWs. This was repeated for time t_o-1 day and time t_o+1 day.
- The composite of wind anomalies was plotted to study the structure of 3-5 days AEWs, while the composite rainfall anomalies was plotted to study the rainfall anomalies pattern associated with the wave. The characteristics of the waves studied include the latitudinal extent, wavelength, phase speed, and the maximum meridional wind speed. The location and strength of the corresponding African Easterly Jet were also studied.

To extract the 6-9 days AEWs, the above procedure was repeated but using a 6-9 days spectral band pass on the daily V700 time series from at 1^{o}W and 17.5^{o}N. The 17.5^{o}N is the track of the 6-9 days AEWs. To examine how well the model simulates the characteristics of AEWs, we compare the characteristics of the simulated AEWs with those obtained from ERAINT. To study the impact of climate change on the AEWs, we examine and compare the characteristics of the simulated AEWs in the past and future climate.

The spatial distribution of the AEWs variance (an indication of the wave strength) over West Africa was obtained by repeating the first two steps in the above procedure at each grid point over the study area and for each of the wave types (3-5 and 6–9 days AEWs). The capability of the models in replicating the observed spatial distribution of the variance was assessed, and the impact of climate change on the variance was studied by comparing the projected values in the future climate with the simulated values in the past climate.

3.3.3 Calculating the Percentage Contribution of African Eastern Waves to Extreme Rainfall Events

The percentage contribution of the AEWs (3-5 days and 6-9 days) to extreme rainfall events is obtained as the number (%) of extreme rainfall events that occur during the strongest (top 10%) northerly or southerly phases of the AEWs (3-5 days and 6-9 days, respectively) to the total number of extreme rainfall events over West Africa within the study period. This was calculated for both reanalysis and model simulations, and it was obtained for the past and future climate-simulation datasets.

Chapter 4: Model Evaluation

Before examining future climate-change projections from the RCA4, it is important to first assess the capability of the model in simulating the West African climate, because confidence in any model's projection depends on the ability of the model to reproduce past climate. This chapter evaluates how well the downscaling of the global climate datasets (ERAINT and GCMs) with RCA4 reproduces the West African climate. However, our evaluation focuses on the performance of the model in simulating the atmospheric parameters needed for the present study (i.e. rainfall, AEWs, and the interaction between AEWs and rainfall). In the evaluation, the simulated rainfall is compared with the GPCP, TRMM and ERAINT products, while the simulated AEW is compared with the ERAINT reanalysis. The RCA4 simulations evaluated here also provide the baseline for the climate-change projections presented in the next section.

4.1 Characteristics of West African Rainfall

Figure (4.1) presents the spatial distribution of the annual rainfall and the threshold of extreme rainfall (i.e. 95th percentile of daily rainfall) over West Africa (1971-2005) as given by GPCP, TRMM, ERAINT, and the RCA4 downscaling of ERAINT (hereafter, R_ERAINT). Similar results for the RCA4 downscaling of the GCMs (hereafter, R_CCMA, R_CNRM, R_GFDL, R_HADGEM, R_ICHEC, R_MIROC, R_MPI, and R_NCCN) are shown in Figure (4.2). For comparison purposes, the original results of the GCMs (i.e. CCMA, CNRM, RGFDL, HADGEM, ICHEC, MIROC, MPI, and NCCN, respectively) are displayed in Figure (4.3).

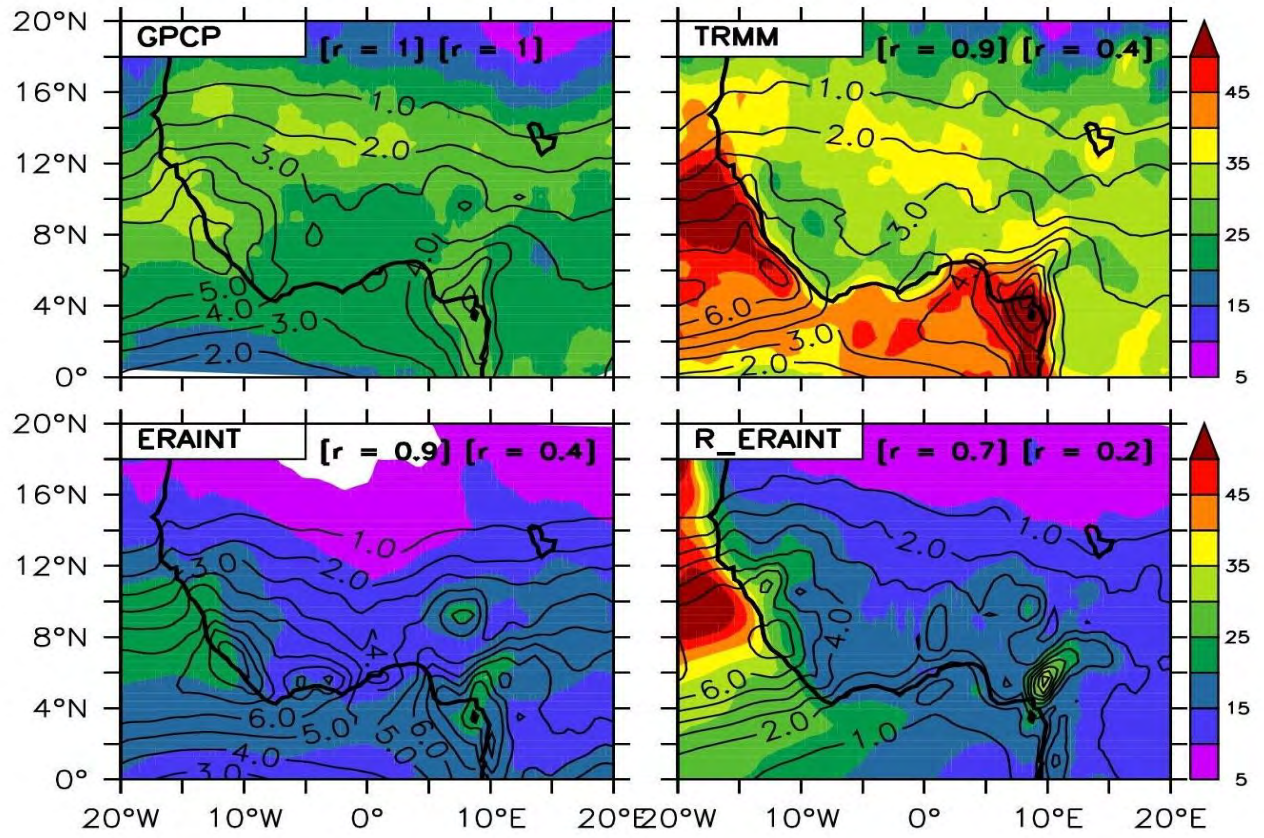

Figure 4.1: The spatial distribution of annual mean rainfall (contours, mm day^{-1}) and extreme rainfall thresholds (i.e. 95th percentile of daily rainfall, mm day^{-1}) as depicted by observations (GPCP and TRMM), reanalysis (ERAINT) and RCA4-dowscalling of ERAINT (R-ERAINT) over West Africa for the period 1998-2013 (GPCP and TRMM), 1981-2005 (ERAINT and R-ERAINT). The left and right r-values in each panel represent the correlations between the represent the correlations between the simulated and observed mean-annual rainfall, and between simulated and observed extreme rainfall thresholds, respectively.

Figure (4.1) shows that R_ERAINT gives a realistic simulation of annual rainfall over West Africa because the model reproduces all the essential features in the observation (TRMM and GPCP). For instance, the model captures the zonal-distribution in the rainfall pattern, replicates the meridional rainfall gradient between the Guinea and Sahel, and simulates the rainfall maxima over the high topography (i.e. Cameroon Mountains and Guinean Highlands) as in GPCP, TRMM, and ERAINT. In addition, the structure and magnitude of small-scale features in the observed rainfall patterns are well depicted in R_ERAINT and the correlation between R_ERAINT and GPCP rainfall pattern is high (r = 0.7). However, this correlation is smaller than the one between ERAINT and GPCP (r = 0.9), possibly because R_ERAINT fails to simulate the band of maximum rainfall over Cameroon and Congo and underestimates the rainfall over the Gulf of Guinea (i.e. South of 4^{o}N). While these two biases may be related to shortcomings in the convective parameterisation scheme in RCA4, the first may also be due to inadequate representation of land cover (over Cameroon and Congo) in the model. The biases could also be due to the difference in the period of analyses between simulation

(1981-2005) and the observation (GPCP: 1997-2013). Although none of the GCMs (Fig. 4.3; CCCMA, GFDL, HADGEM, MIROC and MPI) performs better than ERAINT (Fig. 4.1) in simulating the annual rainfall, the RCA4 downscaling of some GCMs (Fig. 4.2; R_CCCMA, R_GFDL, R_HADGEM, R_MIROC and R_MPI) produces better results than R_ERAINT. For instance, the rainfall pattern from these simulations has a higher correlation (r = 0.8) with GPCP than R_ERAINT has. Nevertheless, the correlation is still smaller than that of the forcing GCMs with GPCP, and the correlation of the RCA-simulations ensemble mean with GPCP (r = 0.7) is lower than that of GCM ensemble mean with GPCP (r = 0.8). Assessing the performance of the RCA4 simulations with the correlation results might be erroneous. For example, it can be concluded that the RCA4 downscaling does not improve on simulated rainfall fields from GCMs; however, a qualitative comparison of the GCMs and RCA4 simulations with the observations reveals that the downscaling does add value to the rainfall fields by simulating local-scale features that are in the observation but not in the GCMs results.

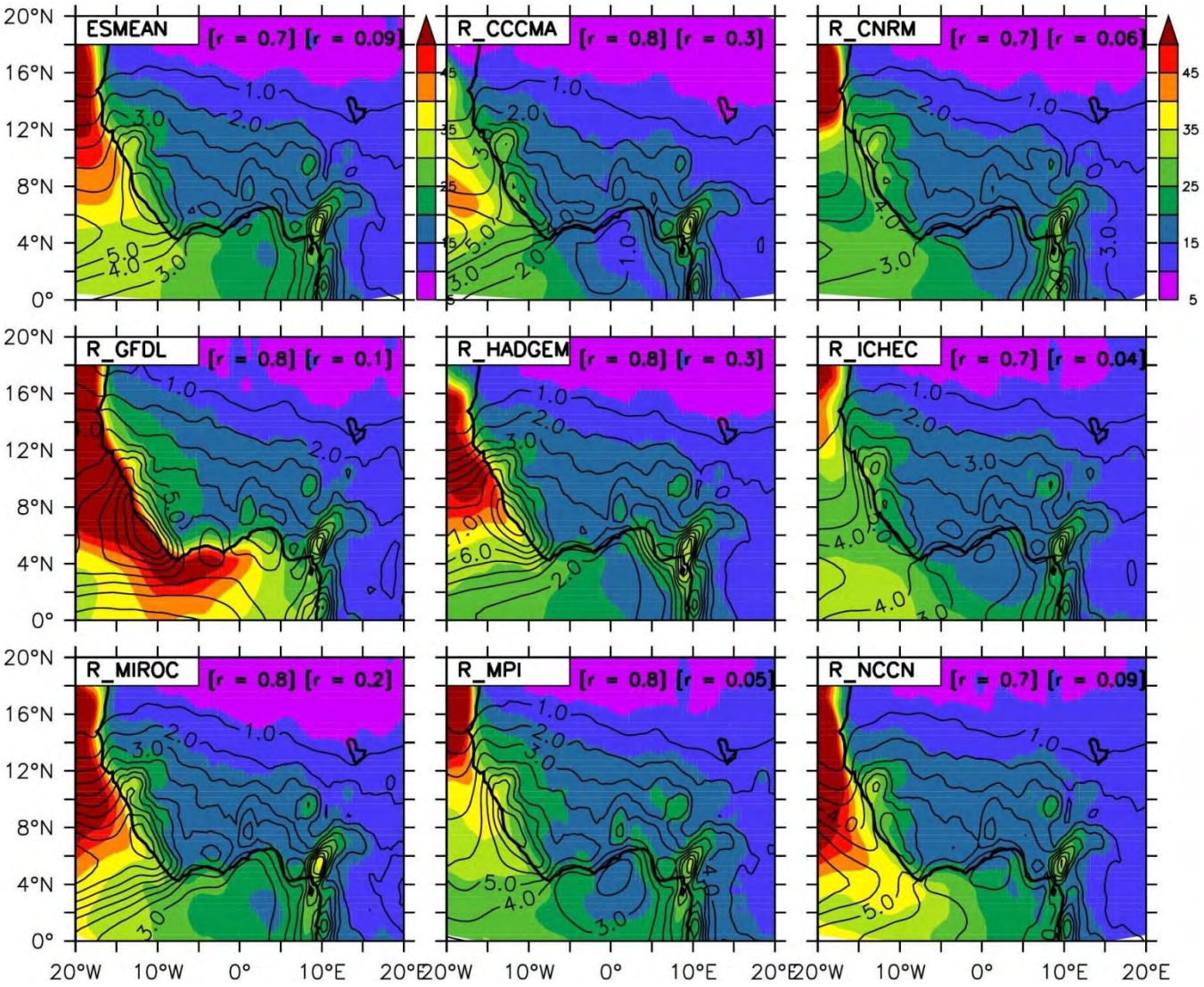

Figure 4.2: The spatial distribution of annual mean rainfall (contours, mm day^{-1}) and extreme rainfall thresholds (i.e. 95th percentile of daily rainfall, mm day^{-1}) obtained from RCA4-dowscaling of eight GCMs (R_CCMA, R_CNRM, R_GFDL, R_HADGEM, R_ICHEC, R_MIROC, R_MPI, and R_NCCN) over West Africa (1971-2005). The correlation between GPCP and mean rainfall pattern (left) and extreme rainfall threshold (right) in each panel is indicated in brackets at the top right-hand corner.

There are some common features between the spatial distributions of the extreme rainfall threshold from the observation datasets (GPCP and TRMM), especially over land. For instance, both indicate that the maximum threshold value is located within 11-16^{o}N (i.e. northern Savannah and southern Sahel). However, there are notable discrepancies between the two observation datasets, as evidenced by their weak correlation (r = 0.4). While GPCP observed a threshold maximum over the Guinean mountain of about 30 mm day^{-1}, the TRMM reports threshold minima of about 20 mm day^{-1} over the same mountain. In addition, the threshold values are generally higher in TRMM than in GPCP, especially over the ocean. Masking out the threshold over the ocean increases the correlation (r = 0.6) between the two datasets. Hence, the correlation between the two datasets over the ocean is

poor. This may be related to differences in how the two satellite products handle cloudiness in estimating the rainfall amount (Jain et al., 2011). The threshold patterns from ERAINT and R_ERAINT also show poor correlations with that of GPCP (i.e. r = 0.4 and 0.2, respectively). They both underestimate the threshold value over land and fail to reproduce the band of maximum threshold within 11–16^{o}N as in GPCP and TRMM. Similarly, all the GCMs (except MIROC) have a weak correlation with GPCP; r ranges from 0.3-0.4. MIROC has the highest correlation (r = 0.6) because it reproduces the band of maximum threshold and simulates the threshold maxima over the Guinean Mountain. The RCA4 downscaling of the GCMs simulation does not improve simulated threshold pattern. Instead, in most cases, it makes the results deviate more from those of GPCP. However, all the RCA simulations produce threshold maxima over the Atlantic Ocean (off the West African Coast), in agreement with the high resolution TRMM observation (though with less magnitude). Yet the maxima are absent in the low-resolution GPCP observation, and not in the ERAINT and GCMs results. Therefore, the discrepancy between the two observation datasets regarding the spatial distribution of extreme rainfall threshold patterns makes it difficult to evaluate the capability of RCA4 in simulating this parameter.

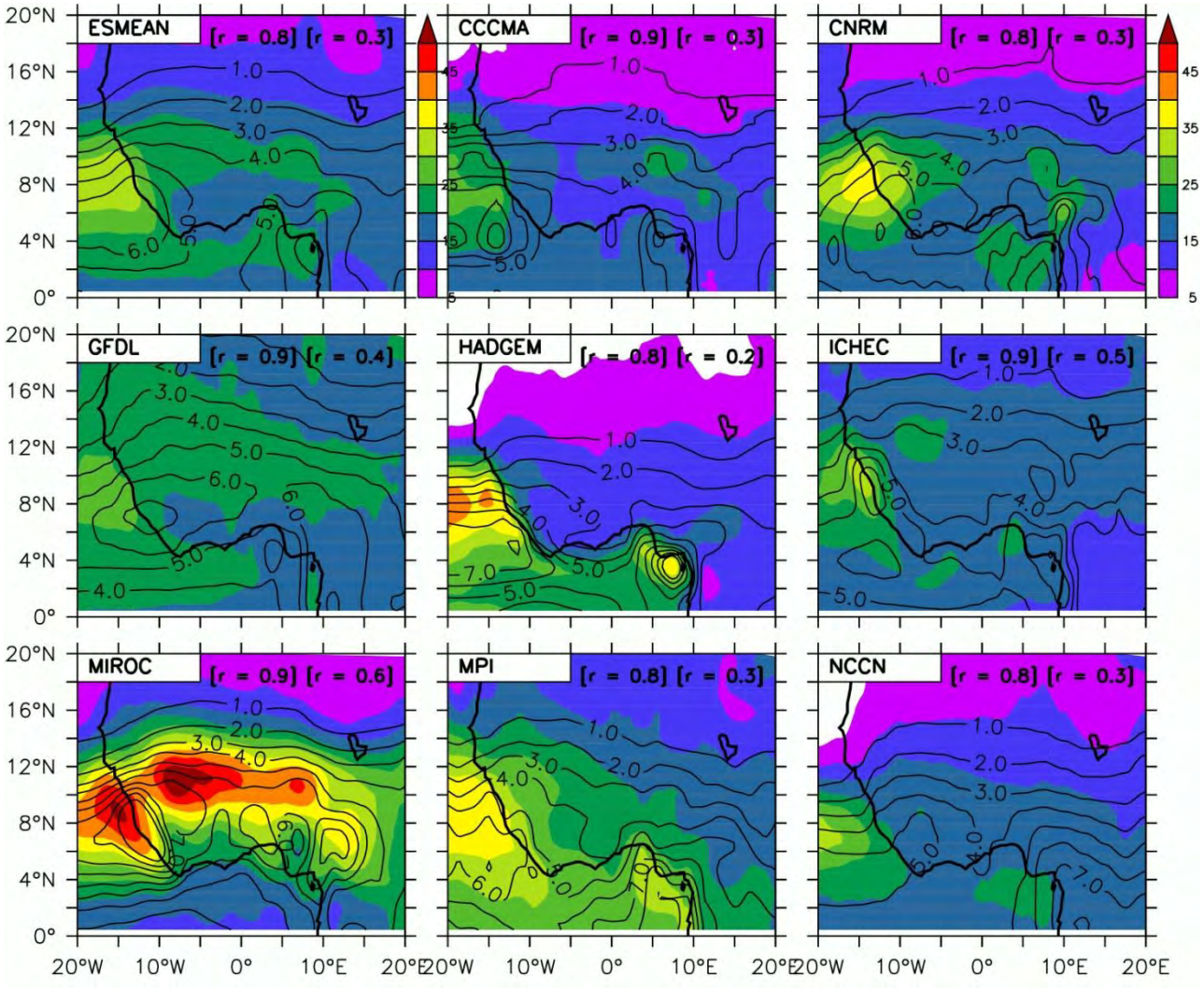

Figure 4.3: Same as figure 4.2, but for the GCMs (CCMA, CNRM, GFDL, HADGEM, ICHEC, MIROC, MPI, and NCCN).

4.2 The Structure of AEWs and Rainfall Pattern

R_ERAINT reproduces the structure of AEWs (3-5 and 6-9 days), and the link between AEW and rainfall, as in ERAINT (Figure 4.4; Tables 2 and 3 below). In ERAINT, the 3-5 days AEWs (depicted by the 700 hPa wind anomalies) extend from about 4° S to 25°N (i.e. the latitudinal extent is about 29°) with a wavelength of about 3,330 km and a phase speed of about 9.6 m s^{-1}. The AEJ that feeds the wave is located at 15°N with a maximum speed of 10.8 m s^{-1}. The associated rainfall pattern features positive rainfall anomalies in the northerly wind and ahead of the trough, and shows negative rainfall anomalies in the southerly wind anomalies and behind the trough. This link between the AEW structure and rainfall anomalies is consistent with previous observational and modelling studies (i.e. Diedhiou et al. 1999; Cifelli et al. 2010; Barthe et al. 2010; Crétat et al. 2014). The downscaling of ERAINT with RCA4 (R_ERAINT) retains the structure of the 3-5 days AEW wave, the location of the AEJ, and the associated rainfall pattern, although there are few biases: the wind anomalies, rainfall anomalies, and AEJ speed (8 m s^{-1}) are weaker in R_ERAINT.

Furthermore, in contrast with ERAINT, R_ERAINT simulates another AEJ south of West Africa (at 1^{o}N; speed = 9.2 m s^{-1}). The characteristics of 3-5 days AEWs, the associated AEJ, and wind anomalies in the RCA-downscaling of the GCMs are similar to that of R_ERANT in some cases, but differ in other cases (Table 4.1; detail results are in Appendix A). Only R_HADGEM produces double AEJ as in R_ERAINT; other simulations produce a single AEJ as in ERAINT. Among the simulations, R_HADGEM produces the weakest AEJ (7.1 m s^{-1}) over the sub-continent, and the location of the simulated single AEJ has the southernmost position (5^{o}N) in R_CCCMA. The simulated 3-5 days AEW has the narrowest latitudinal extent (18^{o}) in R_HADGEM, the shortest wavelength (2,222 km) in R_HADGEM and R_NCCN, the slowest phase speed (6.4 m s^{-1}) in R_GFDL and R_NCCN, and the fastest phase speed (12.8 m s^{-1}) in R_CCCMA. The associated wind anomalies are lowest in R_HADGEM and highest in R_CNRM, while the corresponding rainfall anomalies are strongest in R_CNRM and weakest in R_HADGEM and R_MPI.

R_ERAINT also captures the differences between the structure of 6-9 days and 3-5 days AEWs as in ERAINT, but with some notable biases. In ERAINT, the 6-9 days AEW is characterised by wider latitudinal extent (30^{o}), longer wavelength (4,440.0 km), and lower phase speed (about 7.7 m s^{-1}) than that of 3-5 days AEWs, but the location and speed of the AEJ that produces both waves remain the same (Table 4.2; see detailed results in Appendix A). The spatial distribution of the rainfall anomalies (with respect to the wind anomalies) are also the same as for the 3-5 days AEWs, except that the rainfall anomalies are lower and the wind anomalies are also lower. All these differences are well captured in R_ERAINT, except that ERAINT associated a strong AEJ (8.0 m s^{-1}) with the 6-9 days AEWs.

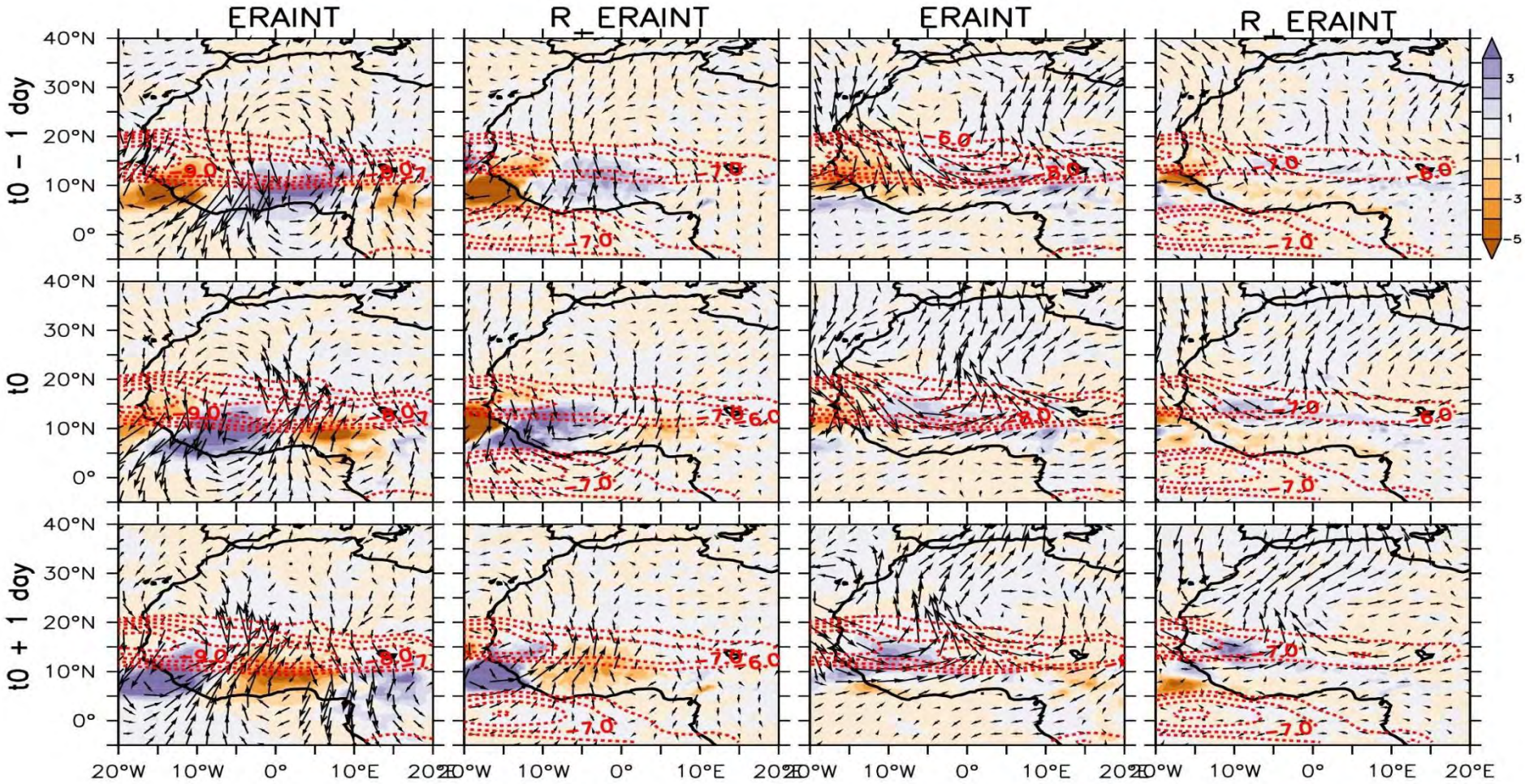

Figure 4.4: Composite anomalies for 3 – 5 days (two left-most columns) and 6 – 9 days (two right-most columns) African Easterly Waves (AEWs) from t_o – 1 to t_o + 1 days over West Africa as shown by reanalysis (ERAINT) and simulated by RCA4 forced with ERAINT (R_ERAINT) for the period 1981-2005. Vectors are 700 hPa wind anomalies (m s^{-1}). Rainfall anomalies (mm day^{-1}) are shaded. The contour (dashed red line) indicates the position of the African Easterly Jet (AEJ).

Table 4.1: The characteristics of 3-5 days AEWs and the associated AEJ, wind anomalies, and rainfall anomalies in the past climate (1971-2005; Historical), as depicted ERAINT and RCA4 forced with ERAINT and GCMs. The projected future changes (2031-2065) under RCP4.5 and RCP8.5 scenarios (ΔRCP4.5 and ΔRCP8.5) are indicated (Detailed figures are in Appendix A).

	ERAINT	R_ERAINT	R_CCCMA	R_CNRM	R_GFDL	R_HADGEM	R_ICHEC	R_MIROC	R_MPI	R_NCCN	ENSM
Latitudinal Extent (^{o})											
Historical	29.0	26.0	26.0	26.0	26.0	18.0	26.0	26.0	26.0	26.0	25.0
ΔRCP4.5	-	-	0.0	0.0	-4.0	0.0	0.0	0.0	0.0	0.0	-0.5
ΔRCP8.5	-	-	0.0	0.0	-4.0	0.0	0.0	0.0	0.0	0.0	-0.5
Wavelength (km)											
Historical	3330.0	3330.0	3330.0	3330.0	3330.0	2220.0	3330.0	3330.0	3330.0	2220.0	3052.5
ΔRCP4.5	-	-	0.0	0.0	0.0	0.0	0.0	0.0	0.0	0.0	0.0
ΔRCP8.5	-	-	0.0	0.0	0.0	0.0	0.0	0.0	0.0	0.0	0.0
Phase Speed (m s^{-1})											
Historical	9.6	9.6	12.8	9.6	6.4	9.6	9.6	9.6	9.6	6.4	9.2
ΔRCP4.5	-	-	0.0	0.0	0.0	0.0	0.0	0.0	0.0	0.0	0.0
ΔRCP8.5	-	-	0.0	0.0	0.0	0.0	0.0	0.0	0.0	0.0	0.0
Wind Anomalies (m s^{-1})											
Historical	4.3	2.3	2.6	5.3	2.2	1.6	2.9	2.8	2.9	3.2	2.9
ΔRCP4.5	-	-	-0.2	-0.6	1.5	0.0	0.2	0.7	1.6	-0.3	0.4
ΔRCP8.5	-	-	-0.1	-0.4	1.6	-0.2	0.0	0.8	1.2	0.2	0.4
Rain Anomalies (mm day^{-1})											
Historical	9.5	10.1	4.8	14.5	7.9	4.0	7.5	8.3	2.4	7.5	7.1
ΔRCP4.5	-	-	-1.6	-0.6	4.0	2.4	-0.1	0.9	8.5	0.1	1.7
ΔRCP8.5	-	-	-1.0	1.1	8.0	0.0	-0.1	1.5	8.3	1.8	2.5
AEJ location											
Historical (^{o}N)	15.0	15.0	5.0	15.0	10.0	10.0	15.0	15.0	15.0	15.0	12.5
ΔRCP4.5	-	-	0.0	0.0	5.0	0.0	0.0	0.0	0.0	0.0	0.6
ΔRCP8.5	-	-	0.0	0.0	5.0	0.0	0.0	0.0	0.0	0.0	0.6
AEJ Speed (m s^{-1})											
Historical	10.8	9.2	9.2	10.0	9.4	7.1	8.5	8.9	8.8	9.8	9.0
ΔRCP4.5	-	-	0.0	-0.5	0.8	-0.2	0.3	0.4	0.9	0.1	0.2
ΔRCP8.5	-	-	0.1	0.0	0.7	-0.1	0.6	0.0	0.8	0.2	0.3

Table 4.2: Same as Table (4.1) but for 6-9 days AEWs

	ERAINT	R_ERAINT	R_CCCMA	R_CNRM	R_GFDL	R_HADGEM	R_ICHEC	R_MIROC	R_MPI	R_NCCN	ENSM
Latitudinal Extent (^{o})											
Historical	30.0	30.0	30.0	30.0	30.0	25.0	25.0	30.0	15.0	20.0	25.6
ΔRCP4.5	-	-	0.0	0.0	0.0	0.0	0.0	0.0	0.0	0.0	0.0
ΔRCP8.5	-	-	0.0	0.0	0.0	0.0	0.0	0.0	0.0	0.0	0.0
Wavelength (km)											
Historical	4884.0	4440.0	4440.0	4440.0	4218.0	4440.0	3552.0	4440.0	3774.0	3774.0	4134.8
ΔRCP4.5	-	-	0.0	0.0	0.0	0.0	0.0	0.0	0.0	0.0	0.0
ΔRCP8.5	-	-	0.0	0.0	0.0	0.0	0.0	0.0	0.0	0.0	0.0
Phase Speed (m s^{-1})											
Historical	7.7	7.7	7.7	7.7	6.4	6.4	6.4	6.4	6.4	6.4	6.7
ΔRCP4.5	-	-	0.0	0.0	0.0	0.0	0.0	0.0	0.0	0.0	0.0
ΔRCP8.5	-	-	0.0	0.0	0.0	0.0	0.0	0.0	0.0	0.0	0.0
Wind Anomalies (m s^{-1})											
Historical	2.9	1.8	2.8	2.7	3.2	2.1	2.8	2.9	2.8	3.6	2.9
ΔRCP4.5	-	-	-0.4	0.1	1.6	0.0	0.6	1.1	0.2	-0.6	0.3
ΔRCP8.5	-	-	0.3	0.2	0.5	-0.2	0.1	-0.2	-0.2	-0.4	0.0
Rain Anomalies (mm day^{-1})											
Historical	3.7	5.9	4.5	7.1	16.0	5.0	7.2	11.7	3.3	11.0	8.2
ΔRCP4.5	-	-	-0.4	-1.0	4.9	0.0	1.8	2.9	4.6	-1.5	1.4
ΔRCP8.5	-	-	1.1	2.2	-0.5	1.0	2.9	0.4	-0.5	-1.7	0.6
AEJ location											
Historical (^{o}N)	15.0	15.0	5.0	15.0	10.0	10.0	15.0	15.0	15.0	15.0	12.5
ΔRCP4.5	-	-	0.0	0.0	0.0	0.0	0.0	0.0	0.0	0.0	0.0
ΔRCP8.5	-	-	0.0	0.0	0.0	0.0	0.0	0.0	0.0	0.0	0.0
AEJ Speed (m s^{-1})											
Historical	10.5	9.5	8.8	9.9	9.4	6.5	8.2	8.5	8.6	9.6	8.7
ΔRCP4.5	-	-	0.2	-0.3	0.7	0.2	0.5	0.4	0.7	0.4	0.3
ΔRCP8.5	-	-	-0.1	-0.1	-0.3	0.1	0.3	-0.4	0.0	-0.1	-0.1

4.3 Contribution of AEWs to Extreme Rainfall Events

The spatial distributions of AEWs variance in ERAINT and R_ERAINT are the same, but the values are smaller in R_ERAINT (Fig 4.5). This implies that the strength of AEWs is weaker in R_ERAINT. In ERAINT, the variance increases from east to west (i.e. 2.0 m s^{-1} → 3.5 m s^{-1} for 3-5 days AEW and 1.0 m s^{-1} → 1.5 m s^{-1} for 6-9 days AEW), but in R_ERAINT, the gradient is weaker (i.e. 0.5 → 1.5 m s^{-1} for 3-5 days AEW and 0.4 m s^{-1} → 0.5 m s^{-1} for 6-9 days AEW). This zonal gradient suggests that, once AEJ triggers AEWs in the east, the waves will generally amplify as they traverse West Africa, at the expense of the jet that fuels them (Hsieh and Cook, 2005). This amplification is weaker in R_ERAINT, possibly because of boundary-condition errors or the weaker AEJ in R_ERAINT. However, the weaker variance in R_ERAINT is consistent with the weaker wind and rainfall anomalies seen in Fig (4.4). Nevertheless, the spatial distribution and magnitude of the AEWs variance simulated by RCA depend on the GCM that provide the boundary forcing (Figs. 4.6 and 4.7). While all the simulations produce the zonal gradient in the AEWs variance, the magnitude of the variance of the AEWs differs in the simulations. For 3-5 days AEWs, the variance is highest in R_CNRM (1.0 m s^{-1} → 3.5 m s^{-1}) and lowest in R_HADGEM (1.0 m s^{-1} → 3.5 m s^{-1}) (Fig. 4.6), while for 6-9 days AEWs, the variance is highest in R_GFDL (1.0 m s^{-1} → 3.0 m s^{-1}) and lowest in R_CNRM (0.5 m s^{-1} →1.0 m s^{-1}) (Fig. 4.7). Nevertheless, the RCA4 ensemble mean produces the AEWs variances that are comparable in patterns and in magnitudes with ERAINT results.

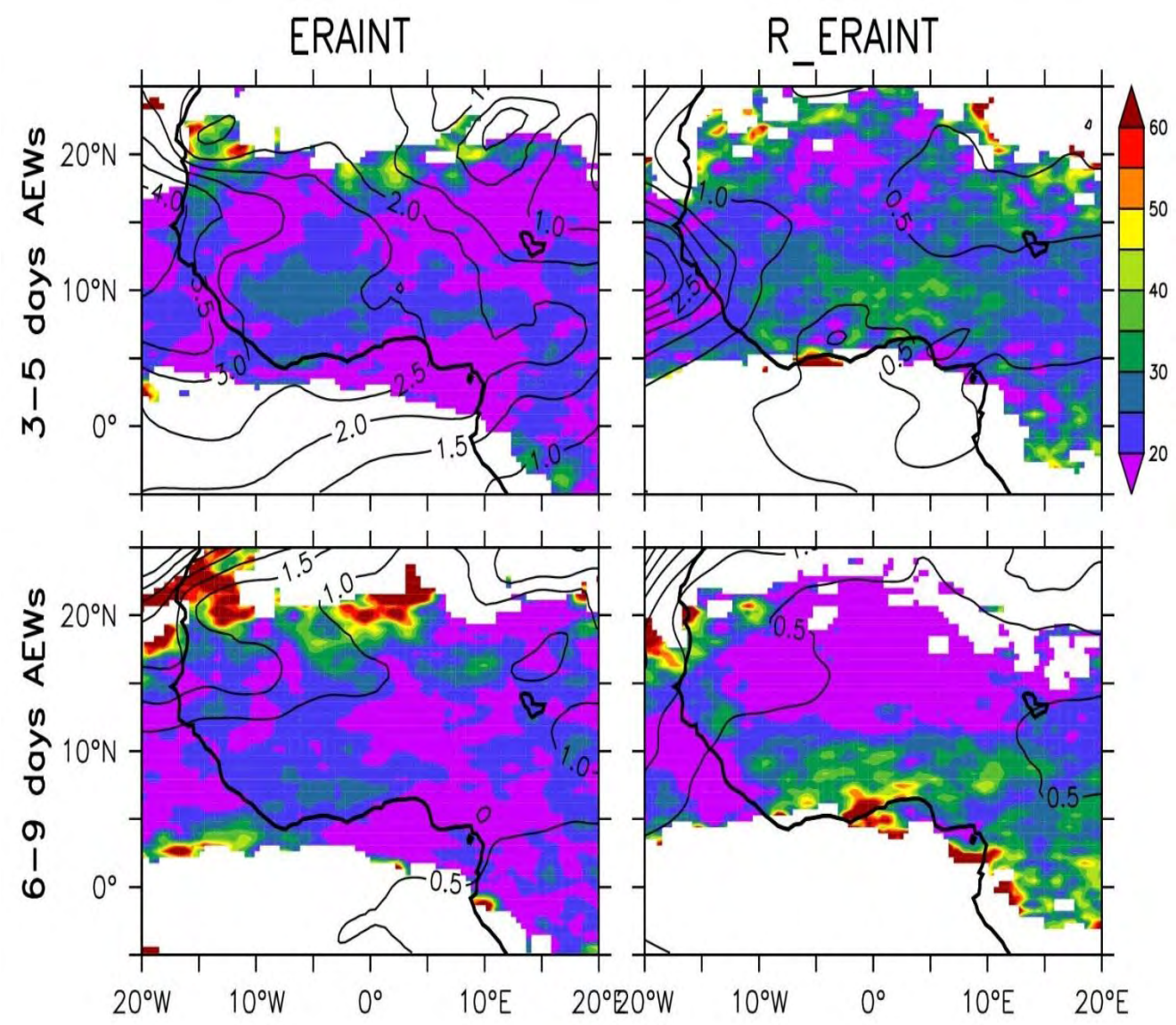

Figure 4.5: The spatial variance of AEWs (3–5 days and 6–9 days; contour, m/s) and the percentage contribution (%) of the waves to occurrence of extreme rainfall events over West Africa (1981–2005), as produced by ERAINT and R_ERAINT.

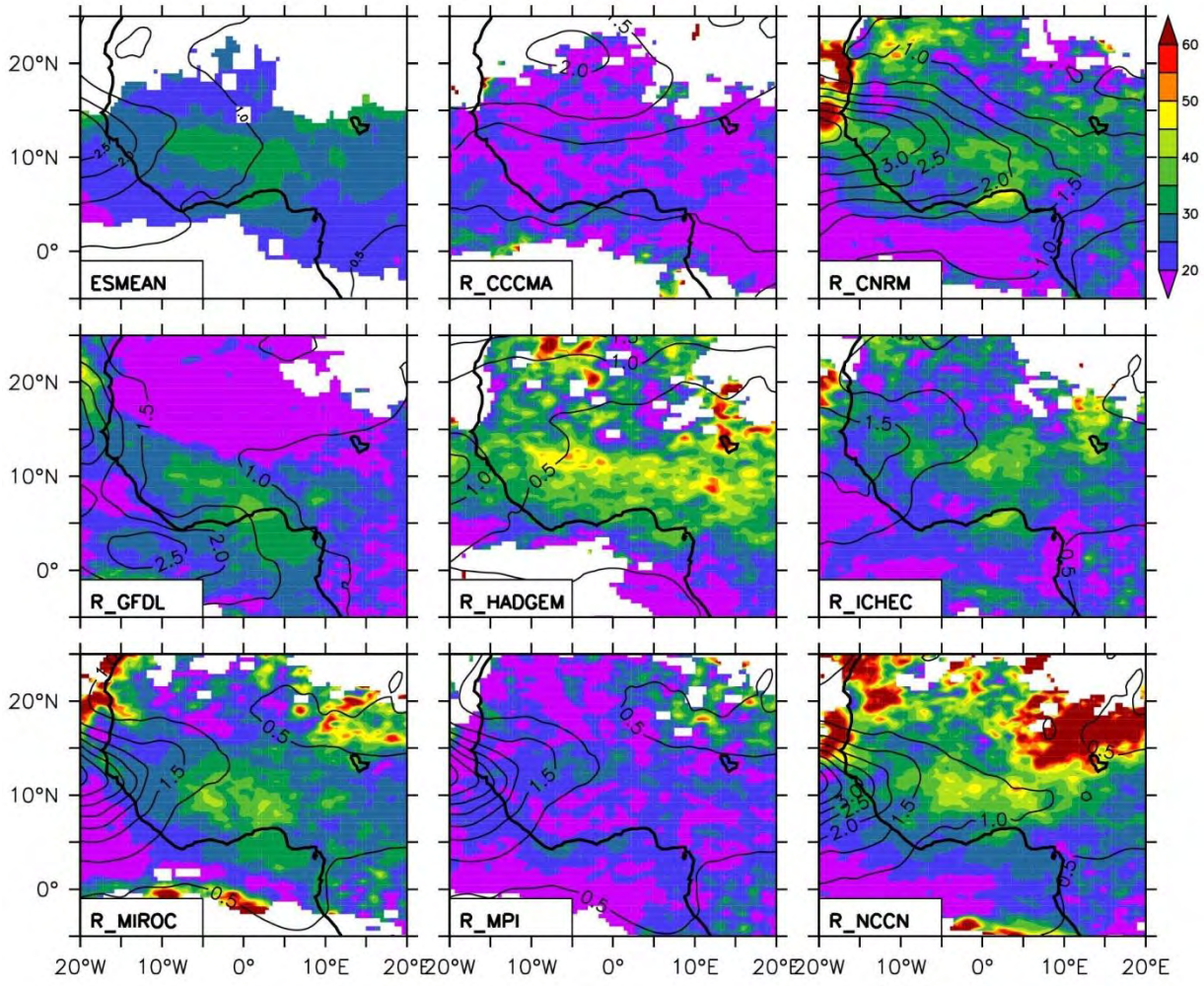

Figure 4.6: The spatial variance of 3–5 days AEWs (contour, m/s) and the percentage contribution (%) of the waves to occurrence of extreme rainfall events over West Africa (1971-2005) as simulated by RCA4 forced with different GCMs.

ERAINT shows that AEWs contribute to the occurrence of extreme rainfall events over West Africa. However, the percentage of the contribution varies (i.e. 20-60%) over the sub-continent, and patterns are similar for both 3-5 days and 6-9 days AEWs (Figs. 4.6 and 4.7). R_ERAINT clearly reproduces these characteristics, except that it attributes more percentage contribution south of 15^{o}N and less north of 15^{o}N which is consistent with the findings of Crétat et al. (2014). In both ERAINT and R_ERAINT, there is no discernible link between AEWs and the percentage contribution to extreme rainfall events, because the region of maximum percentage contribution is not confined to the areas of maximum AEWs variance and vice versa. This, of course, does not mean that the strength of AEWs is not important in the occurrence of extreme events. Several studies have established the importance of AEWs to intense rainfall. However, the results in this study reveal that AEWs are not the only determinant of extreme rainfall events. Other factors (i.e. moisture and large CAPE) are also important (Omotosho and Abiodun, 2007). The spatial

distribution of the percentage contribution remains fairly the same as RCA4 with the different GCMs forcing, although magnitude is more pronounced in R_NCCN and R_HADGEM than in any other simulation (Fig. 4.6). However, the RCA4 ensemble mean reproduces the spatial pattern of the percentage contribution as in ERAINT and R_ERAINT, especially south of 20°N.

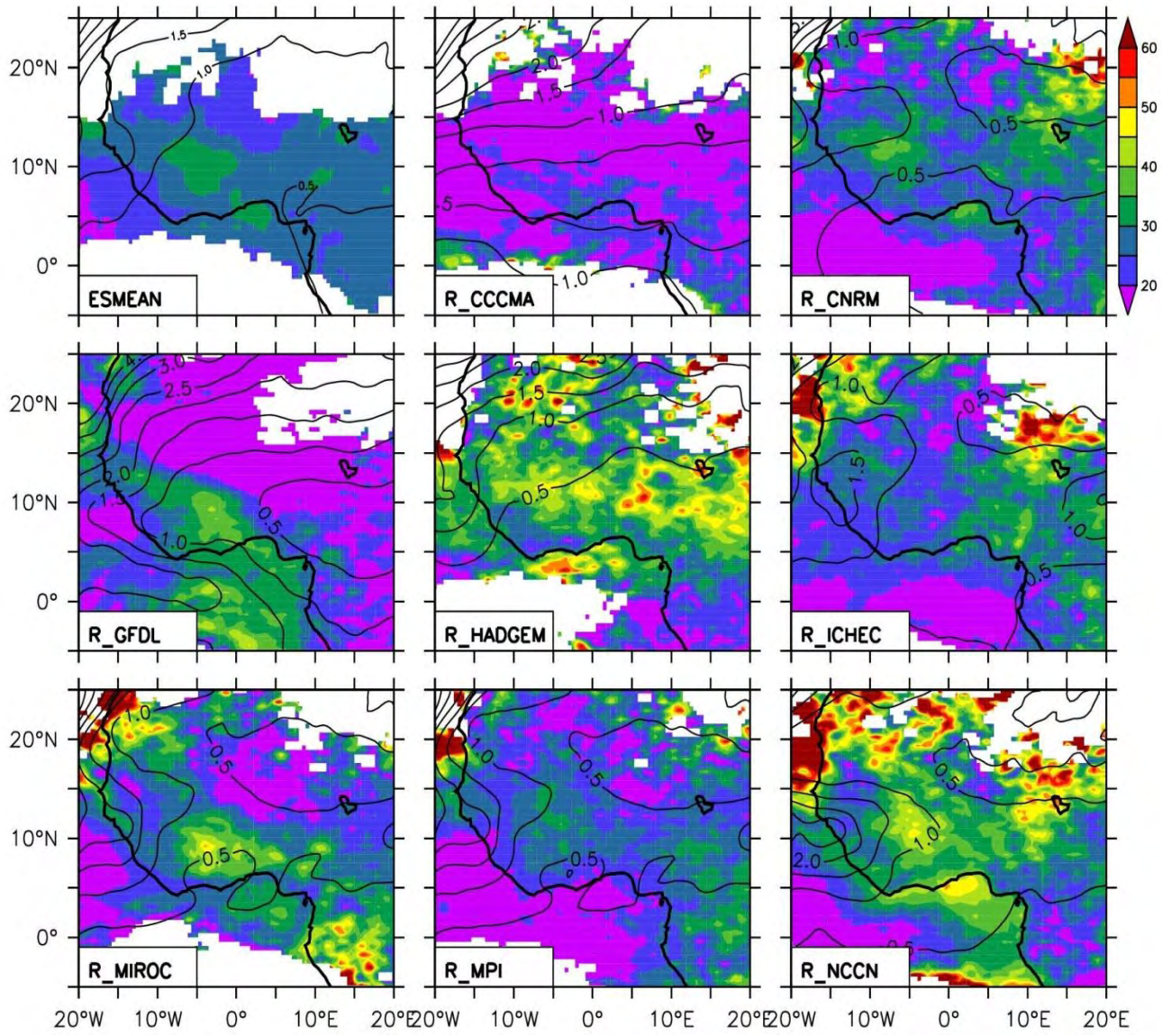

Figure 4.7: Same as figure (7), but for 6–9 days AEWs.

Chapter 5: Projected Changes in Rainfall and African Easterly Waves over West Africa

In this section, we discuss the projected changes in the West African climate in the mid-century (2035-2065) under the RCP4.5 and RCP8.5 scenarios. The projections are from RCA4 simulations forced with eight GCMs, and our discussion focuses on changes in annual rainfall, the characteristics of AEWs, and the contribution of AEWs to extreme rainfall events. The future changes are calculated with reference to past climate (1971-2005)—that is, future minus past. And, for easy comparison, the extreme rainfall threshold for the past climate is used for identifying the future extreme event.

5.1 Annual Rainfall and Extreme Rainfall Events

Figures 5.1 and 5.2 present the projected changes in annual rainfall and extreme rainfall intensity (i.e. threshold) for the RCP4.5 and RCP8.5 scenarios. For both scenarios, the RCA-ensemble mean projects an increase in annual rainfall over the region, but the magnitude of increase is generally higher for the RCP8.5 scenario than for the RCP4.5 scenario, especially over the Savannah and Sahel zones. The maximum increase over the sub-continent occurs along the Guinean coast (about 0.6 mm day^{-1}). The increase may be attributed to the enhanced evaporation of moisture from the ocean following greenhouse-gas (GHG) induced warming, because with warming, the atmosphere will have a higher capability for moisture. Hence, it will evaporate more over the ocean and transport more moisture inland to produce more rainfall over the sub-continent. However, there are discrepancies among the simulations regarding the signs of the rainfall changes. While some simulations project increased rainfall along the coast and decreased rainfall inland, some project the opposite pattern. Both cases (maximum increase and maximum decrease of rainfall over the coast) are plausible under the warning. Following the increased atmospheric moisture in the warmer climate, it is logical that the highest increase in rainfall would occur along the coast. This is so because, once the moisture is released as rain falls along the coast, the atmosphere would depend on the evaporation of soil moisture to meet the additional demand for moisture imposed by the warming to produce rainfall further inland, and the soil moisture may not be sufficient to meet the demand. On the other hand, this decrease of rainfall along the coast may be attributed to a stronger subsidence motion (from the downward arm of Hadley circulation) over the Guinean coast. Several studies (e.g. Lu et al. 2007; Johanson and Fu, 2009; Kang and Lu, 2012) have projected a strong Hadley cell and a northward expansion of the cell with global warming. The maximum impact of

the subsidence (decreased convection and rainfall) will be along the coast. However, the majority of simulations project increased rainfall over most parts of West Africa.

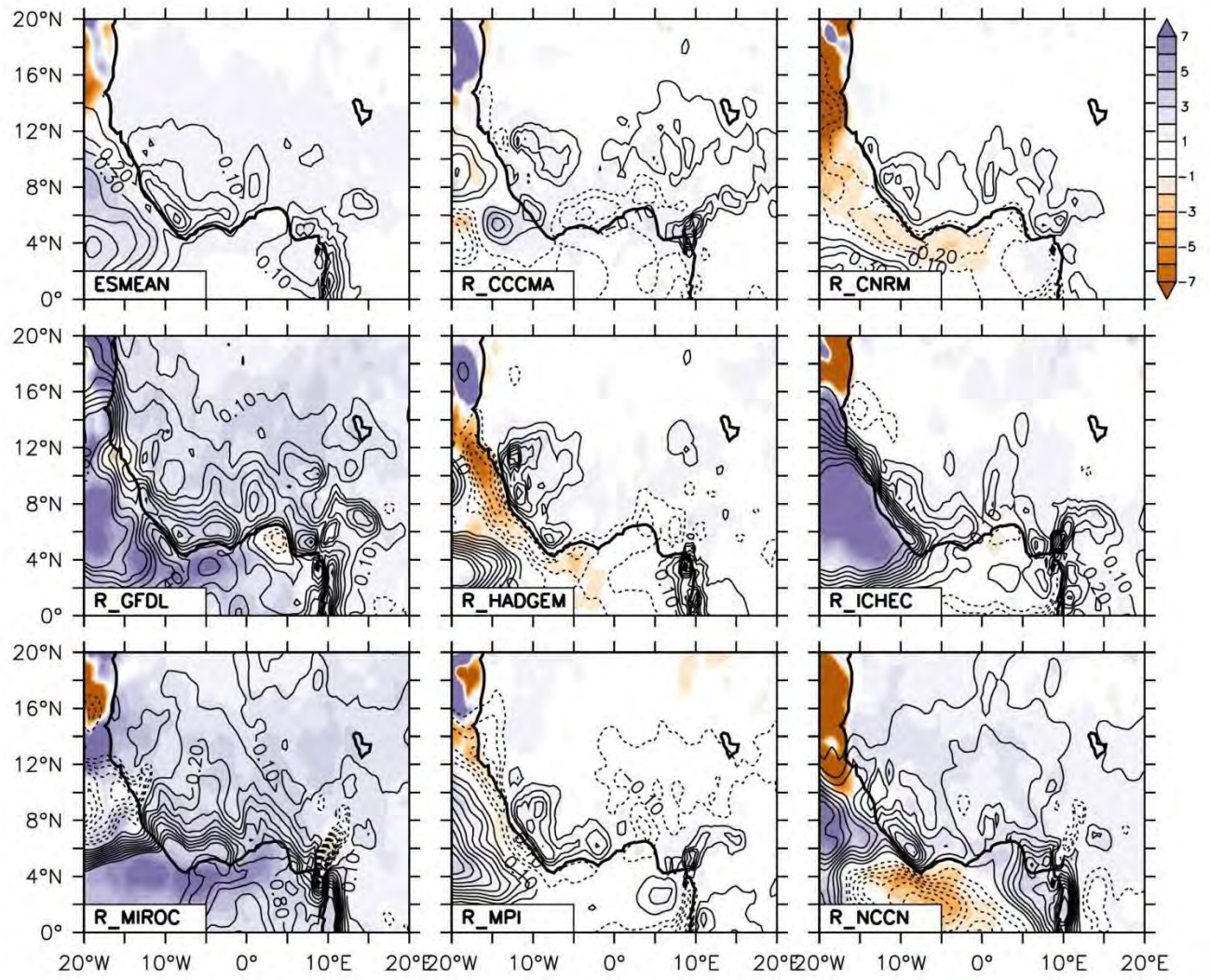

Figure 5.1: Projected changes in annual mean rainfall (contour, mm day^{-1}) and the 95th percentile threshold (shaded, mm day^{-1}) of daily rainfall over West Africa for the period 2031–2065 under RCP4.5 emission scenario.

The RCA ensemble-mean also projects an increase in rainfall intensity over the region for both the RCP4.5 and RCP8.5 scenarios (Figs. 5.1 and 5.2). For RCP.45, the increase is uniform (about 1 mm day^{-1}) over the sub-continent, while the increase is up to 2.0 mm day^{-1} over the Guinean coast for RCP8.5. However, for both scenarios, the increase is up to 7 mm day^{-1} over the ocean. The increased rainfall intensity is consistent with the increased atmospheric boundary layer (ABL) moisture in the warmer climate. Most of the West African rainfall is from convection, which acts to stabilise the atmosphere (and remove excess boundary moisture) within a time period (typically, about 30-60 minutes (Chou and Neelin, 2004; Omotosho and Abiodun, 2007). Therefore, with the

warmer and moister ABL, the rate at which convection would remove the excess moisture from the atmosphere would be higher. All the simulations agree on the increase of the rainfall intensity over the sub-continent, but with different magnitudes of increase. For example, with the RCP4.5 scenario, while R_CNRN and R_MPI show less than 1.0 mm day^{-1}, R_GFDL and R_MIROC show more than 1.0 mm day^{-1}. While all the simulations agree on the magnitude of the rainfall changes, they disagree on the sign of the changes; some simulations project a decrease in rainfall over the Ocean, while others project an increase in some areas and a decrease in other areas.

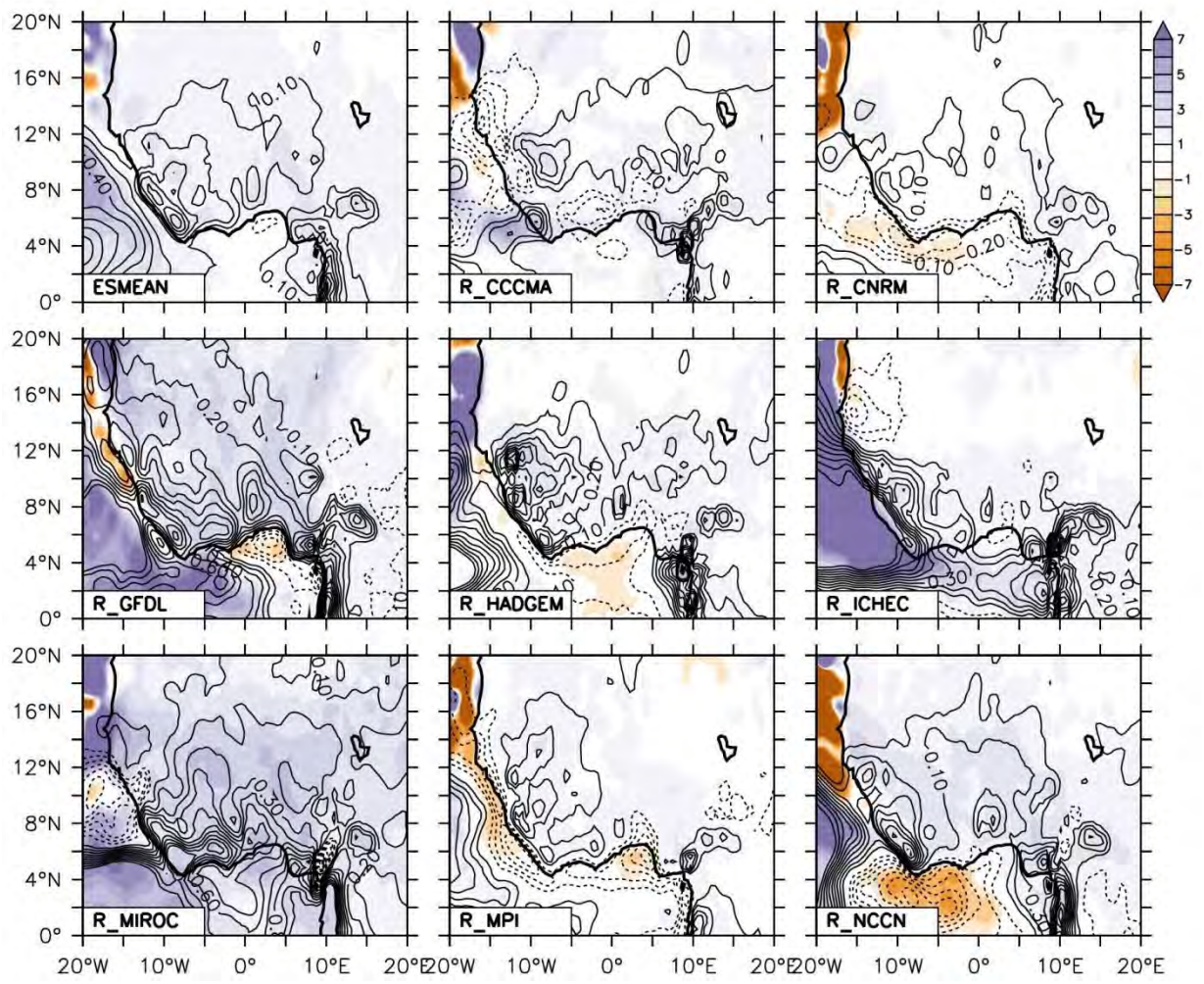

Figure 5.2: Same as figure (5.1), except for the RCP8.5 emission scenario.

For both scenarios, the RCA4 ensemble-mean projects a decrease in the number of rain days (NRD), but an increase in the number of extreme rainfall days (NED) over West Africa (Figs. 5.3 and 5.4). The magnitudes of these changes are higher for RCP8.5 than for RCP4.5. The maximum decrease in NRD (–7 days year^{-1} for RCP4.5 and –8 days year^{-1} for RCP8.5) is projected over south-west Nigeria, where the maximum increase in NED (5 event year^{-1} for RCP4.5 and 6 days year^{-1} for RCP.85) is also located. These opposite signs in the NRD and NED changes suggest that

the warmer ABL with a higher capacity for moisture would take a longer time to be saturated and produce rainfall (hence less rain days), but once saturated it would produce heavier rainfall (more extreme rainfall days) over a short period. All the simulations agree on the signs and spatial pattern of the NRD and NED changes, though they project different magnitudes of the changes. While R_MIROC projects the highest magnitude (i.e. NRD: > 15 events year^{-1} for RCP4.5 and NED: 12 events year^{-1} for RCP8.5), R_CNCM projects the lowest magnitudes (i.e. NRD: < 5 events year^{-1} for RCP4.5 and NED: < 2 events year^{-1} for RCP8.5). Nevertheless, there is no consensus among the simulations on how NRD and NED would change over the ocean. For example, while some simulations project a decrease in NRD over the entire ocean, others project an increase, and still others project an increase in one part and a decrease in another part. The same is true for NED. Hence, with RCA, the future projections for NRD and NED are more robust over the sub-continent than over the ocean.

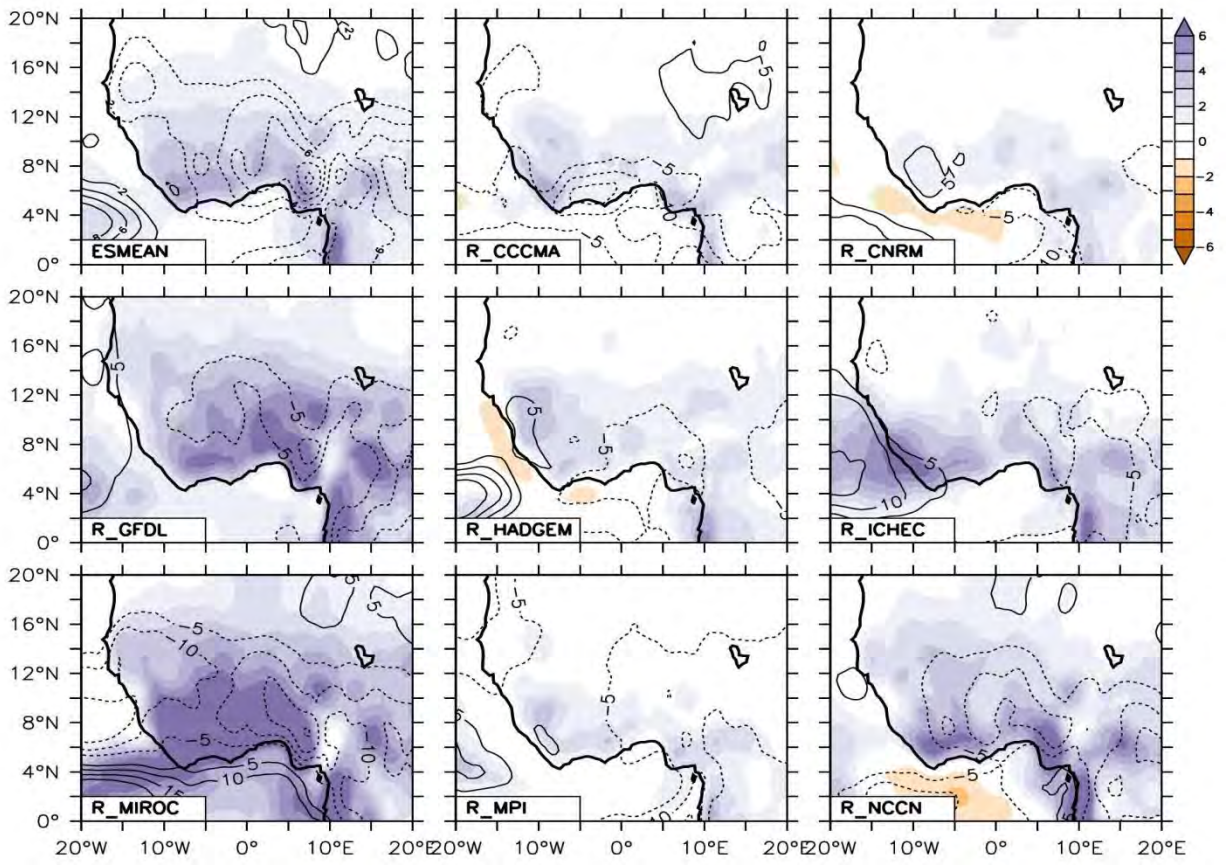

Figure 5.3: Projected changes in frequency of rainy days (contour, day decade^{-1}) and frequency of rainfall events (shaded, day decade^{-1}) over West Africa for the period 2031–2065 under RCP4.5 emission scenario. All changes are calculated with reference to 1971–2005 climatology.

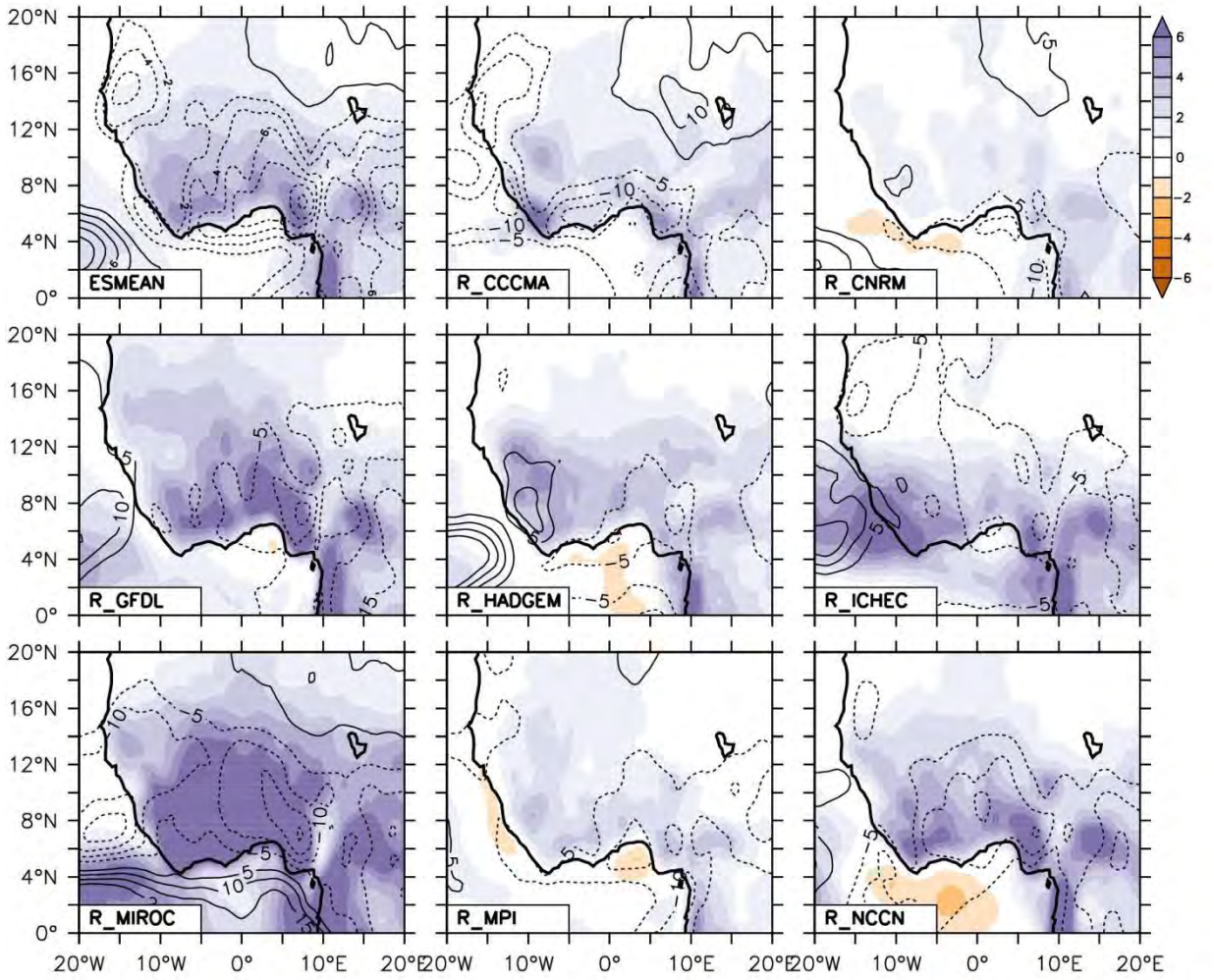

Figure 5.4: Same as figure (5.3), but for RCP8.5 emission scenario.

5.2 The Structure of AEWs

All the simulations (except R_GFDL) project no visible change in the structure of the AEWs and the location of AEJ in the future for both the RCP4.5 and 8.5 scenarios (Table 4.1 and 4.2). Only R_GFDL projects a decrease (about 4^{o}) in the latitudinal extent of the 3-5 days AEW and a northward shift (about 5^{o}) in the location of AEJ (Table 4.1, see detailed results in Appendix A). Nevertheless, the RCA ensemble-mean projects stronger wind anomalies and higher rainfall anomalies for both 3-5 days and 6-9 days AEWs. For 3-5 days AEW, the increase in the wind anomalies is 0.4 m s^{-1} in both the RCP4.5 and RCP8.5 scenarios (Table 4.1), while for 6-9 days AEW, it is 0.3 m s^{-1} in RCP4.5 and 0.0 m s^{-1} for the RCP8.5 scenario (Table 4.2, see detailed results in Appendix A). The corresponding increase in rainfall anomalies is 1.7 mm day^{-1} in the RCP4.5 scenario and 2.5 mm day^{-1} in the RCP8.5 scenario for AEW, but ±1.4 mm day^{-1} in the RCP4.5 scenario and 0.6 in the RCP8.5 scenario for 6-9 days AEW. However, few simulations disagree with the increase in wind and rainfall anomalies; instead, they project a decrease in wind anomalies,

or in rainfall anomalies, or in both. However, the projected increase in the wind anomalies is consistent with the projected increase in the speed of AEJ (i.e. 0.2-0.3 m s^{-1} for 3-5 days AEW in the RCP4.5 scenario).

5.3 Contribution of AEWs to Extreme Rainfall Events

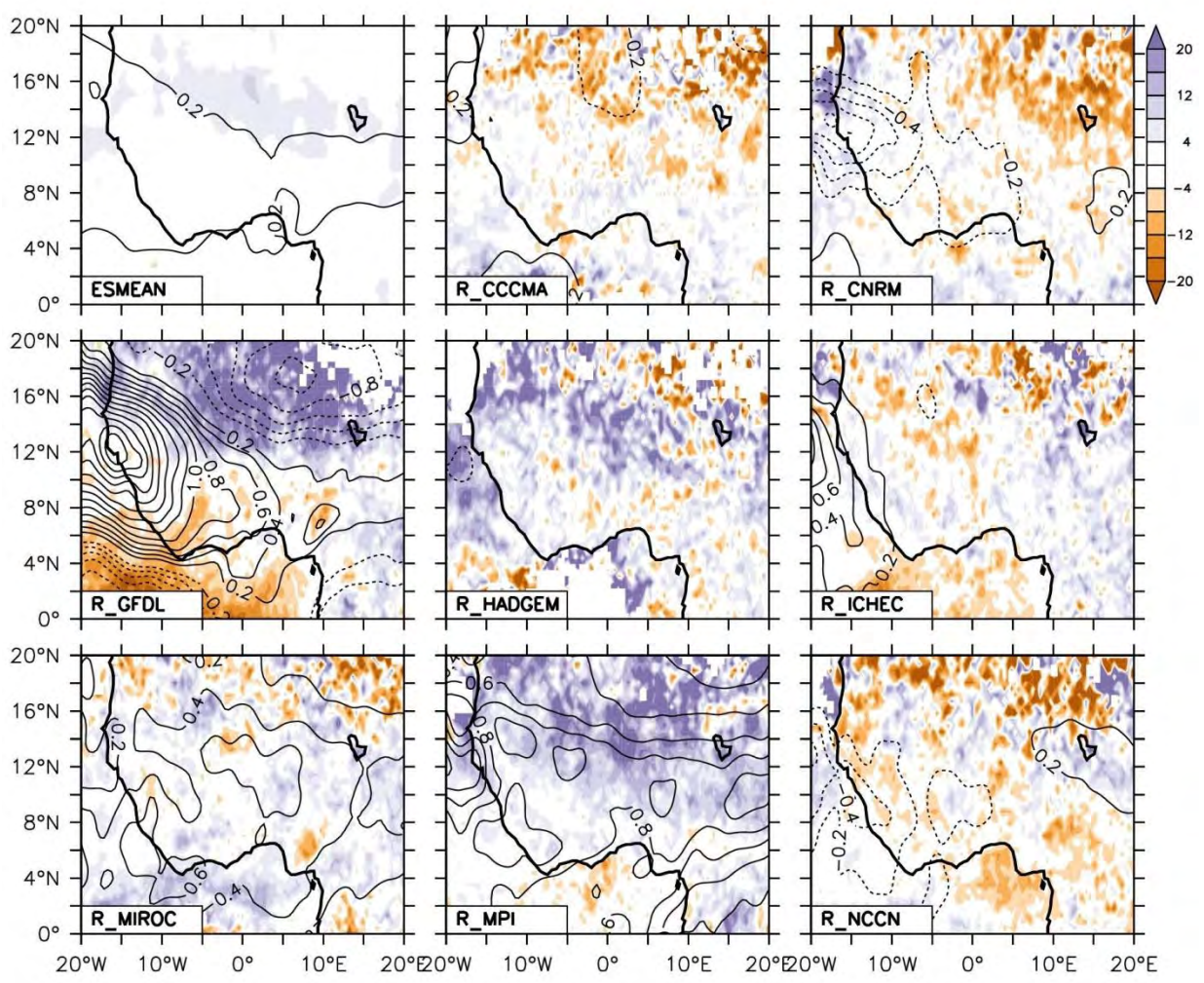

Figure 5.5: Projected changes in the variance of 3-5 days AEWs (contour, m/s) and the percentage contribution (shaded, %) of the waves to occurrence of extreme rainfall events over West Africa in the future (2031–2065) under the RCP4.5 emission scenario. All changes are calculated with reference to 1971-2005 climatology.

The enhanced wind anomalies seen in the AEWs structure also manifests in the strength (i.e. variance) of the waves over the entire sub-continent (Figs. 5.5-5.8). The RCA ensemble-mean projection shows an increase in the variance for AEWs in both the RCP4.5 and RCP8.5 scenarios. For 3-5 days AEW, the maximum increase in the variance is about 0.3 m s^{-1} for the RCP4.5 scenario and 0.4 for the RCP8.5 scenario, while for 6-9 days AEW, it is about 0.4 m s^{-1} for both scenarios. The projected increase in AEW strength here agrees with the results of Skinner and

Diffenbaugh (2014), who associate it with enhance monsoon flow and wind convergence following low-level warming.

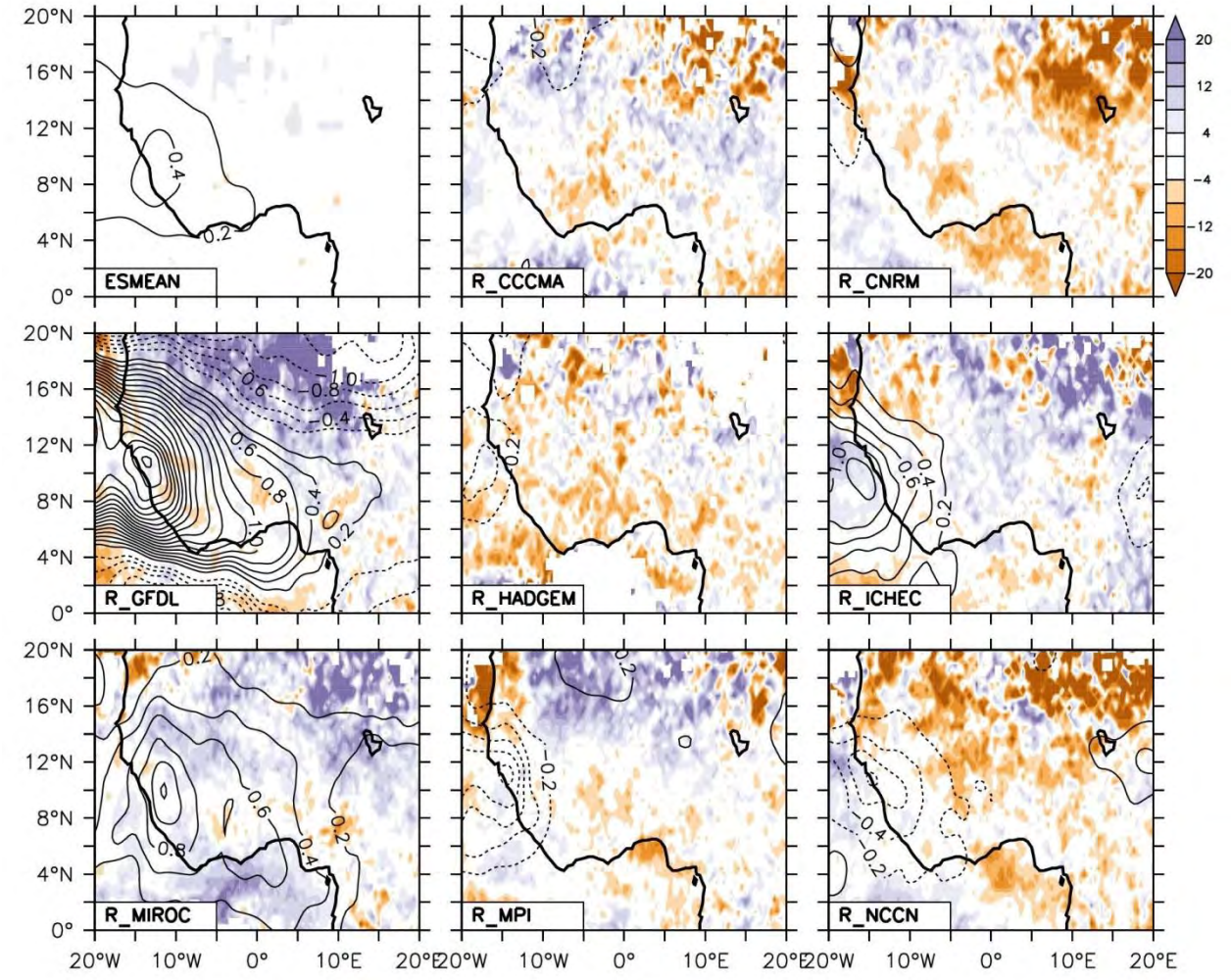

Figure 5.6: Same as figure (5.5), but for 6–9 days AEWs.

However the ensemble mean shows no substantial changes in the contribution of AEW to extreme rainfall events in the RCP4.5 and 8.5 scenarios. This is not because individual simulations do not project substantial changes in the contribution, but rather because the signs of the projected differ among the simulations and most of the changes cancel out when averaging. For instance, north of 12^{o}N, R_GFDL projects an increase (about +20%) in the percentage contribution, while R_ICHEC projects a decrease of a similar magnitude (about +20%). In addition, there is no consistent relationship between the change in the strength of AEWs and the percentage contribution of the wave to extreme rainfall events. In some simulations, stronger AEWs are associated with a higher percentage contribution, and vice versa; but the inverse is the case in some models (i.e. north of 12^{o}N for 3-5 and 6-9 days AEWs under the RCP4.5 and RCP8.5 scenarios in R_GFDL, and along the west coast of Senegal to Liberia in 6-9 days AEWs under the RCP8.5 scenario in R_NCCN).

This suggests that an increase in AEWs may not necessarily produce more extreme rainfall events, because AEWs only acts to trigger convection. In the warmer future climate, the lower atmosphere requires more moisture and large convective available potential energy (CAPE) to become conditionally unstable and to produce an extreme rainfall event. But, with stronger AEWs, the instability may be released before the CAPE is large enough for a deep convention that can induce extreme rainfall events. Hence, a decrease in the strength of AEWs may favour more extreme rainfall events because it would allow the CAPE to be larger. In addition, in a warmer climate, as the moist boundary layer is more buoyant with larger CAPE, the instability can be released by any other mechanism (which may produce a vertical lifting as much as that of AEWs), thereby weakening the dependency of extreme events on AEWs. However, the differences in the simulations suggest a non-linear relationship between the stronger AEWs and the increase in extreme rainfall events in the future climate. Hence, the projected increase in extreme rainfall events may be better linked with changes in other atmospheric processes, especially local-scale systems.

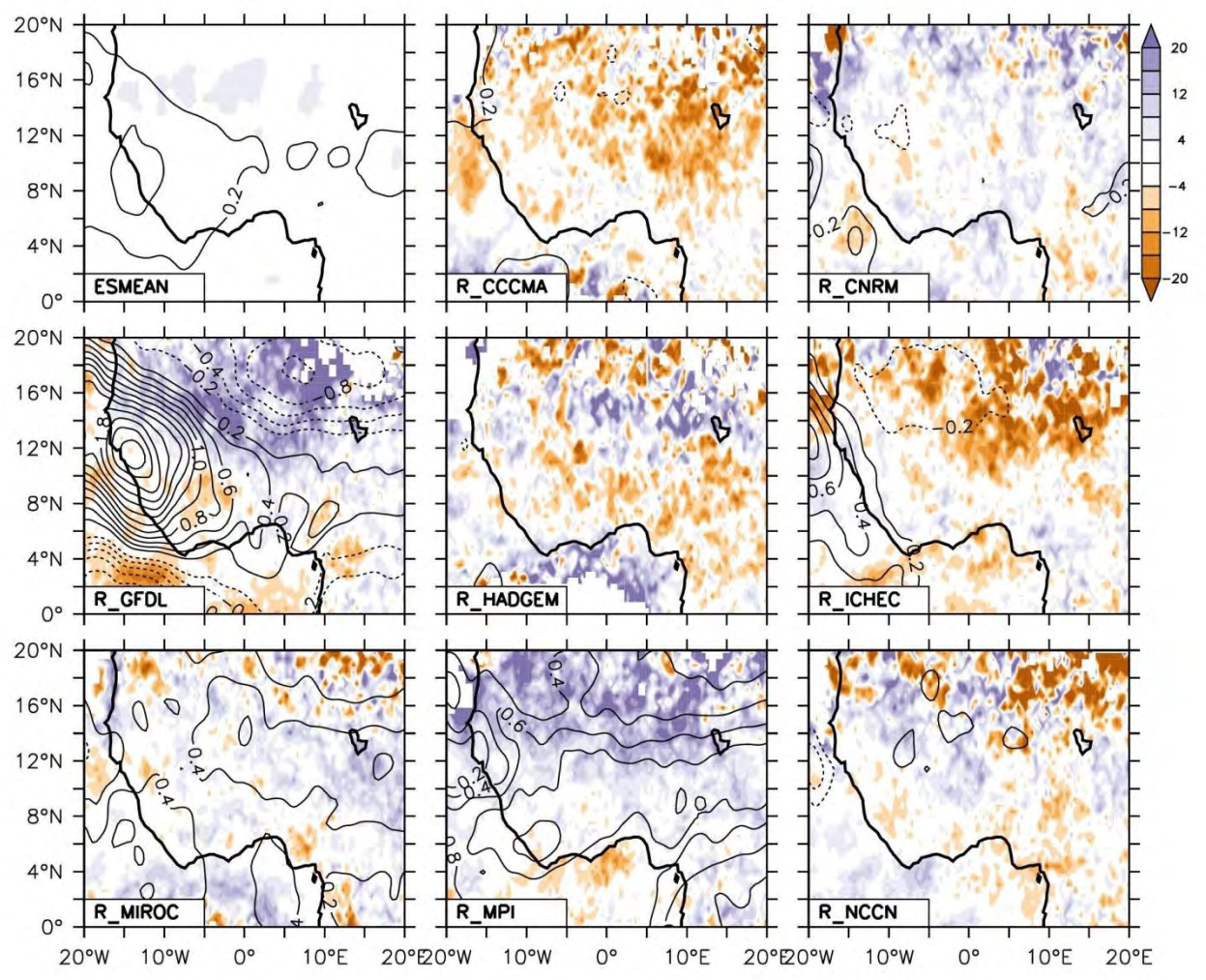

Figure 5.7: Same as figure (5.5), but for the RCP8.5 emission scenario.

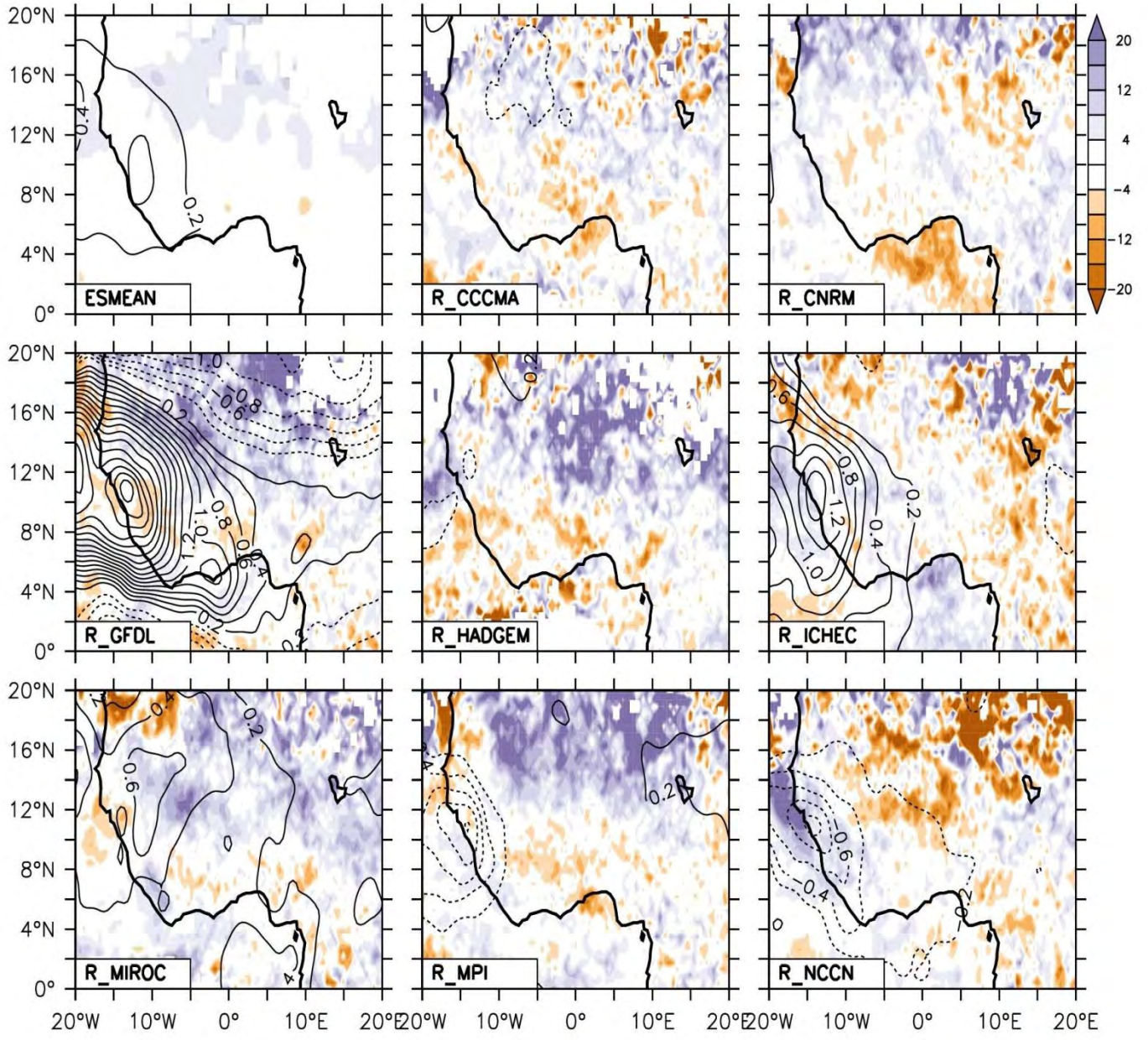

Figure 5.8: Same as figure (5.6), but for 6–9 days AEWs and the RCP8.5 emission scenario.

Chapter 6: Conclusion and Recommendations

6.1 Conclusion

This study has analysed observation, reanalysis and RCA-ensemble simulations data and investigated the relationship between African Easterly Waves (AEWs) and extreme rainfall events over West Africa, as well as how climate change could alter this relationship in the future. The RCA simulations were obtained from CORDEX. The model downscaled the eight global climate results for past climate (2031-2065) and future climate (2031-2065) under RCP4.5 and RCP8.5 radiative forcing. The study used the 95^{th} percentile of daily rainfall as a threshold to identify extreme rainfall events and applied spectral analysis to extract 3-5 days and 6-9 days AEWs from the 700hPa meridional wind component over West Africa. The capability of RCA4 to reproduce the rainfall climatology, extreme rainfall events, and the characteristics of AEWs and the contribution of AEWs to extreme rainfall events over the region during the past climate (1971-2005) was examined and quantified using statistical analysis. The future changes (2031-2065) in these parameters were projected for the RCP4.5 and RCP8.5 climate-change scenarios.

The results of our study can be summarised below:

- The RCA4 ensemble simulations give a realistic simulation of the West African climate, including the annual rainfall pattern, AEWs, and the African Easterly Jet that feeds AEWs. The model shows a strong correlation ($r \geq 0.7$) with observation in annual rainfall pattern over West Africa. However, RCA4 shows a weak correlation ($r \leq 0.4$) with both observation datasets (GPCP and TRMM) in the simulated threshold of extreme rainfall, but the bias in the simulated threshold of extreme rainfall is within the uncertainty of the observed values.
- The model also captures the link between the structure of AEWs and the rainfall pattern over West Africa, and shows that the percentage contribution of AEWs to extreme rainfall events over the region ranges from 20 to 60%, as depicted by reanalysis data.
- For the RCP4.5 and RCP8.5 scenarios, the RCA4 ensemble mean projects a future increase in annual rainfall and in the frequency and intensity of extreme rainfall events over the sub-continent, but the increase is generally higher for the RCP8.5 scenario. The increase in the frequency of extreme rainfall events implies more damage and a more devastating impact of extreme rainfall events across the region as a result of flooding via heavy and extreme rainfall.
- RCA4 also projects a decrease in the frequency of rain days, no changes in the structure of the AEWs, and an increase in variance of the waves. The decrease in rain-days frequency suggests a period of dry spells over the region. Also, the increase in variance of the waves

shows an increase in AEW strength in the future under the RCP4.5 and 8.5 scenarios.

- The simulations from the ensemble mean show no substantial changes in the contribution of AEWs to the extreme rainfall events, suggesting that the increase in the frequency and intensity of the extreme rainfall events may not be attributed to the changes in AEWs. Hence, using AEWs to monitor or investigate the characteristics (intensity and frequency) of extreme rainfall events may underestimate the characteristics of the events over West Africa.

6.2 Limitation and Recommendations

6.2.1 Limitation

As in any research, we identified a limitation that needs to be addressed and may help improve our knowledge on the relationship and contribution of AEWs to extreme rainfall events over West Africa. The present study on the relationship between AEWs and extreme rainfall events for present-day and near-future climate over West Africa was carried out using only one RCM. The result will be more consistent and comprehensive if other RCMs are included. This can only be done if more wind data are available over 700hPa from other CORDEX models.

6.2.2 Recommendations

The present study has enhanced our understanding of how RCMs may be used to investigate the projection of the future characteristics of extreme rainfall due to the impact of climate change over West Africa. However, the findings from this study can be improved and made more robust through more extensive analysis. Such research is needed to help guide policy makers at both the national and the regional level in reducing the impact and risk associated with future extreme rainfall events in West Africa.

Future studies may investigate the future characteristics of extreme rainfall over the region using more RCMs other than the single RCM with the different forcing GCMs used in this study. This may help resolve the bias observed in RCA4 and the challenge of uncertainty in the future characteristics of extreme rainfall events over West Africa. In addition, the result will make the study more robust and improve our knowledge on the relationship between AEWs and extreme rainfall events over West Africa.

The present study only considers AEWs among the West African monsoon systems. Future work may examine how other systems, such as the Tropical Easterly Jet, may induce or contribute to

extreme rainfall events in the region, by investigating how they may alter the characteristics of extreme rainfall events in West Africa.

Nevertheless, the present work has established that using RCM, RCA4 to downscale GCMs simulations may improve the simulation and projection of future extreme rainfall characteristics (frequency and intensity) in West Africa. In addition, the study also shows that, although there exists a good relationship between AEWs and daily rainfall over West Africa, the projected future increase in the strength of AEWs may not be responsible for the projected increases in the intensity and frequency of extreme rainfall over the region.

References

Abatan, Abayomi Abiodun, "West African extreme daily precipitation in observations and stretched-grid simulations by CAM-EULAG" (2011). *Graduate Theses and Dissertations*. Paper 10401. http://lib.dr.iastate.edu/etd/10401

Abba Omar, S. (2014). Capability of CORDEX RCMs in simulating extreme rainfall events over South Africa (Master's Dissertation, University of Cape Town).

Abiodun, B. J., Pal, J. S., Afiesimama, E. A., Gutowski, W. J., & Adedoyin, A. (2008). Simulation of West African monsoon using RegCM3 Part II: impacts of deforestation and desertification. *Theoretical and Applied Climatology*, *93*(3-4), 245-261.

Abiodun, B. J., Adeyewa, Z. D., Oguntunde, P. G., Salami, A. T., & Ajayi, V. O. (2012a). Modeling the impacts of reforestation on future climate in West Africa. *Theoretical and Applied Climatology*, *110*(1-2), 77-96.

Abiodun, B. J., Salami, A. T., Matthew, O. J., & Odedokun, S. (2013). Potential impacts of afforestation on climate change and extreme events in Nigeria. *Climate dynamics*, *41*(2), 277-293.

Abiodun, B. J., Abba Omar, S., Lennard, C. and Jack, C. (2015), Using regional climate models to simulate extreme rainfall events in the Western Cape, South Africa. Int. J. Climatol., 36: 689–705.

Adedokun, J. A. (1978). West African precipitation and dominant atmospheric mechanisms. *Archiv für Meteorologie, Geophysik und Bioklimatologie, Serie A*, *27*(3-4), 289-310.

Adler, B., Kalthoff, N., & Gantner, L. (2011a). Initiation of deep convection caused by land-surface inhomogeneities in West Africa: a modelled case study. *Meteorology and Atmospheric Physics*, *112*(1-2), 15-27.

Adler, B., Kalthoff, N., & Gantner, L. (2011b). The impact of soil moisture inhomogeneities on the modification of a mesoscale convective system: An idealised model study. *Atmospheric Research*, *101*(1), 354-372.

Afiesimama, E. A., Pal, J. S., Abiodun, B. J., Gutowski Jr, W. J., & Adedoyin, A. (2006). Simulation of West African monsoon using the RegCM3. Part I: model validation and interannual variability. *Theoretical and Applied Climatology*, *86*(1-4), 23-37.

Bain, C. L., Williams, K. D., Milton, S. F., & Heming, J. T. (2014). Objective tracking of African easterly waves in Met Office models. *Quarterly Journal of the Royal Meteorological Society*, *140*(678), 47-57.

Barnston, A. G., & Mason, S. J. (2011). Evaluation of IRI's seasonal climate forecasts for the extreme 15% tails. *Weather and Forecasting*, *26*(4), 545-554.

Barthe, C., Asencio, N., Lafore, J. P., Chong, M., & Campistron, B. (2010). Cloud-resolving model simulation of the 25–27 July 2006 convective period over Niamey: comparison with radar data and other observations. *Quarterly Journal of the Royal Meteorological Society*, *136*, 190-208.

Benestad, R. E., Hanssen-Bauer, I., & Chen, D. (2008). *Empirical-statistical downscaling*. Singapore: World Scientific Publishing Company Incorporated.

Berrisford, P., Dee, D., Fielding, K., Fuentes, M., Kallberg, P., Kobayashi, S. and Uppala, S., (2009) *The ERA-Interim Archive.* ERA Report Series. 1. Technical Report. European Centre for Medium-Range Weather Forecasts, Shinfield Park, Reading. p 16.

Berry, G. J., & Thorncroft, C. (2005). Case study of an intense African easterly wave. *Monthly Weather Review*, *133*(4), 752-766.

Berry, G. J., & Thorncroft, C. D. (2012). African easterly wave dynamics in a mesoscale numerical model: The upscale role of convection. *Journal of the Atmospheric Sciences*, *69*(4), 1267-1283.

Biasutti, M., Held, I. M., Sobel, A. H., & Giannini, A. (2008). SST forcings and Sahel rainfall variability in simulations of the twentieth and twenty-first centuries. *Journal of Climate*, *21*(14), 3471-3486.

Brown, S. J., Caesar, J., & Ferro, C. A. (2008). Global changes in extreme daily temperature since 1950. *Journal of Geophysical Research: Atmospheres (1984–2012)*, *113*(D5).

Browne NAK, Sylla MB. (2012). Regional climate model sensitivity to domain size for the simulation of the West African monsoon rainfall. Int. J. Geophys. Article ID 625831.

Burpee, R. W. (1972). The origin and structure of easterly waves in the lower troposphere of North Africa. *Journal of the Atmospheric Sciences*, *29*(1), 77-90.

Burpee, R. W. (1974). Characteristics of North African easterly waves during the summers of 1968 and 1969. *Journal of the Atmospheric Sciences*, *31*(6), 1556-1570.

Caminade, C., & Terray, L. (2010). Twentieth century Sahel rainfall variability as simulated by the ARPEGE AGCM, and future changes. *Climate Dynamics*, *35*(1), 75-94.

Carlson, T. N. (1969). Synoptic histories of three African disturbances that developed into Atlantic hurricanes. *Monthly Weather Review*, *97*(3), 256-276.

Charney, J. G. (1975). Dynamics of deserts and drought in the Sahel. *Quarterly Journal of the Royal Meteorological Society*, *101*(428), 193-202.

Chou, C., & Neelin, J. D. (2004). Mechanisms of global warming impacts on regional tropical precipitation*. *Journal of climate*, *17*(13), 2688-2701.

Christensen, J. H., Hewitson, B., Busuioc, A., Chen, A., Gao, X., Held, R., ... & Dethloff, K. (2007). Regional climate projections. *Climate Change, 2007: The Physical Science Basis. Contribution of Working group I to the Fourth Assessment Report of the Intergovernmental Panel on Climate Change, University Press, Cambridge, Chapter 11*, 847-940.

Chu, P. S., Zhao, X., Ruan, Y., & Grubbs, M. (2009). Extreme rainfall events in the Hawaiian Islands. *Journal of Applied Meteorology and Climatology*, *48*(3), 502-516.

Cifelli, R., Lang, T., Rutledge, S. A., Guy, N., Zipser, E. J., Zawislak, J., & Holzworth, R. (2010). Characteristics of an African easterly wave observed during NAMMA. *Journal of the Atmospheric Sciences*, *67*(1), 3-25.

Clark, D. B., Taylor, C. M., & Thorpe, A. J. (2004). Feedback between the land surface and rainfall at convective length scales. *Journal of Hydrometeorology*, *5*(4), 625-639.

Cook, K. H., & Vizy, E. K. (2006). Coupled model simulations of the West African monsoon system: Twentieth-and twenty-first-century simulations. *Journal of climate*, *19*(15), 3681-3703.

Cornforth, R. J., Hoskins, B. J., & Thorncroft, C. D. (2009). The impact of moist processes on the African easterly jet–African easterly wave system. *Quarterly Journal of the Royal Meteorological Society*, *135*(641), 894-913.

Crétat, J., Vizy, E. K., & Cook, K. H. (2013). How well are daily intense rainfall events captured by current climate models over Africa?. *Climate dynamics*, *42*(9-10), 2691-2711.

Crétat, J., Vizy, E. K., & Cook, K. H. (2014). The relationship between African easterly waves and daily rainfall over West Africa: observations and regional climate simulations. *Climate Dynamics*, *44*(1-2), 385-404.

Cuxart J, Bougeault P, Redelsperger J-L. (2000). A turbulence scheme allowing for mesoscale and large-eddy simulations. Quart. J. Roy. Meteor. Soc. 126: 1–30.

Dee, D. P., Uppala, S. M., Simmons, A. J., Berrisford, P., Poli, P., Kobayashi, S., ... & Vitart, F. (2011). The ERA-Interim reanalysis: Configuration and performance of the data assimilation system. *Quarterly Journal of the Royal Meteorological Society*, *137*(656), 553-597.

de Elía, R., & Laprise, R. (2003). Distribution-oriented verification of limited-area model forecasts in a perfect-model framework. *Monthly weather review*, *131*(10), 2492-2509.

De Felice, P., Monkam, D., Viltard, A., & Ouss, C. (1990). Characteristics of North African 6-9 day waves during summer 1981. *Monthly weather review*, *118*(12), 2624-2633.

DeMott, P. J., Sassen, K., Poellot, M. R., Baumgardner, D., Rogers, D. C., Brooks, S. D., ... & Kreidenweis, S. M. (2003). African dust aerosols as atmospheric ice nuclei. *Geophysical Research Letters*, *30*(14).

Deser, C., Phillips, A. S., & Alexander, M. A. (2010). Twentieth century tropical sea surface temperature trends revisited. *Geophysical Research Letters*, *37*(10).

Diallo, I., M. B. Sylla, F. Giorgi, A. T. Gaye, and Camara, M. (2012). Multimodel GCM-RCM ensemble-based projections of temperature and precipitation over West Africa for the early 21st century. Int. J. Geophys., 2012, 972896.

Diedhiou, A., Janicot, S., Viltard, A., & de Felice, P. (1998). Evidence of two regimes of easterly waves over West Africa and the tropical Atlantic. *Geophysical Research Letters*, *25*(15), 2805-2808.

Diedhiou, A., Janicot, S., Viltard, A., De Felice, P., & Laurent, H. (1999). Easterly wave regimes and associated convection over West Africa and tropical Atlantic: results from the NCEP/NCAR and ECMWF reanalyses. *Climate Dynamics*, *15*(11), 795-822.

Dieterich, C., Schimanke, S., Wang, S., Väli, G., Liu, Y., Hordoir, R., ... & Meier, H. E. M. (2013). Evaluation of the SMHI coupled atmosphere-ice-ocean model RCA4_NEMO. SMHI Report Oceanography No.47, SMHI, Norrköping, pp. 1–80.

Di Vittorio, A. V., & Miller, N. L. (2013). Evaluating a modified point-based method to downscale cell-based climate variable data to high-resolution grids. *Theoretical and applied climatology*, *112*(3-4), 495-519.

Douville, H., Salas-Mélia, D., & Tyteca, S. (2006). On the tropical origin of uncertainties in the global land precipitation response to global warming. *Climate Dynamics*, *26*(4), 367-385.

Druyan, L. M., Fulakeza, M., & Lonergan, P. (2004). Land surface influences on the West African summer monsoon: implications for synoptic disturbances. *Meteorology and Atmospheric Physics*, *86*(3-4), 261-273.

Dyson, L. L. (2009). Heavy daily-rainfall characteristics over the Gauteng Province. *Water SA*, *35*(5).

Endris, H. S., Lennard, C., Hewitson, B., Dosio, A., Nikulin, G., & Panitz, H. J. (2015). Teleconnection responses in multi-GCM driven CORDEX RCMs over Eastern Africa. *Climate Dynamics*, 1-26.

FAO (1985): Integrating crops and livestock in West Africa. Agriculture and Consumer Protection. Available online 19/08/2014: http://www.fao.org/docrep/004/x6543e/X6543E01.htm#ch1

Fink, A. H., & Reiner, A. (2003). Spatiotemporal variability of the relation between African easterly waves and West African squall lines in 1998 and 1999. *Journal of Geophysical Research: Atmospheres (1984–2012)*, *108*(D11).

Fink, A. H., Vincent, D. G., & Ermert, V. (2006). Rainfall types in the West African Sudanian zone during the summer monsoon 2002. *Monthly weather review*, *134*(8), 2143-2164.

Fontaine, B., Trzaska, S., & Janicot, S. (1998). Evolution of the relationship between near global and Atlantic SST modes and the rainy season in West Africa: statistical analyses and sensitivity experiments. *Climate Dynamics*, *14*(5), 353-368.

Fortune, M. (1980). Properties of African squall lines inferred from time-lapse satellite imagery. *Monthly Weather Review*, *108*(2), 153-168.

Frich, P., Alexander, L. V., Della-Marta, P., Gleason, B., Haylock, M., Klein Tank, A. M., & Peterson, T. (2002). Observed coherent changes in climatic extremes during the second half of the twentieth century. *Climate research*, *19*(3), 193-212.

Gachon, P., Gauthier, N., Bokoye, A. I., Parishkura, D., Cotnoir, A., Tramblay, Y., & Vigeant, G. (2007). Working Group II: variability, extremes and climate change in the Sahel: from observation to modelling. *Report on Canadian Contributions to the CIDA–CILSS Project (A030978-002) Climate Change Adaptation Capacity Support*, *220*.

Gaye, A., Viltard, A., & De Felice, P. (2005). Squall lines and rainfall over Western Africa during summer 1986 and 87. *Meteorology and Atmospheric Physics*, *90*(3-4), 215-224.

Giannini, A., Saravanan, R., & Chang, P. (2003). Oceanic forcing of Sahel rainfall on interannual to interdecadal time scales. *Science*, *302*(5647), 1027-1030.

Giorgi, F., & Mearns, L. O. (1991). Approaches to the simulation of regional climate change: a review. *Reviews of Geophysics*, *29*(2), 191-216.

Giorgi, F., Christensen, J., Hulme, M., Von Storch, H., Whetton, P., Jones, R., ... & Semazzi, F. (2001). Regional climate information-evaluation and projections. *Climate Change 2001: The Scientific Basis. Contribution of Working Group to the Third Assessment Report of the Intergouvernmental Panel on Climate Change [Houghton, JT et al.(eds)]. Cambridge University Press, Cambridge, United Kongdom and New York, US*.

Giorgi, F. (2006, December). Regional climate modelling: Status and perspectives. In *Journal de Physique IV (Proceedings)*, *139*, 101-118.

Giorgi, F., Jones, C., & Asrar, G. R. (2009). Addressing climate information needs at the regional level: the CORDEX framework. *World Meteorological Organization (WMO) Bulletin*, *58*(3), 175.

Goswani, B. N., Venugopal, V., Sengupta, D., Madhusoodanan, M. S., & Xavier, P. K. (2006). Increasing trend of extreme rain events over India in a Warming environment. *Science*, *314*(5804), 1442-1445.

Gouvernement de la République du Bénin (2011) Inondations au Benin: Rapport d'Evaluation des Besoin Post Catastrophe. Rapport Final préparé avec l'appui de la Banque Mondial et du Système des Nations Unies, Avril, 2011.

Grimm, A. M., & Tedeschi, R. G. (2009). ENSO and extreme rainfall events in South America. *Journal of Climate*, *22*(7), 1589-1609.

Grist, J. P., & Nicholson, S. E. (2001). A study of the dynamic factors influencing the rainfall variability in the West African Sahel. *Journal of climate*, *14*(7), 1337-1359.

Groisman, P. Y., Knight, R. W., & Karl, T. R. (2001). Heavy precipitation and high stream flow in the contiguous United States: Trends in the twentieth century. *Bulletin of the American Meteorological Society*, *82*(2), 219-246.

Grolle, J. (1997). Heavy rainfall, famine, and cultural response in the West African Sahel: the 'Muda'of 1953–54. *GeoJournal*, *43*(3), 205-214.

Gu, G., Adler, R. F., Huffman, G. J., & Curtis, S. (2004). African easterly waves and their association with precipitation. *Journal of Geophysical Research: Atmospheres (1984–2012)*, *109*(D4).

Haensler, A., F. Saeed, and D. Jacob, (2013): Assessing the robustness of projected precipitation changes over central Africa on the basis of a multitude of global and regional climate projections. *Climate change*, 121(2), 349-363

Hall, N. M., Kiladis, G. N., & Thorncroft, C. D. (2006). Three-dimensional structure and dynamics of African easterly waves. Part II: Dynamical modes. *Journal of the atmospheric sciences*, *63*(9), 2231-2245.

Hewitson BC, Crane RG (1996) Climate downscaling: techniques and application. *Clim Res 07*(2): 85-95

Hountondji, Y., De Longueville, F., & Ozer, P. (2011). Trends in extreme rainfall events in Benin (West Africa), 1960-2000. In *1st International Conference on Energy, Environment and Climate Change*.

Hsieh, J. S., & Cook, K. H. (2005). Generation of African easterly wave disturbances: Relationship to the African easterly jet. *Monthly weather review*, *133*(5), 1311-1327.

Hsieh, J. S., & Cook, K. H. (2008). On the instability of the African easterly jet and the generation of African waves: Reversals of the potential vorticity gradient. *Journal of the Atmospheric Sciences*, *65*(7), 2130-2151.

Huffman, G. J., Adler, R. F., Morrissey, M. M., Bolvin, D. T., Curtis, S., Joyce, R., ... & Susskind, J. (2001). Global precipitation at one-degree daily resolution from multisatellite observations. *Journal of Hydrometeorology*, *2*(1), 36-50.

Huffman, G. J., Bolvin, D. T., Nelkin, E. J., Wolff, D. B., Adler, R. F., Gu, G., ... & Stocker, E. F. (2007). The TRMM multisatellite precipitation analysis (TMPA): Quasi-global, multiyear, combined-sensor precipitation estimates at fine scales. *Journal of Hydrometeorology*, *8*(1), 38-55.

Hui, W. J., Cook, B. I., Ravi, S., Fuentes, J. D., & D'Odorico, P. (2008). Dust-rainfall feedbacks in the West African Sahel. *Water Resources Research*, *44*(5).

http://global.britannica.com/place/western-Africa

http://www.oecd.org/migration/38481393.pdf

http://www.feedthefuture.gov/country/west-africa-regional

http://www.slideshare.net/ipsantika/statistical-downscaling-sdsm

http://www.britannica.com/science/Koppen-climate-classification

http://www.britannica.com/science/West-African-monsoon

http://thewatchers.adorraeli.com/2015/08/08/heavy-flooding-across-west-africa-8-people-dead-and-19-779-affected-in-burkina-faso

Ilesanmi, O. O. (1971). An empirical formulation of an ITD rainfall model for the Tropics: A case study of Nigeria. *Journal of Applied Meteorology*, *10*(5), 882-891.

IPCC, (2001): Climate Change 2001: The Scientific Basis. Contribution of Working Group I to the Third Assessment Report of the Intergovernmental Panel on Climate Change [Houghton, J.T., et al. (eds.)]. Cambridge University Press, Cambridge, United Kingdom and New York, NY, USA, pp. 881.

IPCC, (2007): Summary for policymakers. In: Solomon, S., Qin, D., Manning, M., Marquis, M., Averyt, K.B., Tignor, M., Miller, H.L; Chen, Z., Climate Change 2007: The Physical Science Basis. Contribution of Working Group I to the Fourth Assessment Report of the Intergovernmental Panel on Climate Change. Cambridge University Press, Cambridge, United Kingdom and New York, NY, USA, p. 18.

IPCC, 2013: Climate Change (2013): The Physical Science Basis. Contribution of Working Group I to the Fifth Assessment Report of the Intergovernmental Panel on Climate Change [Stocker, T.F., D. Qin, G.-K. Plattner, M. Tignor, S.K. Allen, J. Boschung, A. Nauels, Y. Xia, V. Bex and P.M. Midgley (eds.)]. Cambridge University Press, Cambridge, United Kingdom and New York, NY, USA, pp. 1535.

Jain, D. K., Chakraborty, A., & Nanjundiah, R. S. (2012). On the role of cloud adjustment time scale in simulating precipitation with Relaxed Arakawa–Schubert convection scheme. *Meteorology and Atmospheric Physics*, *115*(1-2), 1-13.

Janicot, S., Moron, V., & Fontaine, B. (1996). Sahel droughts and ENSO dynamics. *Geophysical Research Letters*, *23*(5), 515-518.

Janicot S, Caniaux G, Chauvin F (2011). Intraseasonal variability of the West African monsoon. *Atmospheric Science Letters*, *12*(1), 58–66.

Jenkins, G. S., Gaye, A. T., & Sylla, B. (2005). Late 20th century attribution of drying trends in the Sahel from the Regional Climate Model (RegCM3). *Geophysical Research Letters*, *32*(22).

Johanson, C. M., & Fu, Q. (2009). Hadley cell widening: Model simulations versus observations. *Journal of Climate*, *22*(10), 2713-2725.

Joly, M., Voldoire, A., Douville, H., Terray, P., & Royer, J. F. (2007). African monsoon teleconnections with tropical SSTs: validation and evolution in a set of IPCC4 simulations. *Climate Dynamics*, *29*(1), 1-20.

Jones RG, Noguer M, Hassel D, Hudson D, Wilson S, Jenkins G, Mitchell J. (2004). Generating high resolution climate change scenarios using PRECIS. Met Office Hadley Centre Handbook, pp. 40.
http://www.metoffice.gov.uk/media/pdf/6/5/PRECIS_Handbook.pdf.

Kain, J. S. and Fritsch, J. M. (1990). A one-dimensional entraining/detraining plume model and its application in convective parameterization. *J. Atmos. Sci.*, *47*, 2784–2802.

Kain, J. S., & Fritsch, J. M. (1993). Convective parameterization for mesoscale models: The Kain-Fritsch scheme. In *The representation of cumulus convection in numerical models* (pp. 165-170). American Meteorological Society.

Kalognomou, E. A., Lennard, C., Shongwe, M., Pinto, I., Favre, A., Kent, M., & Büchner, M. (2013). A Diagnostic Evaluation of Precipitation in CORDEX Models over Southern Africa. *Journal of Climate*, *26*(23).

Kamiguchi, K., Kitoh, A., Uchiyama, T., Mizuta, R., & Noda, A. (2006). Changes in precipitation-based extremes indices due to global warming projected by a global 20-km-mesh atmospheric model. *Sola*, *2*, 64-67.

Kang, S. M., & Lu, J. (2012). Expansion of the Hadley cell under global warming: Winter versus summer. *Journal of Climate*, *25*(24), 8387-8393.

Klein Tank, A. M. G., & Zwiers, F. W. (2009). Guidlines on Analysis of Extremes in a Changing Climate in Support of Informed Decisions for Adaptation. Climate Data and Monitoring, 72. World Meteorological Organisation.

Klüser, L., & Holzer-Popp, T. (2010). Relationships between mineral dust and cloud properties in the West African Sahel. *Atmospheric Chemistry and Physics*, *10*(14), 6901-6915.

Konare, A., Zakey, A. S., Solmon, F., Giorgi, F., Rauscher, S., Ibrah, S., & Bi, X. (2008). A regional climate modeling study of the effect of desert dust on the West African monsoon. *Journal of Geophysical Research: Atmospheres (1984–2012)*, *113*(D12).

Lau, K. M., Kim, K. M., Sud, Y. C., & Walker, G. K. (2009). A GCM Study of Responses of the Atmospheric Water Cycle of West Africa and the Atlantic to Saharan Dust Radiative Forcing.

Laurent, H., d'AMATO, N., & Lebel, T. (1998). How important is the contribution of the mesoscale convective complexes to the Sahelian rainfall? *Physics and Chemistry of the Earth*, *23*(5), 629-633.

Lavaysse, C., Diedhiou, A., Laurent, H., & Lebel, T. (2006). African Easterly Waves and convective activity in wet and dry sequences of the West African Monsoon. *Climate Dynamics*, *27*(2-3), 319-332.

Lawal, K. A., Stone, D. A., Aina, T., Rye, C., & Abiodun, B. J. (2015). Trends in the potential spread of seasonal climate simulations over South Africa. *International Journal of Climatology*, *35*(9), 2193-2209.

Lu, J., Vecchi, G. A., & Reichler, T. (2007). Expansion of the Hadley cell under global warming. *Geophysical Research Letters*, *34*(6).

Ly, M., Traore, S. B., Alhassane, A., & Sarr, B. (2013). Evolution of some observed climate extremes in the West African Sahel. *Weather and Climate Extremes*, *1*, 19-25.

Mélice, J. L., & Reason, C. J. (2007). Return period of extreme rainfall at George, South Africa. *South African Journal of science*, *103*(11-12), 499-501.

Mekonnen, A., Thorncroft, C. D., & Aiyyer, A. R. (2006). Analysis of convection and its association with African easterly waves. *Journal of climate*, *19*(20), 5405-5421.

Moufouma-Okia, W., & Rowell, D. P. (2010). Impact of soil moisture initialisation and lateral boundary conditions on regional climate model simulations of the West African Monsoon. *Climate Dynamics*, *35*(1), 213-229.

Naik, M. and Abiodun, B. J. (2016), Potential impacts of forestation on future climate change in Southern Africa. Int. J. Climatol.. doi:10.1002/joc.4652

New, M., Hewitson, B., Stephenson, D. B., Tsiga, A., Kruger, A., Manhique, A., ... & Lajoie, R. (2006). Evidence of trends in daily climate extremes over southern and West Africa. *Journal of Geophysical Research: Atmospheres (1984–2012)*, *111*(D14).

Niang, I., O.C. Ruppel, M.A. Abdrabo, A. Essel, C. Lennard, J. Padgham, and P. Urquhart, (2014): Africa. In: Climate Change 2014: Impacts, Adaptation, and Vulnerability. Part B: Regional Aspects. Contribution of Working Group II to the Fifth Assessment Report of the Intergovernmental Panel on Climate Change [Barros, V.R., C.B. Field, D.J. Dokken, M.D. Mastrandrea, K.J. Mach, T.E. Bilir, M. Chatterjee, K.L. Ebi, Y.O. Estrada, R.C. Genova, B. Girma, E.S. Kissel, A.N. Levy, S. MacCracken, P.R. Mastrandrea, and L.L. White (eds.)]. Cambridge University Press, Cambridge, United Kingdom and New York, NY, USA, pp. 1199-1265.

Nicholson, S. E. (2008). The intensity, location and structure of the tropical rainbelt over west Africa as factors in interannual variability. *International Journal of climatology*, *28*(13), 1775-1785.

Nicholson, S. E. (2009). On the factors modulating the intensity of the tropical rainbelt over West Africa. *International Journal of Climatology*, *29*(5), 673-689.

Nicholson, S. E. (2013). "The West African Sahel: A Review of Recent Studies on the Rainfall Regime and Its Interannual Variability," ISRN Meteorology, vol. 2013, Article ID 453521, pp. 32.

Nikulin, G., Jones, C., Giorgi, F., Asrar, G., Büchner, M., Cerezo-Mota, R., ... & Sushama, L. (2012). Precipitation climatology in an ensemble of CORDEX-Africa regional climate simulations. *Journal of Climate*, *25*(18), 6057-6078.

Norquist, D. C., Recker, E. E., & Reed, R. J. (1977). The energetics of African wave disturbances as observed during phase III of GATE. *Monthly Weather Review*, *105*(3), 334-342.

Odekunle, T. O., Balogun, E. E., & Ogunkoya, O. O. (2005). On the prediction of rainfall onset and retreat dates in Nigeria. *Theoretical and applied Climatology*, *81*(1-2), 101-112.

Okpara, J. N., Tarhule, A. A., & Perumal, M. (2013). Study of Climate Change in Niger River Basin, West Africa: Reality Not a Myth. *CLIMATE CHANGE–REALITIES, IMPACTS OVER ICE CAP, SEA LEVEL AND RISKS*, 1.

Omotosho, J. B. (1992). Long-range prediction of the onset and end of the rainy season in the West African Sahel. *International Journal of Climatology*, *12*(4), 369-382.

Omotosho J, Abiodun BJ (2007) A numerical study of moisture build-up and rainfall over West Africa. *Meteorol Appl*, *14*, 209–225

Ozer, A., & Ozer, P. (2005). Désertification au Sahel: Crise climatique ou anthropique?. *Bulletin des Séances de l'Académie Royale des Sciences d'Outre-Mer= Mededelingen der Zittingen van de Koninklijke Academie voor Overzeese Wetenschappen*, *51*(4).

Paeth, H., Born, K., Girmes, R., Podzun, R., & Jacob, D. (2009). Regional climate change in tropical and northern Africa due to greenhouse forcing and land use changes. *Journal of Climate*, *22*(1), 114-132.

Paeth, H., Fink, A. H., Pohle, S., Keis, F., Mächel, H., & Samimi, C. (2011). Meteorological characteristics and potential causes of the 2007 flood in sub-Saharan Africa. *International Journal of Climatology*, *31*(13), 1908-1926.

Panthou, G., Vischel, T., Lebel, T., Blanchet, J., Quantin, G., & Ali, A. (2012). Extreme rainfall in West Africa: A regional modeling. *Water Resources Research*, *48*(8).

Panthou, G., Vischel, T., & Lebel, T. (2014). Recent trends in the regime of extreme rainfall in the Central Sahel. *International Journal of Climatology*, *34*(15), 3998-4006.

Peel MC, Finlayson BL & McMahon TA (2007), Updated world map of the Köppen-Geiger climate classification, Hydrol. Earth Syst. Sci., 11, 1633-1644.

Peters, M., & Tetzlaff, G. (1988). The structure of West African squall lines and their environmental moisture budget. *Meteorology and Atmospheric Physics*, *39*(2), 74-84.

Pu, B., & Cook, K. H. (2010). Dynamics of the West African westerly jet. *Journal of Climate*, *23*(23), 6263-6276.

Pytharoulis, I., & Thorncroft, C. (1999). The low-level structure of African easterly waves in 1995. *Monthly Weather Review*, *127*(10), 2266-2280.

Rasch PJ, Kristjansson JE. (1998). A comparison of the CCM3 model climate using diagnosed and predicted condensate parameterizations. *J. Climate*, *11*, 1587–1614.

Reed, R. J., Norquist, D. C., & Recker, E. E. (1977). The structure and properties of African wave disturbances as observed during Phase III of GATE. *Monthly Weather Review*, *105*(3), 317-333.

Reed, R. J., Klinker, E., & Hollingsworth, A. (1988). The structure and characteristics of African easterly wave disturbances as determined from the ECMWF operational analysis/forecast system. *Meteorology and Atmospheric Physics*, *38*(1-2), 22-33.

Rummukainen, M. (2010). State-of-the-art with Regional Climate Models. *Wiley Interdisciplinary Reviews: Climate Change*, *1*(1), 82-96.

Ruti, P. M., & Dell'Aquila, A. (2010). The twentieth century African easterly waves in reanalysis systems and IPCC simulations, from intra-seasonal to inter-annual variability. *Climate dynamics*, *35*(6), 1099-1117.

Samuelsson, P., Jones, C. G., Willén, U., Ullerstig, A., Gollvik, S., Hansson, U. L. F., ... & Wyser, K. (2011). The Rossby Centre Regional Climate model RCA3: model description and performance. *Tellus A*, *63*(1), 4-23.

Samuelsson P., Gollvik S. and Ullerstig A. (2006). The land-surface scheme of the Rossby Centre regional atmospheric climate model (RCA3). Report in Meteorology 122. SMHI, SE-60176 Norrkoping, Sweden, pp. 25.

Sanderson, M. (2010). Changes in the frequency of extreme rainfall events for selected towns and cities. *Ofwat, UK*.

Sass B. H., Rontu L., Savijarvi H. and Raisanen P. (1994). HIRLAM-2 Radiation scheme: documentation and tests. Hirlam Technical ReportNo. 16, SMHI, SE-60176 Norrkoping, Sweden, pp. 43.

Savijarvi H. (1990). A fast radiation scheme for mesoscale model and short-range forecast models. *J. Appl. Met.*, *29*, 437–447

Seth, A., Rauscher, S. A., Camargo, S. J., Qian, J. H., & Pal, J. S. (2007). RegCM3 regional climatologies for South America using reanalysis and ECHAM global model driving fields. *Climate Dynamics*, *28*(5), 461-480.

Seneviratne, S. I., Nicholls, N., Easterling, D., Goodess, C. M., Kanae, S., Kossin, J., ... & Zhang, X. (2012). Changes in climate extremes and their impacts on the natural physical environment. *Managing the risks of extreme events and disasters to advance climate change adaptation*, 109-230.

Sighomnou, D., Descroix, L., Genthon, P., Mahé, G., Moussa, I. B., Gautier, E., ... & Hiernaux, P. (2013). La crue de 2012 à Niamey: un paroxysme du paradoxe du Sahel?. *Science et changements planétaires/Sécheresse*, *24*(1), 3-13.

Skinner, C. B., & Diffenbaugh, N. S. (2014). Projected changes in African easterly wave intensity and track in response to greenhouse forcing. *Proceedings of the National Academy of Sciences*, *111*(19), 6882-6887.

Solmon, F., Elguindi, N., & Mallet, M. (2012). Radiative and climatic effects of dust over West Africa, as simulated by a regional climate model. *Climate Research*, *52*, 97-113.

Sylla, M. B., Coppola, E., Mariotti, L., Giorgi, F., Ruti, P. M., Dell'Aquila, A., & Bi, X. (2010). Multiyear simulation of the African climate using a regional climate model (RegCM3) with the high resolution ERA-interim reanalysis. *Climate Dynamics*, *35*(1), 231-247.

Sylla, M. B., Giorgi, F., Ruti, P. M., Calmanti, S., & Dell'Aquila, A. (2011). The impact of deep convection on the West African summer monsoon climate: a regional climate model sensitivity study. *Quarterly Journal of the Royal Meteorological Society*, *137*(659), 1417-1430.

Sylla, M. B., Gaye, A. T., & Jenkins, G. S. (2012). On the fine-scale topography regulating changes in atmospheric hydrological cycle and extreme rainfall over West Africa in a regional climate model projections. *International Journal of Geophysics*, *2012*.

Sylla, M. B., Giorgi, F., Coppola, E., & Mariotti, L. (2013). Uncertainties in daily rainfall over Africa: assessment of gridded observation products and evaluation of a regional climate model simulation. *International Journal of Climatology*, *33*(7), 1805-1817. doi: 10.1002/joc.3551

Tarhule, A. (2005). Damaging rainfall and flooding: the other Sahel hazards. *Climatic change*, *72*(3), 355-377.

Taylor, K. E., Stouffer, R. J., & Meehl, G. A. (2012). An overview of CMIP5 and the experiment design. *Bulletin of the American Meteorological Society*, *93*(4), 485-498.

The Watcher, accessed online on 27th August, 2015 at: http://thewatchers.adorraeli.com/2015/08/08/heavy-flooding-across-west-africa-8-people-dead-and-19-779-affected-in-burkina-faso

Tokinaga, H., & Xie, S. P. (2011). Weakening of the equatorial Atlantic cold tongue over the past six decades. *Nature Geoscience*, *4*(4), 222-226.

Tošić, I., & Unkašević, M. (2012). Extreme daily precipitation in Belgrade and their links with the prevailing directions of the air trajectories. *Theoretical and applied climatology*, *111*(1-2), 97-107.

Tschakert, P., Sagoe, R., Ofori-Darko, G., & Codjoe, S. N. (2010). Floods in the Sahel: an analysis of anomalies, memory, and anticipatory learning. *Climatic Change*, *103*(3-4), 471-502.

Unden, P., Rontu, L., Jarvinen, H., Lynch, P., Calvo, J. and co-authors (2002). HIRLAM-5 scientific documentation. HIRLAM Report, SMHI, SE-601 76 Norrkoping, Sweden, p. 144.

Vezzoli, R., Mercogliano, P., & Pecora, S. (2012). A Brief Introduction to the Concept of Return Period for Univariate Variables. *CMCC Research Paper*, (139). Available at SSRN: http://ssrn.com/abstract=2195426 or http://dx.doi.org/10.2139/ssrn.2195426

Vigaud, N., Roucou, P., Fontaine, B., Sijikumar, S., & Tyteca, S. (2009). WRF/ARPEGE-CLIMAT simulated climate trends over West Africa. *Climate dynamics*, *36*(5-6), 925-944. doi:10.1007/s00382-009-0707-4

Viltard, A. D., De Felice, P., & Oubuih, J. (1997). Comparison of the African and the 6–9 day wave-like disturbance patterns over West-Africa and the tropical Atlantic during summer 1985. *Meteorology and Atmospheric Physics*, *62*(1-2), 91-99.

Viltard, A., Oubuih, J., De Felice, P., & Laurent, H. (1998). Rainfall and the 6–9 day wave-like disturbance in West-Africa during summer 1989. *Meteorology and Atmospheric Physics*, *66*(3-4), 229-234.

Vizy, E. K., & Cook, K. H. (2002). Development and application of a mesoscale climate model for the tropics: Influence of sea surface temperature anomalies on the West African monsoon. *Journal of Geophysical Research: Atmospheres (1984–2012)*, *107*(D3), ACL-2.

Vizy, E. K., & Cook, K. H. (2012). Mid-twenty-first-century changes in extreme events over northern and tropical Africa. *Journal of Climate*, *25*(17), 5748-5767.

Wang, Y., Leung, L. R., McGREGOR, J. L., Lee, D. K., Wang, W. C., Ding, Y., & Kimura, F. (2004). Regional climate modeling: progress, challenges, and prospects. *気象集誌. 第 2 輯*, *82*(6), 1599-1628.

Wang S-Y, Gillies RR. (2011). Observed change in Sahel rainfall, circulations African easterly waves, and Atlantic hurricanes since 1979. International Journal of Geophysics 2011: 259529, DOI:10.1155/2011/259529.

Wang, G., and C. A. Alo, (2012). Changes in precipitation seasonality in West Africa predicted by RegCM3 and the impact of dynamic vegetation feedback. Int. J. Geophys., 2012, 597205, doi:10.1155/2012/597205.

West African monsoon (2015). In Encyclopaedia Britannica. Retrieved from http://www.britannica.com/science/West-African-monsoon

Wiacek, A., Peter, T., & Lohmann, U. (2010). The potential influence of Asian and African mineral dust on ice, mixed-phase and liquid water clouds. *Atmospheric Chemistry and Physics*, *10*(18), 8649-8667.

Williams, C. J. R., Kniveton, D. R., & Layberry, R. (2010). Assessment of a climate model to reproduce rainfall variability and extremes over Southern Africa. *Theoretical and applied climatology*, *99*(1-2), 9-27.

World Meteorological Organization, WMO, (2015). The Climate in Africa: 2013. WMO-No. 1147, Geneva: WMO

Wu, M. L. C., Reale, O., Schubert, S. D., Suarez, M. J., & Thorncroft, C. D. (2012). African easterly jet: Barotropic instability, waves, and cyclogenesis. *Journal of Climate*, *25*(5), 1489-1510.

Wu, M. L. C., Reale, O., & Schubert, S. D. (2013). A characterization of African easterly waves on 2.5–6-day and 6–9-day time scales. *Journal of Climate*, *26*(18), 6750-6774.

Yabi, I., & Afouda, F. (2012). Extreme rainfall years in Benin (West Africa). *Quaternary International*, *262*, 39-43.

Zaroug, M. A., Sylla, M. B., Giorgi, F., Eltahir, E. A., & Aggarwal, P. K. (2013). A sensitivity study on the role of the swamps of southern Sudan in the summer climate of North Africa using a regional climate model. *Theoretical and applied climatology*, *113*(1-2), 63-81.

Zhang, X., Alexander, L., Hegerl, G. C., Jones, P., Tank, A. K., Peterson, T. C., ... & Zwiers, F. W. (2011). Indices for monitoring changes in extremes based on daily temperature and precipitation data. *Wiley Interdisciplinary Reviews: Climate Change*, *2*(6), 851-870.

Appendix A (Past Climate)

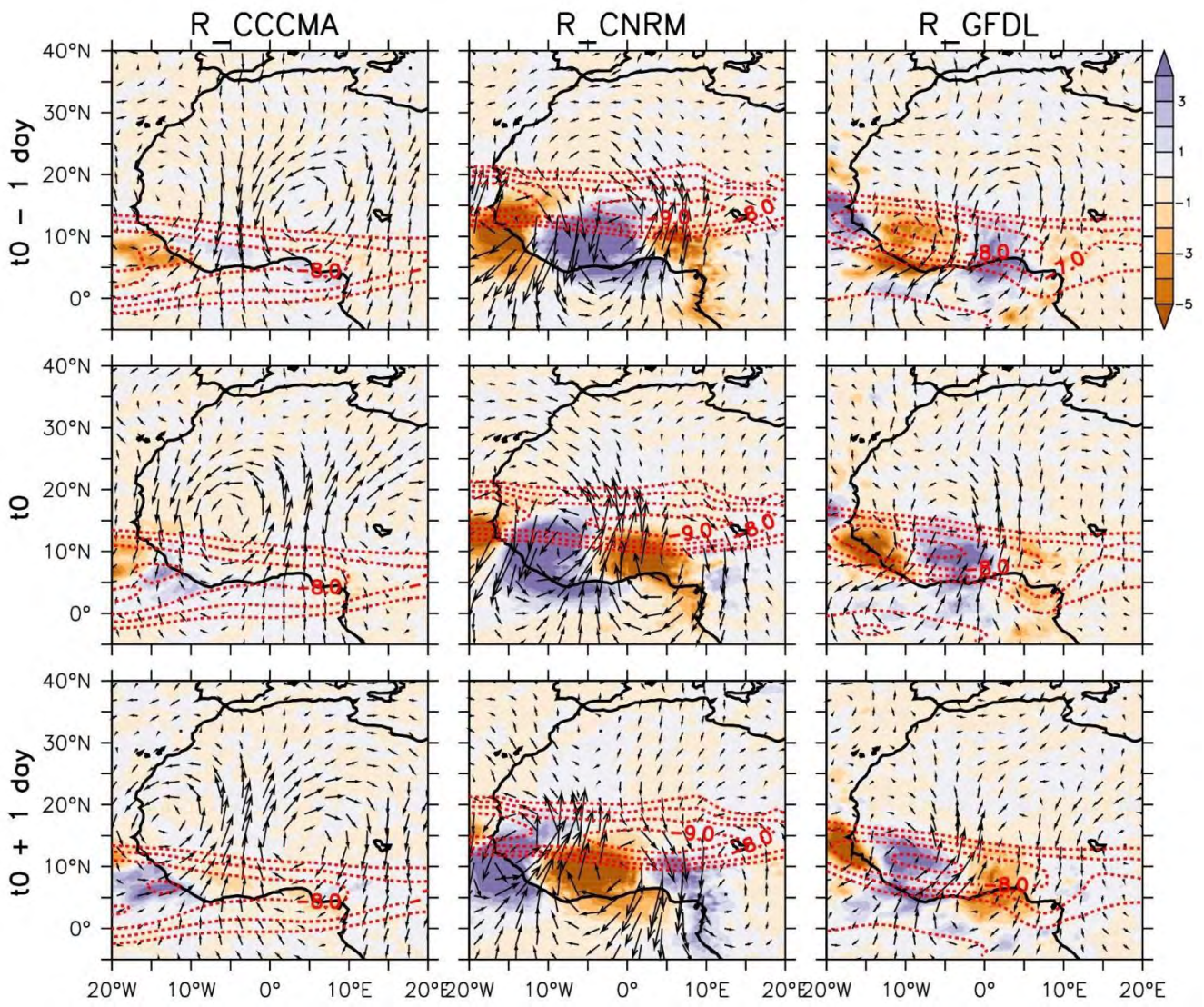

Fig.A1: Composite anomalies for 3-5 African Easterly Waves as simulated by RCA4 forced with 3 GCMs (CCCMA, CNRM5 and GFDL) from time t_o-1 - t_o+1 over West Africa for the period, 1971-2005. Rainfall (mm day^{-1}) is shaded. Vectors are 700 hpa wind anomalies (m s^{-1}). The contour (dashed red line) indicates the position of the African Easterly Jet (AEJ).

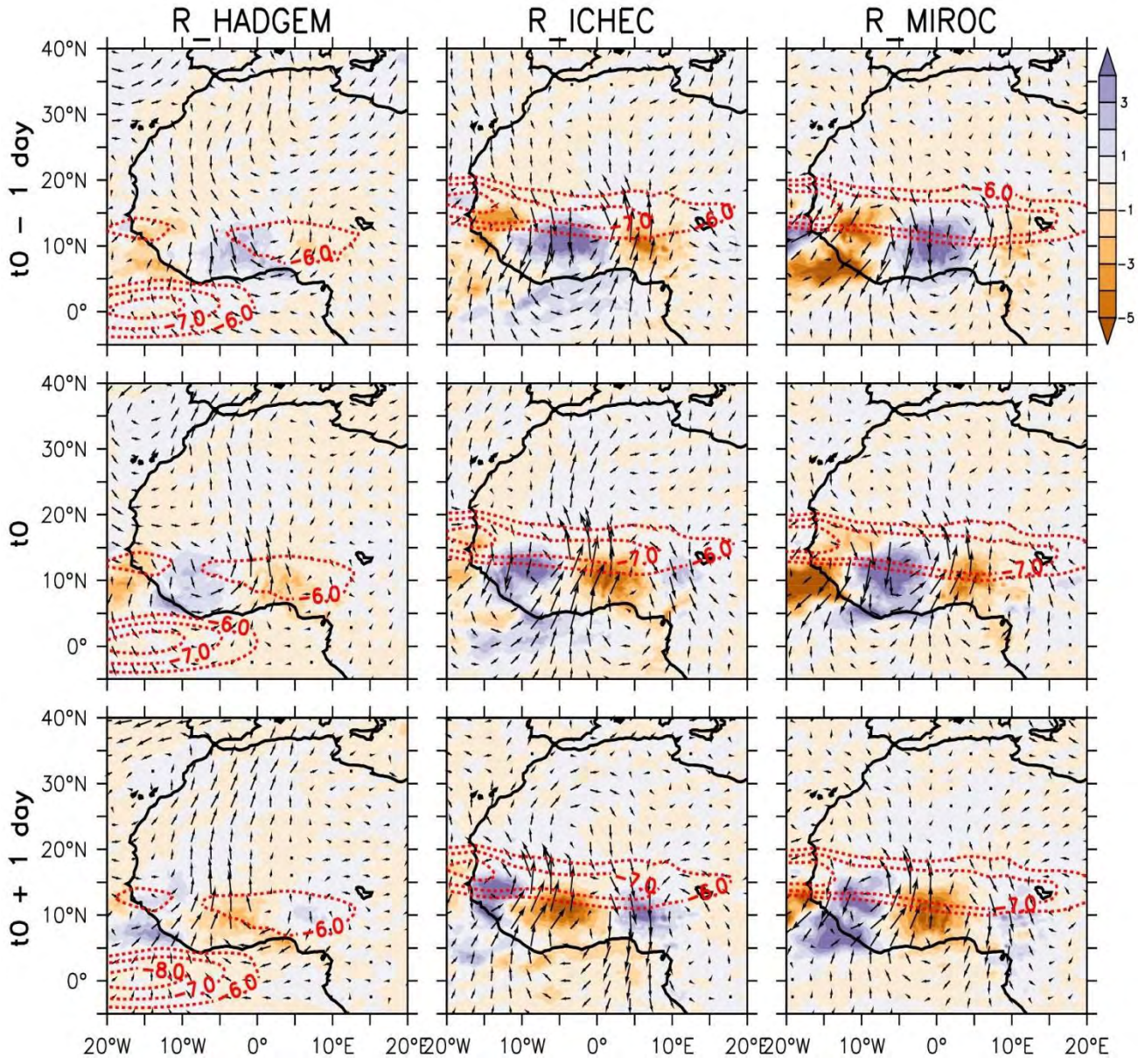

Fig.A2: Same as A1 but for RCA4 forced with HADGEM, ICHEC and MIROC

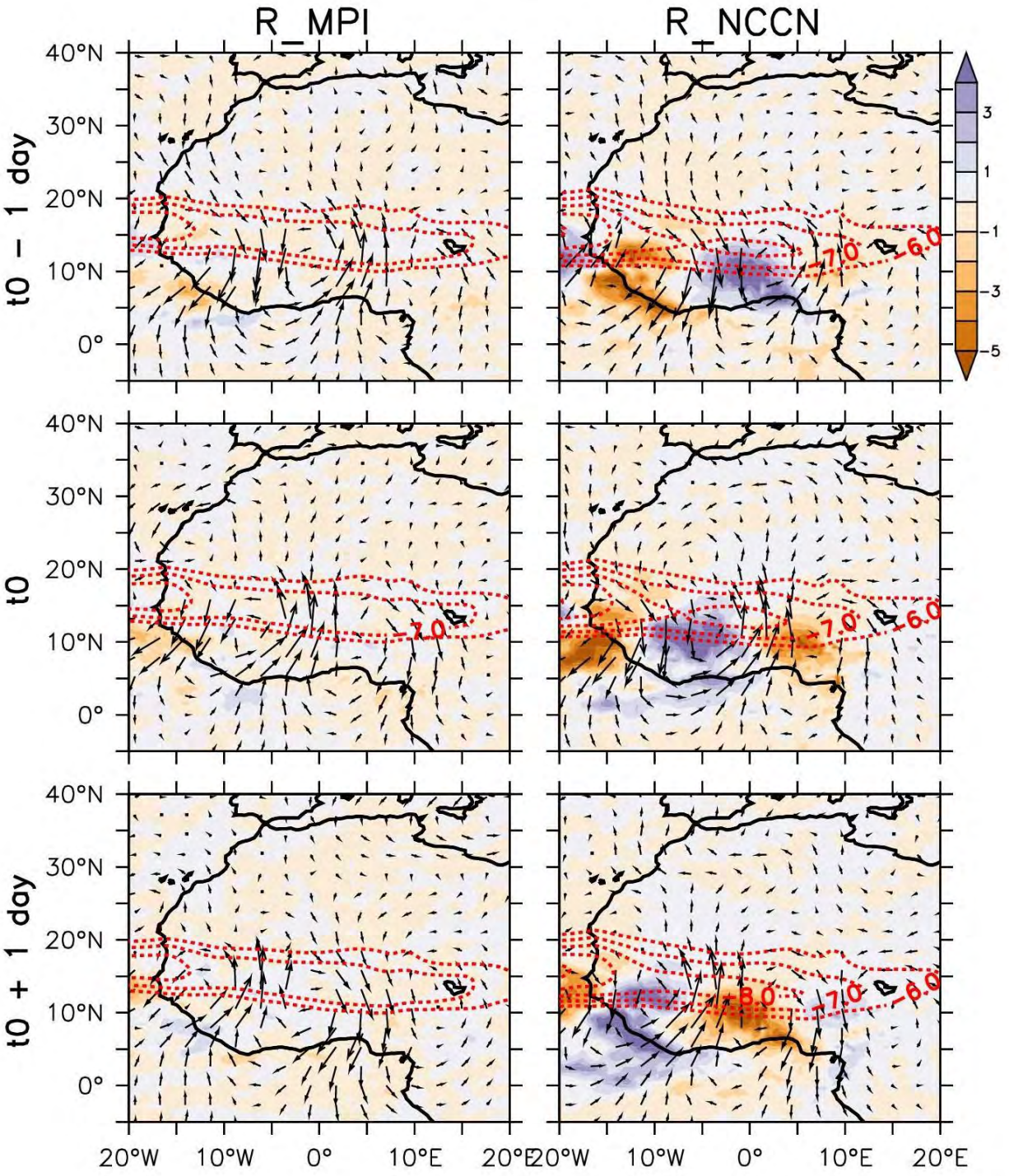

Fig.A3: Same as A1 but for RCA4 forced with MPI and NCCN

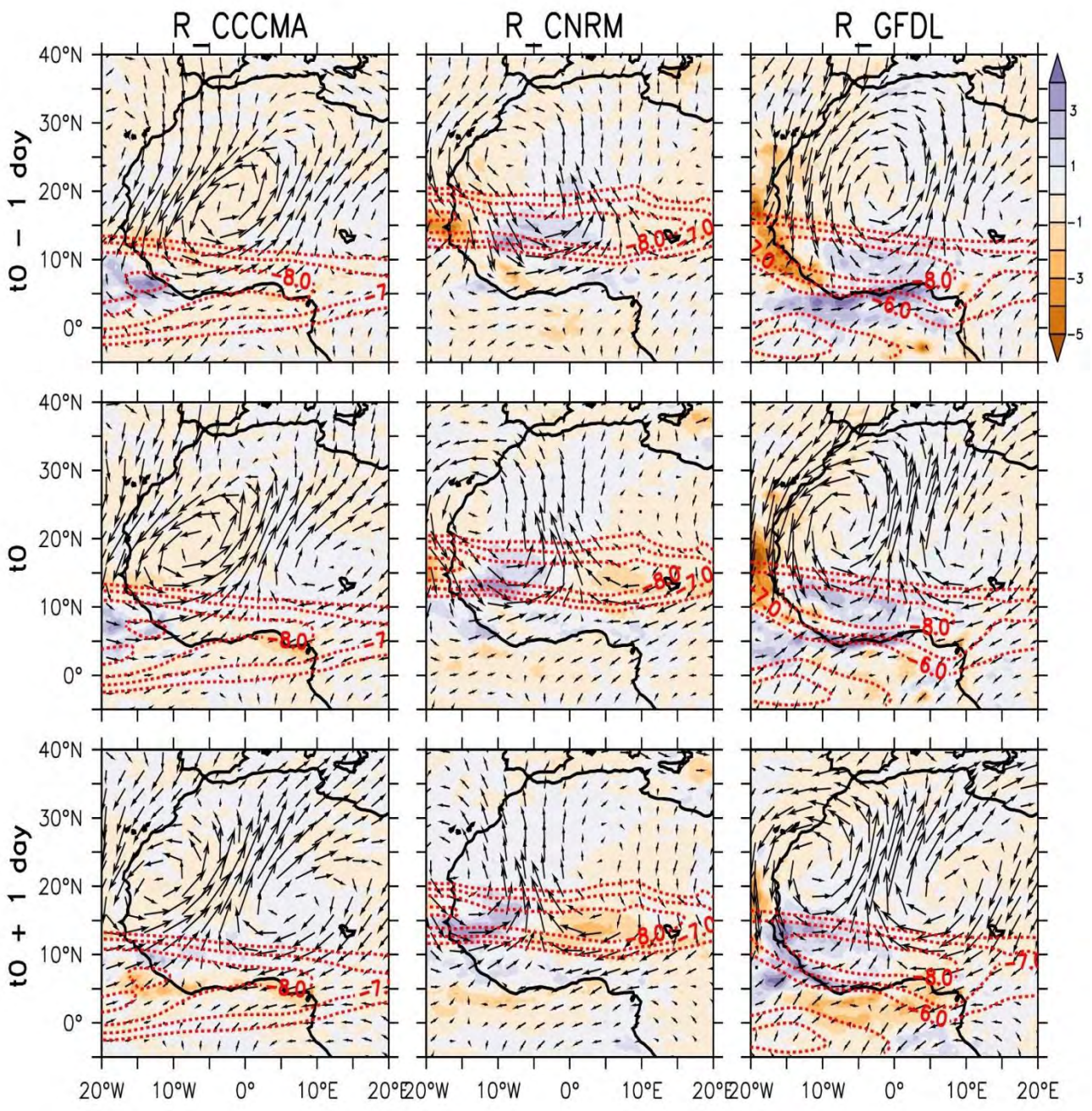

Fig.A4: Same as A1 but for 6-9 days AEWs

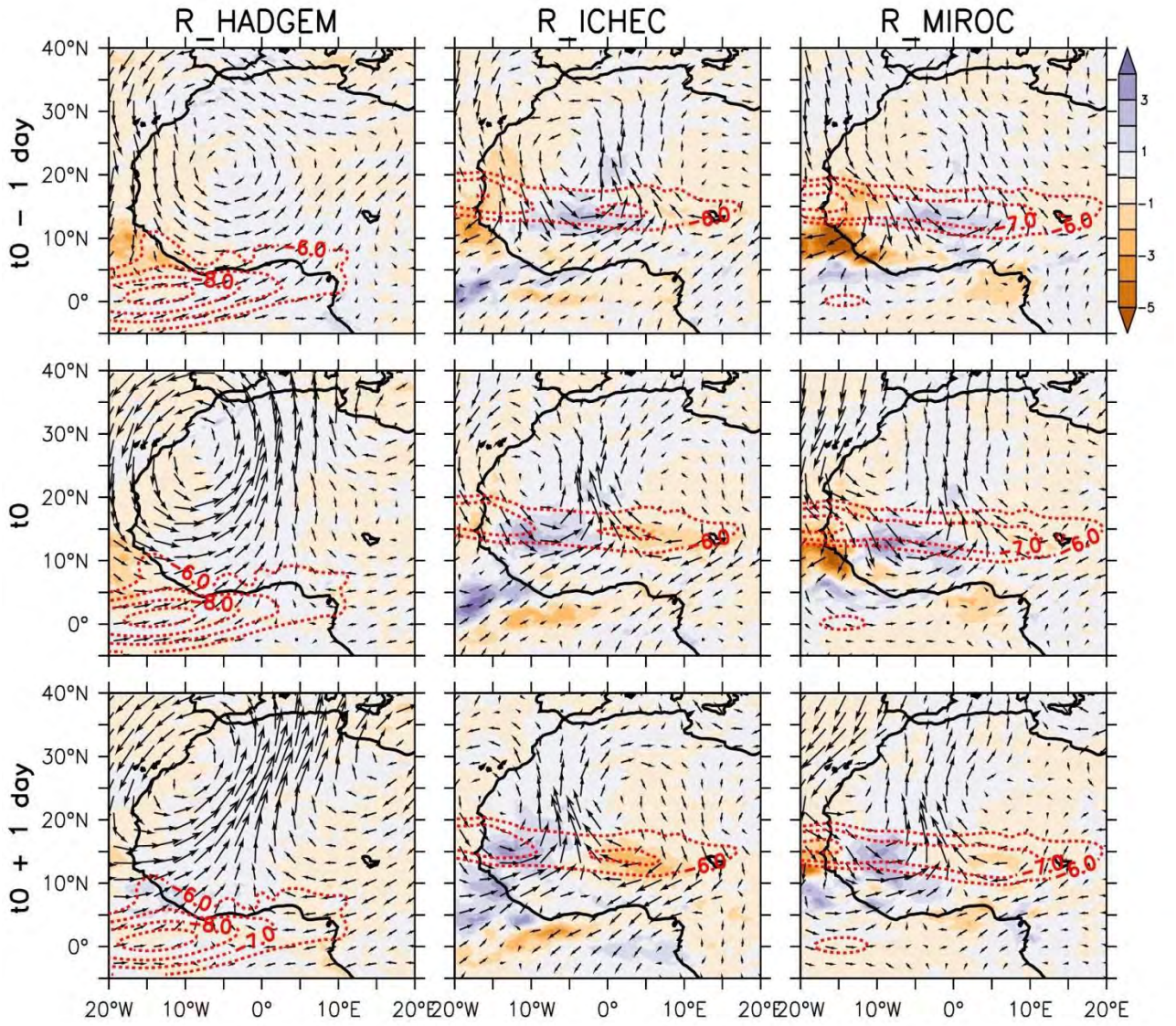

Fig.A5: Same as A2 but for 6-9 days AEWs

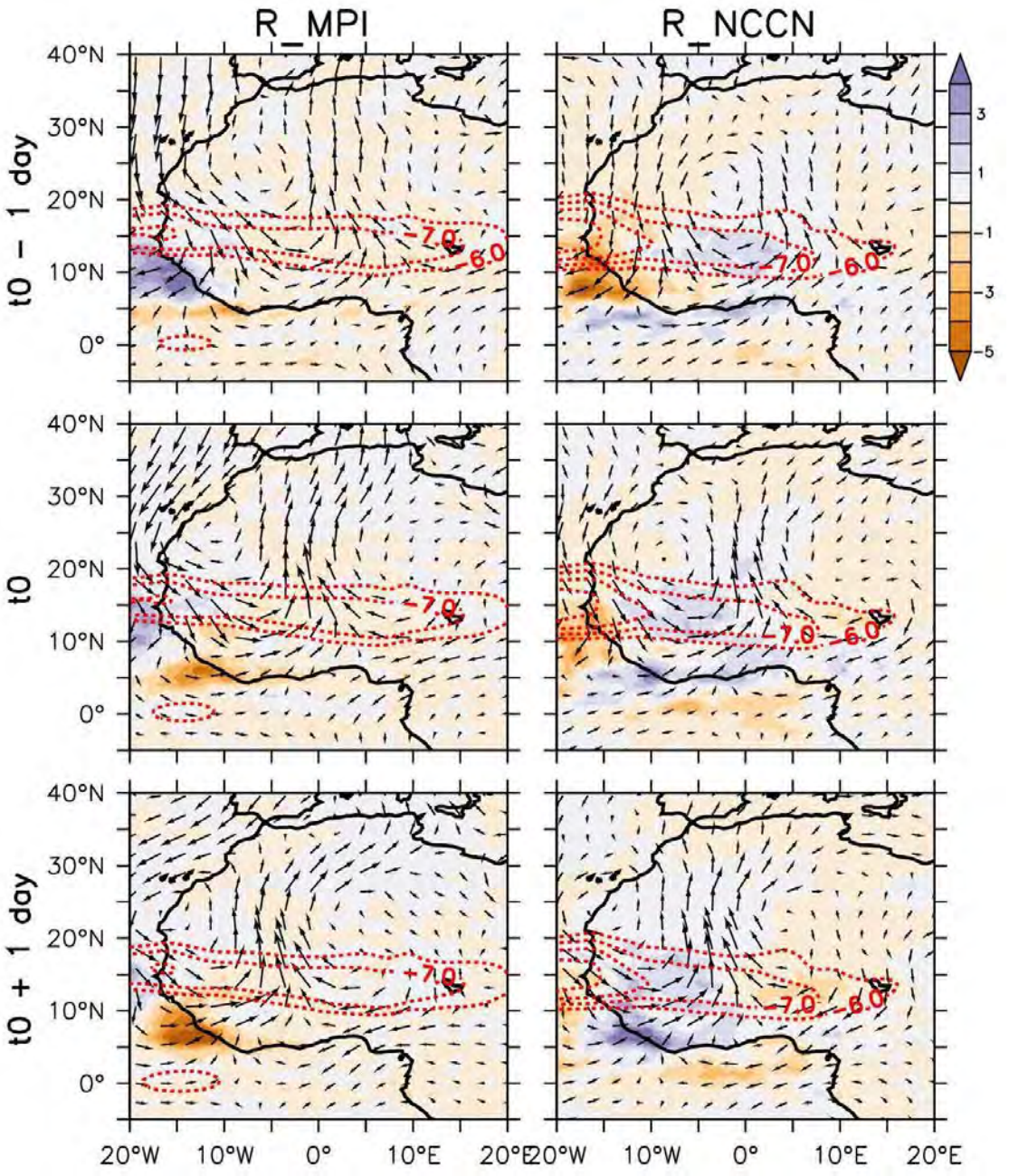

Fig.A6: Same as A3 but for 6-9 days AEWs

Appendix B (Future Changes)

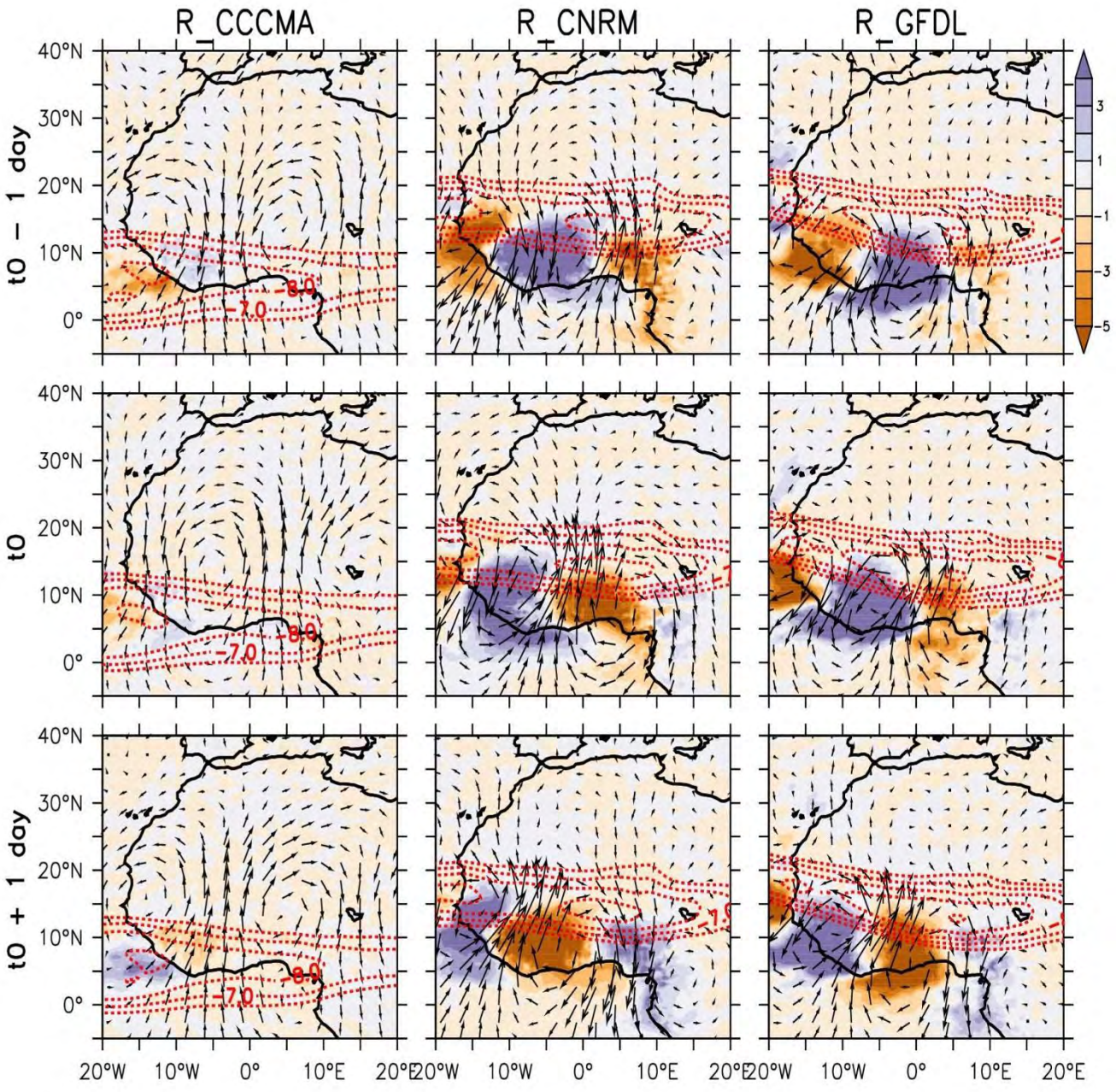

Fig.B1: Composite of projected change for 3-5 days African Easterly Waves as simulated by RCA4 forced with 3GCMs (CCCMA, CNRM5 and GFDL) from time, t_o-1 - t_o+1 over West Africa for the period 2031-2065 under the RCP4.5 emission scenario. Rainfall (mm day^{-1}) is shaded. Vectors are 700hPa wind anomalies (m s^{-1}). The contour (shaded red line) indicates the position of the African Easterly Jet (AEJ).

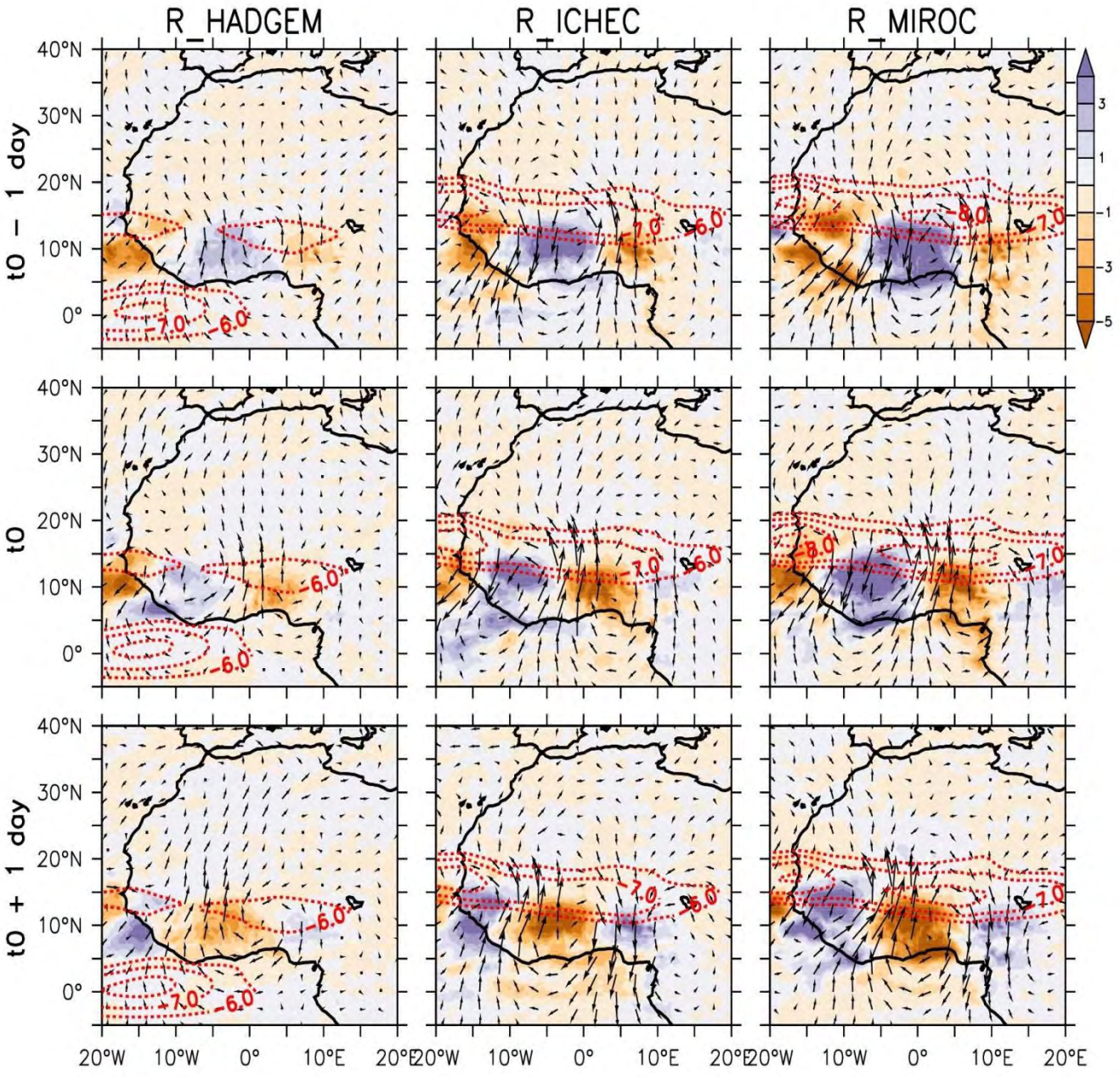

Fig.B2: Same as B1 but for RCA4 forced with HADGEM, ICHEC and MIROC

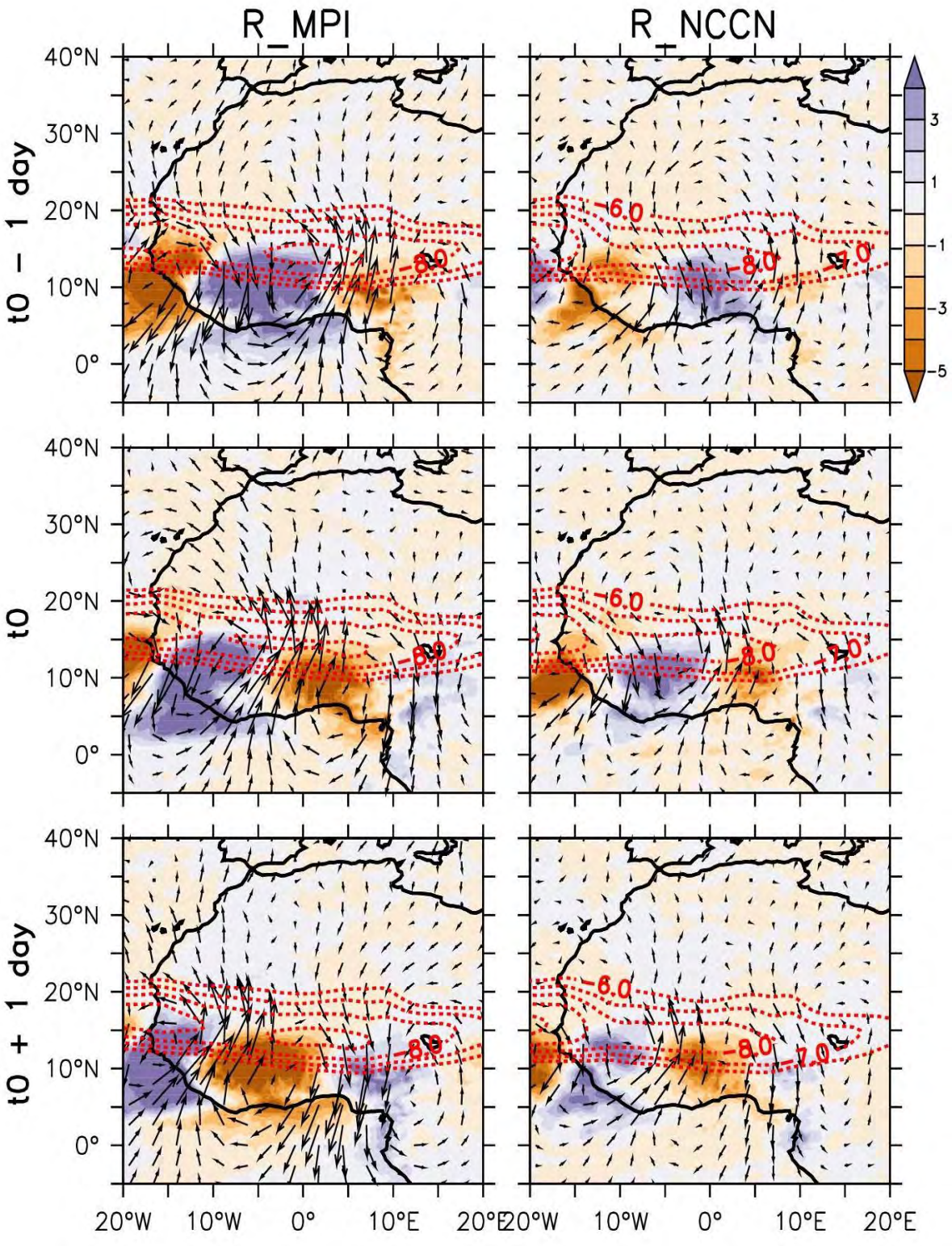

Fig.B3: Same as B1 but for RCA4 forced with MPI and NCCN

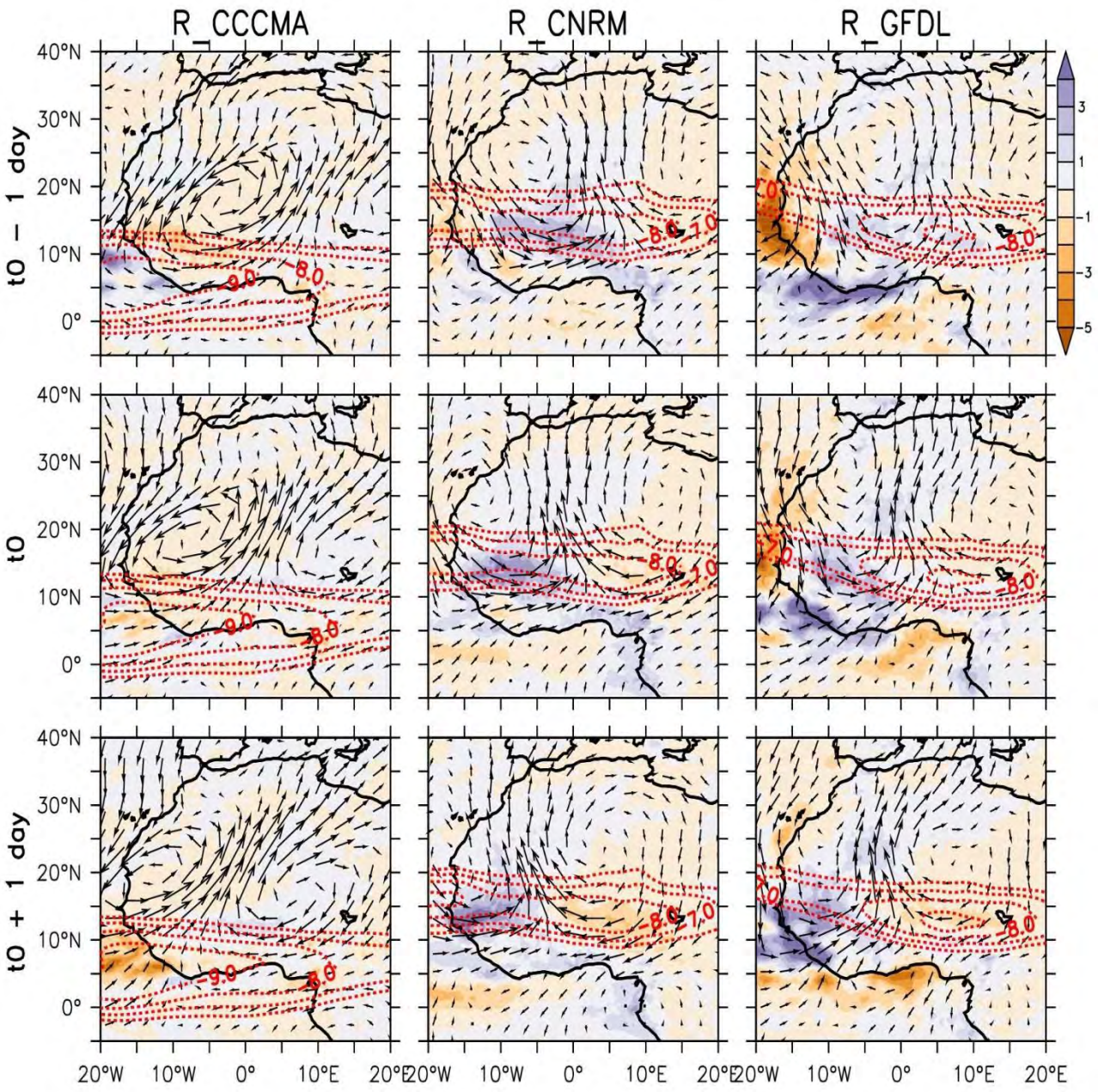

Fig.B4: Same as B1 but for 6-9 days AEWs

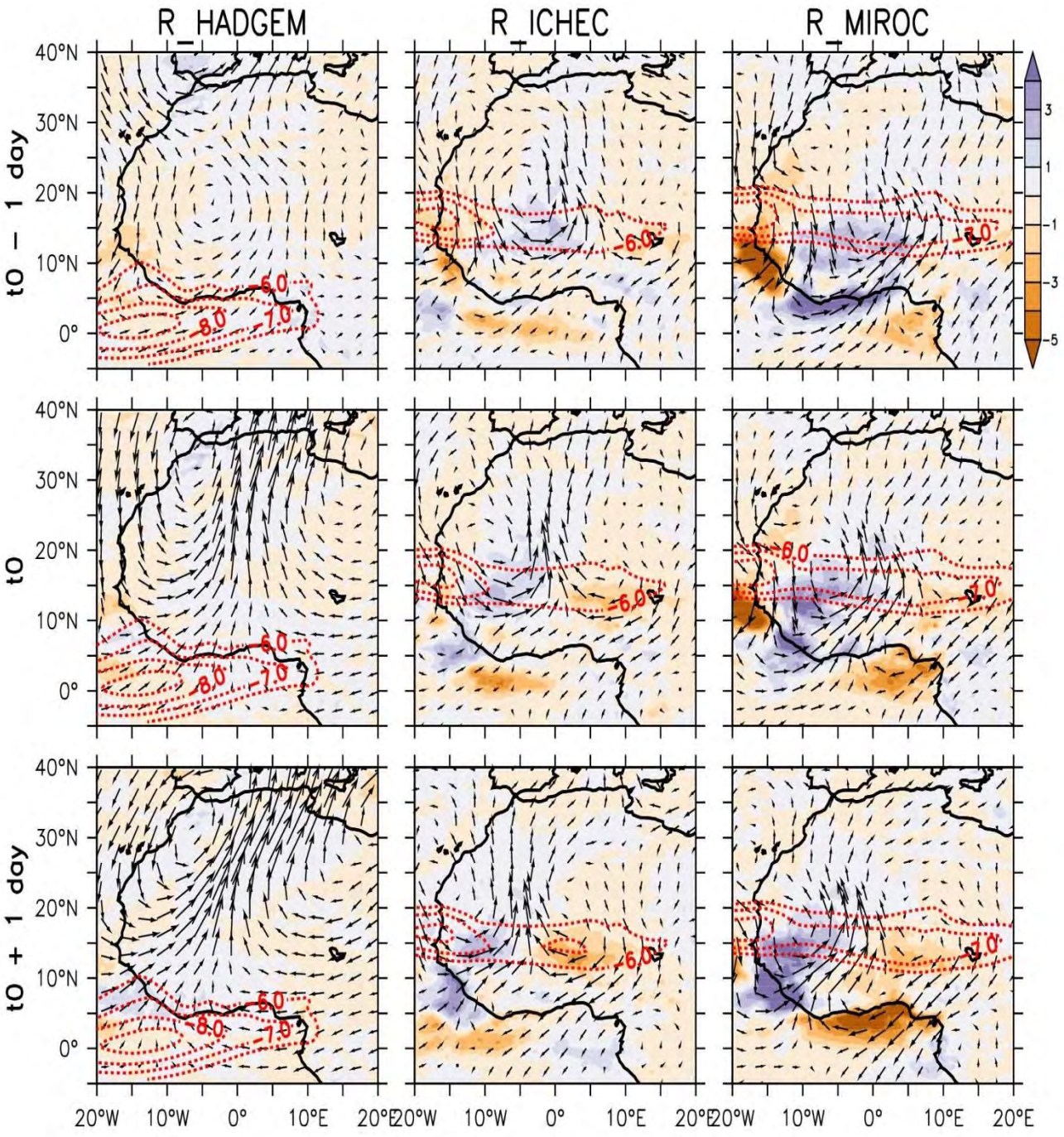

Fig.B5: Same as B2 but for 6-9 days AEWs

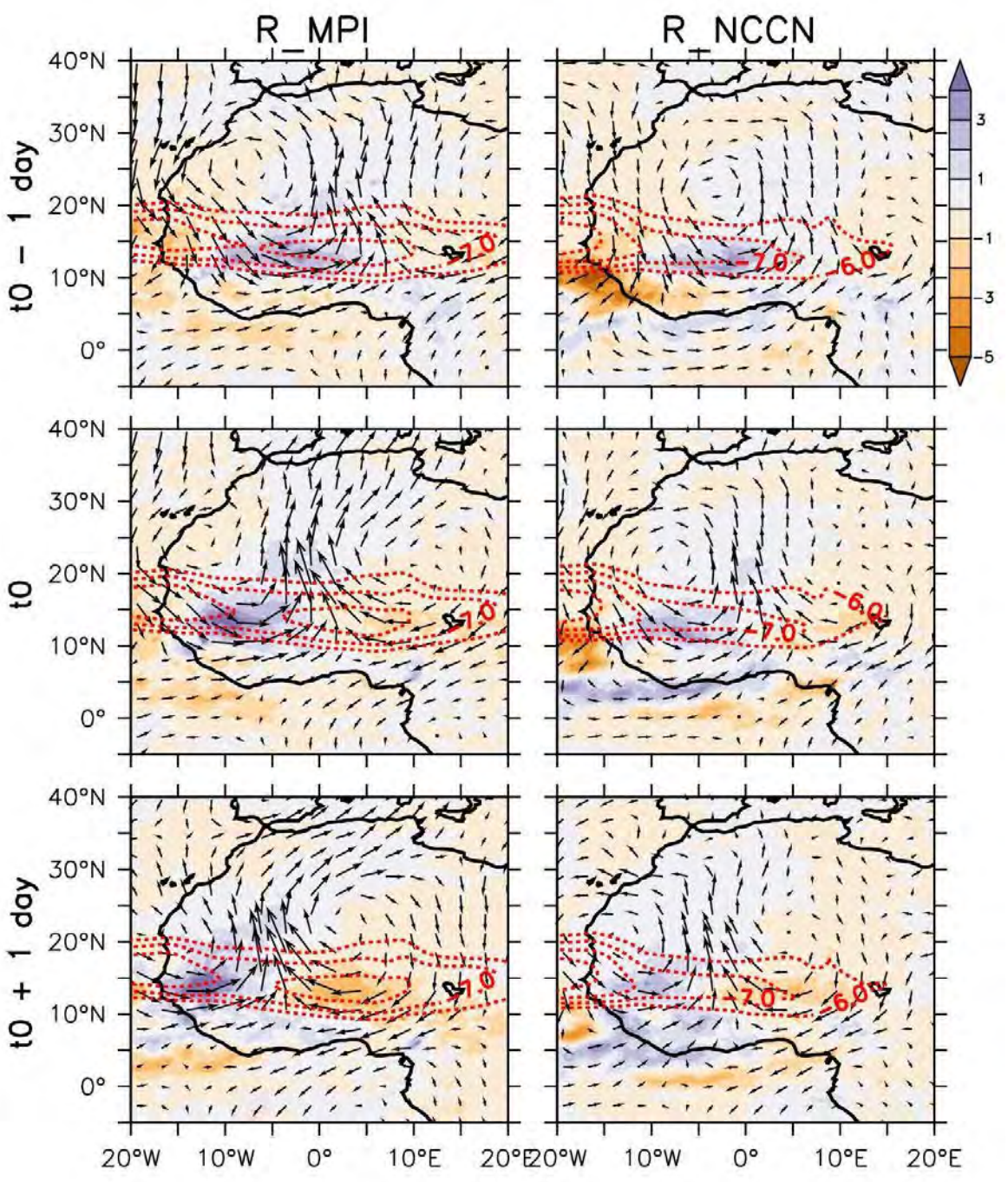

Fig.B6: Same as B3 but for 6-9 days AEWs

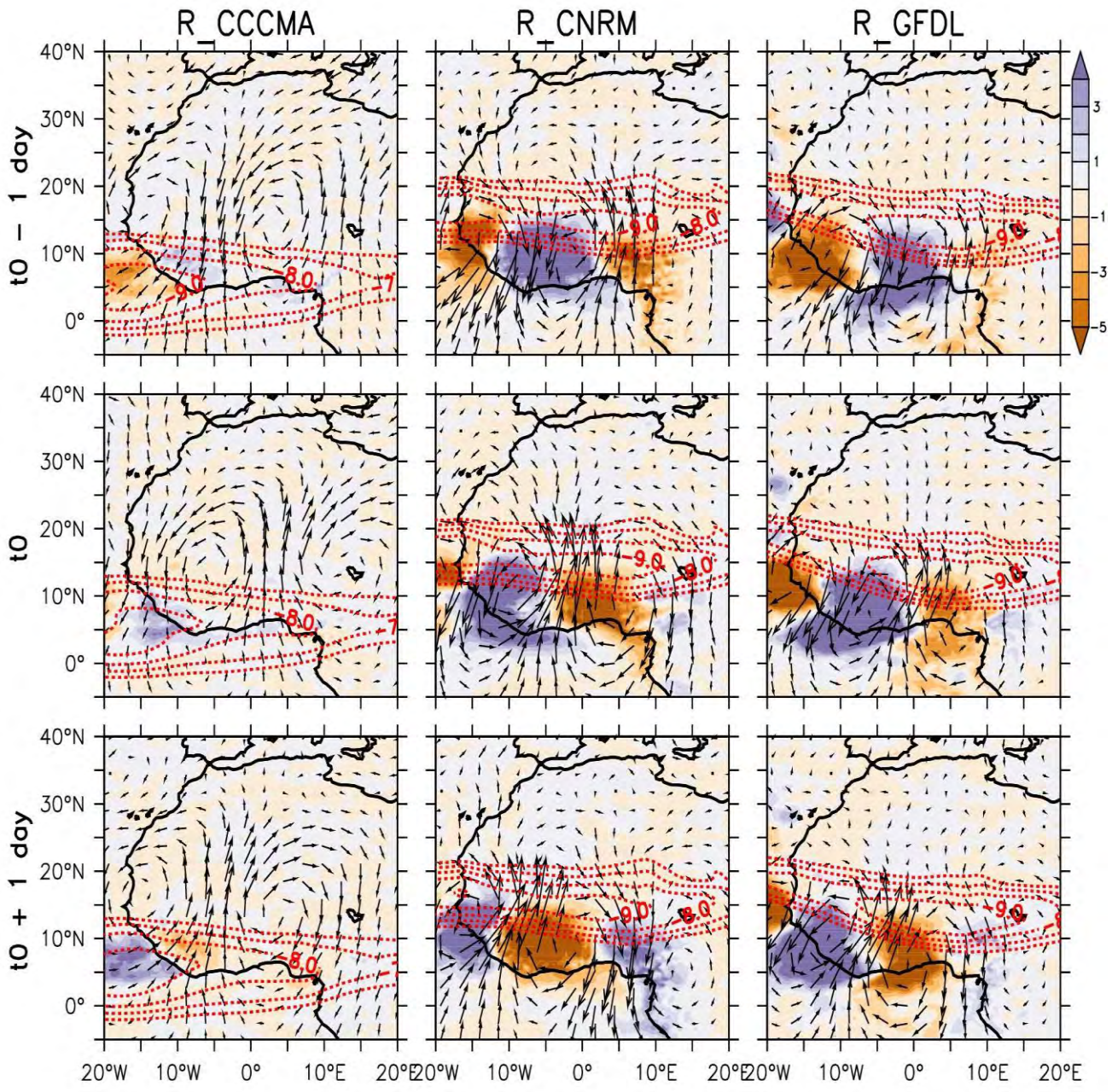

Fig.B7: Same as B1 but under the RCP8.5 emission scenario

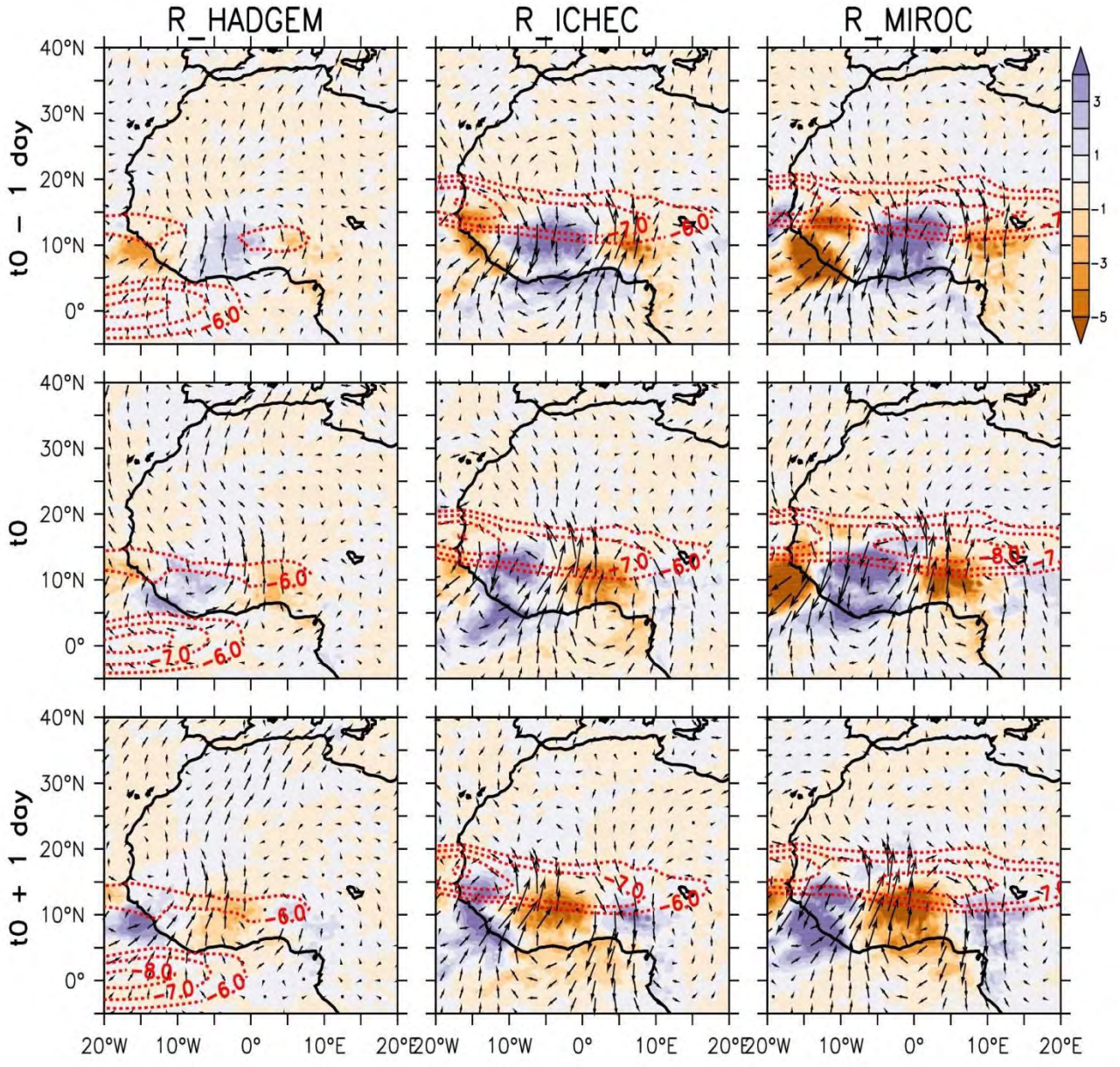

Fig.B8: Same as B2 but under the RCP8.5 emission scenario

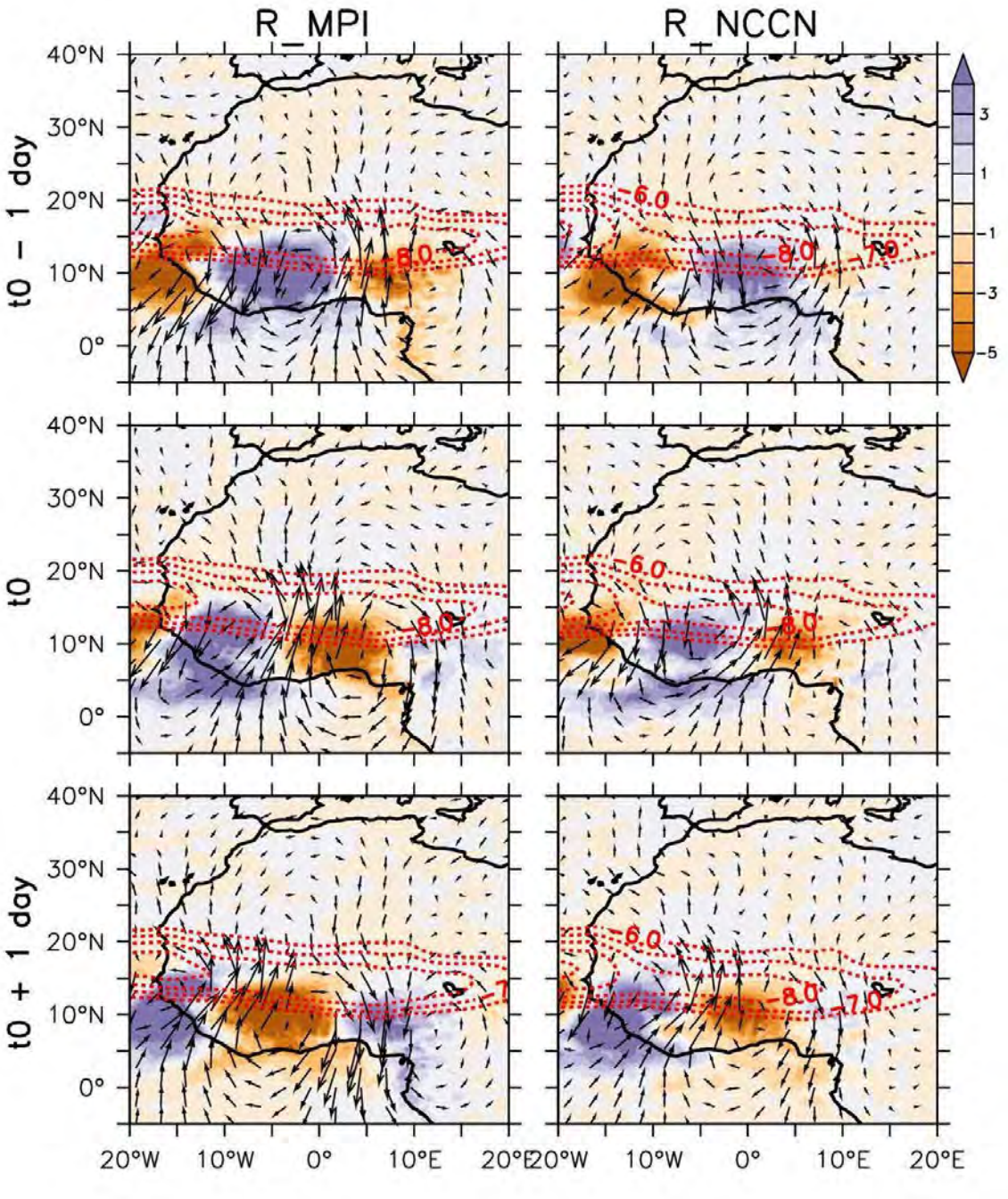

Fig.B9: Same as B3 but under the RCP8.5 emission scenario

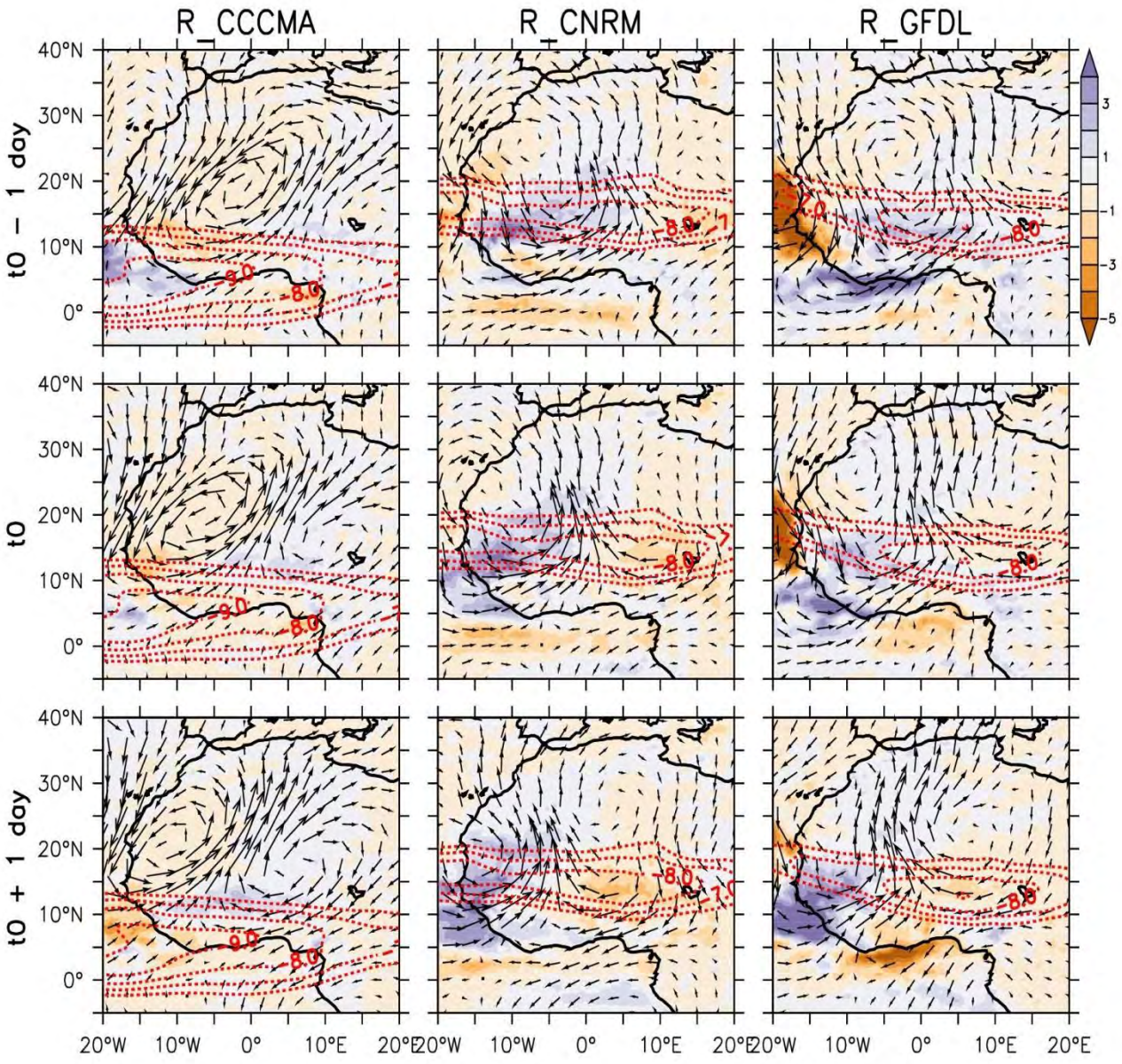

Fig.B10: Same as B4 but under the RCP8.5 emission scenario

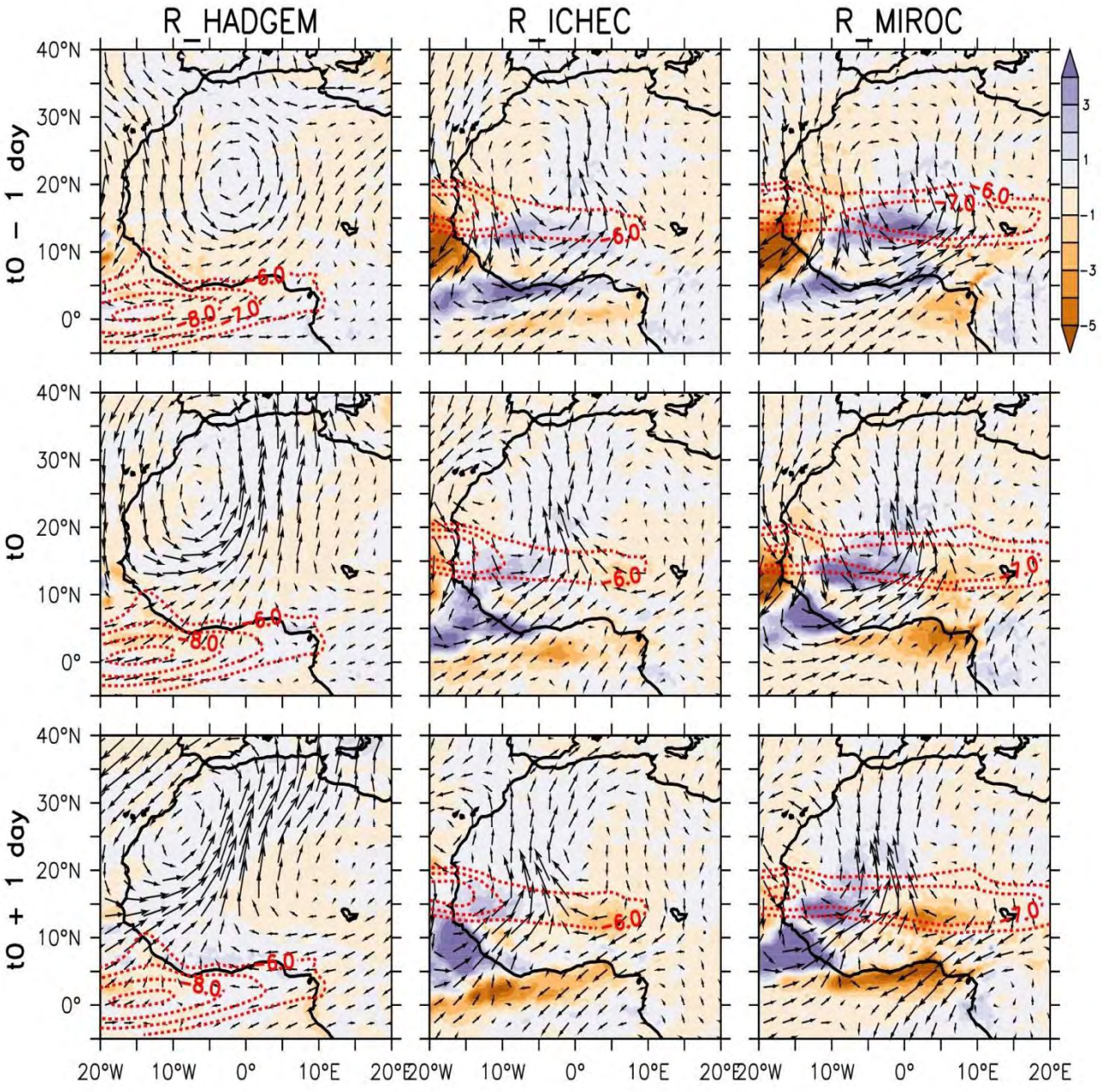

Fig.B11: Same as B5 but under the RCP8.5 emission scenario

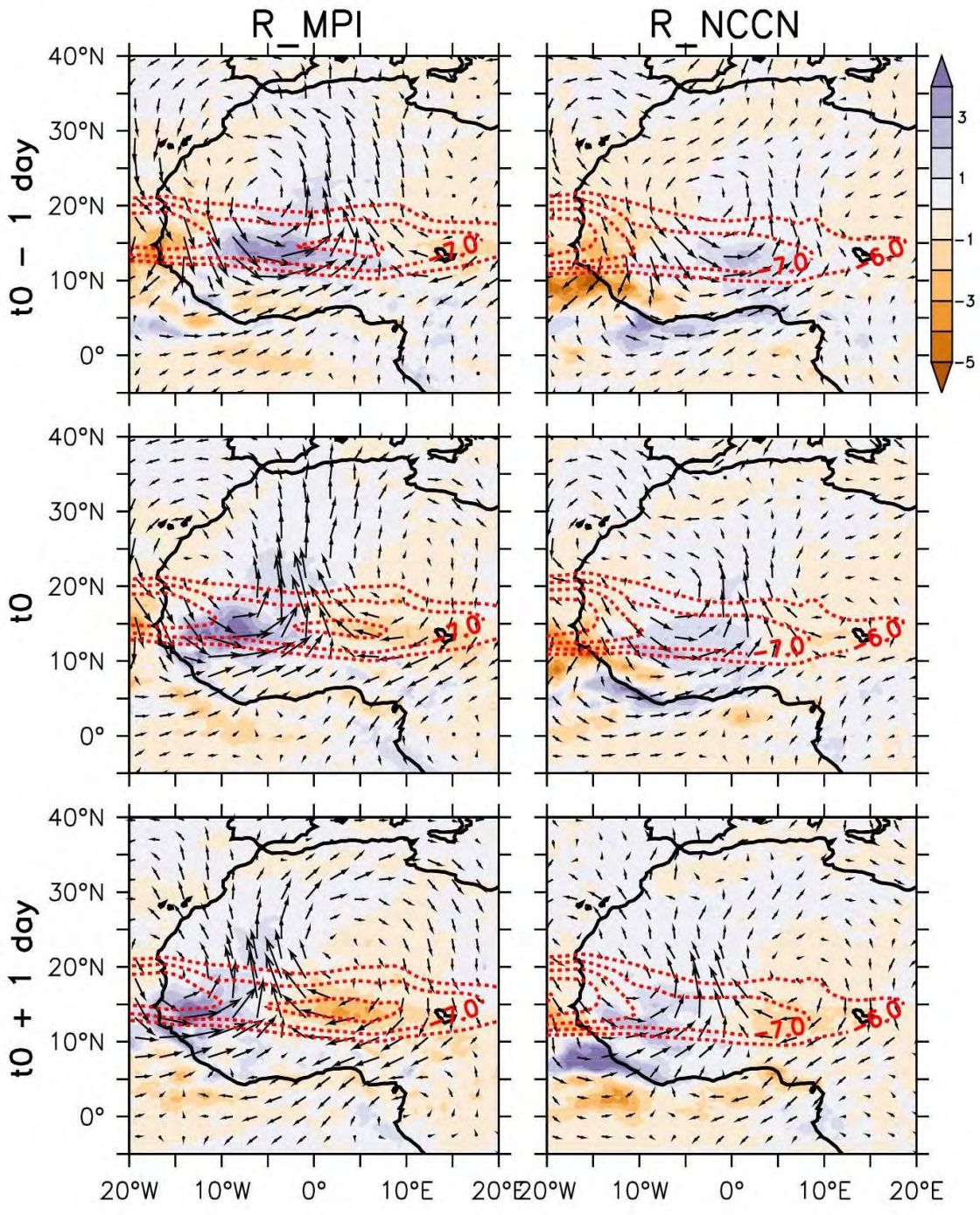

Fig.B12: Same as B6 but under the RCP8.5 emission scenario